November 2015

ROLE OF LIPID-BASED DELIVERY SYSTEMS IN THE BIOLOGICAL FATE OF LIPOPHILIC NUTRACEUTICALS AND INORGANIC NANO-PARTICLES IN THE GASTROINTESTINAL TRACT

Mingfei Yao
University of Massachusetts Amherst

ROLE OF LIPID-BASED DELIVERY SYSTEMS IN THE BIOLOGICAL FATE OF LIPOPHILIC NUTRACEUTICALS AND INORGANIC NANO-PARTICLES IN THE GASTROINTESTINAL TRACT

A Dissertation Presented

by

MINGFEI YAO

Submitted to the Graduate School of the
University of Massachusetts Amherst in partial fulfillment
of the requirements for the degree of

DOCTOR OF PHILOSOPHY

September 2015

Food Science

ROLE OF LIPID-BASED DELIVERY SYSTEMS IN THE BIOLOGICAL FATE OF LIPOPHILIC NUTRACEUTICALS AND INORGANIC NANO-PARTICLES IN THE GASTROINTESTINAL TRACT

A Dissertation Presented

by

MINGFEI YAO

Approved as to style and content by:

_____
Hang Xiao, Chair

_____
David Julian McClements, Member

_____
Eric A. Decker, Member

_____
Richard J. Wood, Member

_____
Eric A. Decker, Department Head
Food Science

DEDICATION

I dedicate this thesis to
my family and my husband
for their constant support and unconditional love.
I love you all dearly.

ACKNOWLEDGMENTS

First and Foremost, I would like to express my sincere gratitude to my advisor, Dr. Hang Xiao, for his guidance, support and assistant of my Ph.D study and research. It has been my honor to be his Ph.D. student and to be in his group. I am indebted and thankful for the fresh new opportunities he offered and supporting my attendance at various academic conferences. My experience in this lab is great treasure in my life. Also, I gratefully acknowledge the government scholarship by Chinese Scholarship Council (CSC) for my graduate study.

I will be forever thankful to Dr. David Julian McClements, who provided me with valuable instruction and inspiration in every stage of my research. Without his impressive kindness and patience, I could not have completed my thesis. My sincere thanks also goes to Dr. Eric Decker for not only providing much advice and insight for this thesis, but gave me the motivation to improve in my weaker areas. I would also like to thank my committee member Dr. Richard Wood, for serving on my committee and his academic suggestion and foresight for my research.

All special thanks to Dale A. Callahan, without his expertise and patience, I couldn't get so many amazing TEM images and my project might not have ever come to fruition. Also thanks for his encouragement, which inspired me to make every efforts to go after things I am interested. I need to extend my thanks to Dr. Faqing Zhao, Dr. Gregory Hendricks and Prof. Craig. Roger from Umass medical school for their help of the cryo-tem images. I would thank Jean Alamed and Fran Kostek for their help in the past three years.

Also I need to express my thanks to my lab mates, those who helped me during

the past three years. It was great pleasure to chat and share experience with you. It also produced tremendous energy in the work of research every time we encouraged each other. Besides, the knowledge of law, finance and psychology I learnt from you made me feel I am a real Ph.D.

To my dear friends in this Department, Cansu, Jennifer, Ziyuan and Sibel, thanks for the fun and support. I am grateful to have all of you as my friends.

Last but not least, I especially thank my grandma, my parents and my husband. Thanks for encouraging me to be an independent thinker, be confident in my abilities, go after things inspired me, be brave when facing any difficulties, stick to my dreams and most importantly to be a nice person. I am so lucky to have you in my life.

ABSTRACT

ROLE OF LIPID-BASED DELIVERY SYSTEMS IN THE BIOLOGICAL FATE OF LIPOPHILIC NUTRACEUTICALS AND INORGANIC NANO-PARTICLES IN THE GASTROINTESTINAL TRACT

September 2015

MINGFEI YAO, B.A., WUHAN UNIVERSITY, P.R.CHINA

M.A., ZHEJIANG UNIVERSITY, P.R. CHINA

Ph.D., UNIVERSITY OF MASSACHUSETTS AMHERST

Directed by: Professor Hang Xiao

The oral bioavailability of lipophilic bioactive molecules can be greatly increased by encapsulating them within engineered lipid nanoparticles, such as micelles, microemulsions and nanoemulsions. After ingestion these engineered lipid nanoparticles are disassembled in the gastrointestinal tract (GIT), and then reassembled into biological lipid nanoparticles (mixed micelles) in the small intestine. These mixed micelles solubilize and transport lipophilic bioactive components to the epithelium cells. The mixed micelles themselves are then disassembled and reassembled into yet another form of biological lipid nanoparticle (chylomicrons, CMs) within the enterocyte cells. The CMs carry the bioactive components into the systemic (blood) circulation via the lymphatic system, thereby avoiding metabolism in the small intestine and liver.

Polymethoxyflavones (PMFs) are bioactive flavonoids found in citrus fruits that have been shown to have potential health promoting properties. However, their application as nutraceuticals in functional foods and beverages is currently limited

due to their low water solubility and high melting point. The oral bioavailability of lipophilic compounds can be enhanced by promoting their intestinal lymphatic transport through co-administration with digestible lipids. First, we investigated the effects of chylomicron-mediated intestinal lymphatic transport on the bioavailability of 5-hydroxy-6, 7, 8, 3', 4'-pentamethoxylflavone (5-DN), one of representative PMFs in Caco-2 cells. Our results demonstrated that oleic acid and bile acid promoted secretion of CMs in Caco-2 cells, with mean diameter ranged from 70 to 150 nm. The intracellular level of 5-DN increased 3-fold by co-incubation with the mixed micelle solution. Moreover, the basolateral level of 5-DN increased 3-fold due to enhanced chylomicron-mediated transport.

Based on the above results, we then evaluate the influence of different fatty acid types on the properties of mixed micelles, cellular lipid droplets and CMs, and on the uptake of the highly lipophilic nutraceutical 5-DN. There were distinct differences in the structural properties of CMs formed depending on fatty acid unsaturation. Oleic acid ($C_{18:1}$) was most effective at enhancing transport of 5-DN and led to the formation of the largest CMs. Linoleic acid ($C_{18:2}$) and linolenic acid ($C_{18:3}$) also promoted 5-DN incorporation into CMs, but they were less efficient than oleic acid. The metabolism of 5-DN within the epithelium cells was greatly reduced when they were incorporated into CMs, presumably because they were isolated from metabolic enzymes in the cytoplasm. These results have important implications for the design of lipid nanoparticle-based delivery systems for lipophilic drugs and nutraceuticals by targeting them to the lymphatic circulation.

Fatherly, we studied the effects of triglycerides-based nanoemulsion delivery

systems with different fatty acid chain lengths on the bioavailability 5-DN. 5-DN was encapsulated in medium chain triglycerides (MCT) or canola oil (long chain triglycerides, LCT) based nanoemulsion. They were subject to a simulated gastrointestinal digestion model. Finally, the mixed micelle phase was applied to Caco-2 monolayer cell model that mimics intestinal absorption. Higher bioaccessibility of 5-DN was found in MCT nanoemulsion than canola nanoemulsion, 13% vs.7% respectively. However, only 30% 5-DN crossed Caco-2 monolayer while half of them were metabolized for MCT nanoemulsion, up to 60% 5-DN and only 10% were metabolized in canola nanoemulsion. Results also demonstrated more lipid droplets and CMs were formed by canola nanoemulsion, which were responsible for transportation of 5-DN to the lymph. In conclusion, although for lipophilic components like 5-DN, relatively higher bioaccessibility can be achieved by MCT-based nanoemulsion, LCT-based emulsion was more potent in enhancing the bioavailability through increased lymphatic transport.

Lipids especially the ones with polyunsaturated long chain fatty acids (PUFA) are very susceptible to oxidation. Ingestion of oxidized lipids is associated with all kinds of health risk: diabetes, tumor development and atherosclerosis. Meanwhile, the oxidation of lipids may affect the absorption of lipophilic bioactive components in foods. We compared the effect of oxidized and unoxidized PUFA, linoleic acid (LA) on the transport of the highly lipophilic compound 5-hydroxy 6,7,8,4' tetramethoxylflavone (5-DMT) by a Caco-2 cell model. Results turned out that unoxidized LA improved bioavailability of 5-DMT by stimulating CMs. Oxidized LA also showed an effect of improving transport of 5-DMT. However, it significantly

affected the morphology of Caco-2 monolayer especially the tight junction. Accordingly, the transport pathway could be altered compared to the unoxidized LA, which will ultimately influence the distribution and metabolism fate of lipophilic components in the human body.

Recently, the fate of inorganic nanoparticles in foods after ingestion has been attracted highly attention. Based on the above model and experimental methods, we also investigate the transport and toxicity of inorganic nanoparticle (AuNPs) on Caco-2 cell monolayer. AuNPs with different size (15nm, 50nm and 100nm) were applied. Our results demonstrated that more amount of gold was retained in the monolayer and higher toxicity was caused for larger size of AuNPs. Besides, mixed micelles greatly improve the secretion of AuNPs. The influence may be associated with formation abundant lipid droplets and CMs in the monolayer after fatty acids were taken in.

Overall, our results demonstrated for the first time that the bioavailability of PMFs and some inorganic NPs can be enhanced by promoting their incorporation into CMs.

TABLE OF CONTENTS

Page

LIST OF TABLES

LIST OF FIGURES

CHAPTER 1

INTRODUCTION

Many nutraceuticals are highly lipophilic and their oral bioavailability in foods or beverages is very low, such as carotenoids, curcumins and flavonoids[1, 2]. Hence the potential benefits to human health of these nutraceuticals cannot be fully realized. One way to enhance their oral bioavailability is to incorporate them in lipid and lipid-based formulations in pharmaceutical area [3]. Several factors are considered to determine the nutraceutical oral bioavailability: bioaccessibility, absorption and transformation[4]. First, lipid and lipid–based formulations enhanced gastrointestinal solubilization of lipophilic components and absorption by formation of bile salt/phospholipid/fatty acid mixed micelle in the gastrointestinal tract[5, 6]. Then the absorbed nutraceutialcs incorporated into the stimulated lipid carriers chylomicrons were exported directly to the system circulation through lymph, thus avoid being metabolized by the enzymes in intestine and liver[3, 6, 7].

In this article, we focus on improving the bioavailability of highly lipophilic nutraceutical 5-DN and 5-DMT, which are belonging to PMFs, by facilitating their chylomicron-lymphatic pathway on an in vitro Caco-2 monolayer model. The differentiated Caco-2 cell monolayers on membranes were able to assemble ad secrete chylomicrons (CMs)[8]. Besides, lipids types play an important part in the role of facilitating lymphatic pathway. Hence, oleic acid-taurocholate mixed micelles were prepared which has been confirmed to stimulation and secretion of abundant chylomicrons on the Caco-2 cell monolayer model by previous study[7, 9, 10].

The changing of pathway also altered the metabolism behavior of PMFs in the Caco-2 monolayer. In order to further understand the mechanism and control the gastric fate of these nutriceutials, it is also critical to determine the effect of different free fatty acids (FFAs) or different type of lipids (long chain or short chain) on their bioavailability. Morphologies of different FFA-based mixed micelles, formation of lipid droplets and chylomicrons in the monolayer can be clearly characterized by TEM.

Unsaturated lipids are always associated with oxidation. It is also necessary to have the knowledge of the influence of lipid oxidation in lipid-based formulations to the gastrointestinal fate of nutraceuticals, since it is closed related to the function of the delivery system and food safety.

Based on the above study of lipid formation on the in vitro Caco-2 cell monolayer model, we also continue to investigate the transport of inorganic nanoparticles (NPs) on this model and the affect of lipid on their absorption. This information should be useful in the security of food additives in food industry.

CHAPTER 2

LITERATURE REVIEW: DELIVERY OF LIPOPHILIC BIOACTIVES: ASSEMBLY, DISASSEMBLY, AND REASSEMBLY OF LIPID NANOPARTICLES

2.1 Introduction

2.1.1 Lipid Nanoparticles Inside and Outside the Body

Numerous lipophilic constituents within foods have been identified as having health benefits over and above their normal roles as nutrients (Table 2-1), such as bioactive lipids (e.g., ω-3 fatty acids and conjugated linoleic acids), oil-soluble vitamins (e.g., A, D, E and K), carotenoids, flavonoids, and phytosterols[3, 11, 12]. These bioactive components are often highly hydrophobic molecules that have low water-solubility and relatively poor oral bioavailability [3, 13]. Consequently, they are difficult to incorporate into many types of aqueous-based food and beverage products, and their potential beneficial health effects are not fully realized because they are poorly absorbed by the human body [14, 15]. The oral bioavailability of lipophilic bioactive molecules can be greatly enhanced by encapsulating them within colloidal delivery systems, such as micelles, microemulsions, emulsions, and suspensions [3, 16-22]. These delivery systems contain engineered lipid nanoparticles (ELNs) that are normally fabricated using man-made processes outside of the human body, e.g., various physicochemical and mechanical methods [14, 23]. Typically, ELNs consist of a hydrophobic core surrounded by a hydrophilic shell (Figure 2-1). However, their precise composition and structure can be tailored

for specific delivery applications. In particular, they can be designed to enable the bioactive components to be incorporated into particular food and beverage matrices, protect them from degradation, and then release them at an appropriate location within the gastrointestinal tract (GIT) after ingestion.

Table 2-0-1 Examples of poorly water-soluble bioactive components whose bioavailability may be improved by delivery using engineered lipid nanoparticles

Compound	Molar Mass (g mol-1)	Tm (ºC)	Log P
Curcumin	368.4	183	3.07
Capsaicin	305.4	64	3.20
Genistein	270.2	300	3.11
Resveratrol	228.2	255	3.02
Beta-carotene	536.9	180	14.76
Lycopene	536.9	175	14.5
Zeaxanthin	568.9	205	10.9
Astaxanthin	596.8	210	8.24
Lutein	568.9	180	11.5
Beta-sitosterol	414.7	138	10.5
Campesterol	400.7	155	9.97
Stigmasterol	412.7	150	10.07
Alpha-tocopherol	430.7	3	10.96
Tocopherol acetate	472.7	-27.5	10.69
Coenzyme-Q	863.3	49	19.12

There have been numerous, fairly recent reviews on the biological fate of ingested lipids and lipophilic bioactive components in the literature [16, 20, 24-27], and on the development of nanoparticle-based delivery systems for lipophilic bioactive components [28-31]. A number of these delivery systems have been found to increase the bioavailability of lipophilic substances (Table 2- 1). In the current review, we focus on a novel nanotechnology aspect of the behavior of colloidal

delivery systems within the gastrointestinal tract: the disassembly and reassembly of lipid nanoparticles. After ingestion, an engineered lipid nanoparticle may be disassembled and reassembled into various kinds of biological lipid nanoparticles as it passes through the GIT e.g., mixed micelles and CMs. An improved understanding of how these various kinds of lipid nanoparticles are assembled and disassembled could be used to rationally design functional foods with specific health effects. For example, controlling the initial composition and structure of the ELNs in a delivery system could be used to impact the type and amounts of mixed micelles and CMs formed in the gastrointestinal tract. In turn, the nature of the biological lipid nanoparticles formed can determine the amount of bioactive components absorbed, and their subsequent biological fate. For example, when lipophilic bioactive components are incorporated in CMs in the enterocyte cells they are transported into the systemic circulation via the lymphatic system (rather than the portal vein) and so first pass metabolism within the liver is avoided [7]. Hence, the bioactivity of lipophilic components that are susceptible to hepatic metabolism can be improved by designing delivery systems that stimulate chylomicron secretion and lymphatic transport. Although the focus of this review article is on lipid nanoparticles, it should be noted that much of the discussion is also relevant to delivery systems containing larger particles ($d > 200$ nm), such as conventional emulsions, suspensions, and liposomes.

2.1.2 Bioavailability of Lipophilic Bioactive Components

In this review chapter, we focus on bioactive components that are highly lipophilic, i.e., they have a low water-solubility and a high oil-water partition coefficient. These types of compound are often classified as Type II (low solubility/high permeability) or Type III (low solubility/low permeability) compounds using the biopharmaceutical classification system or BCS [22]. The BCS system categorizes bioactive components in terms of their solubility in the aqueous gastrointestinal juices and their permeability across the epithelium cells. Colloidal delivery systems are often required to increase the overall bioavailability of these compounds.

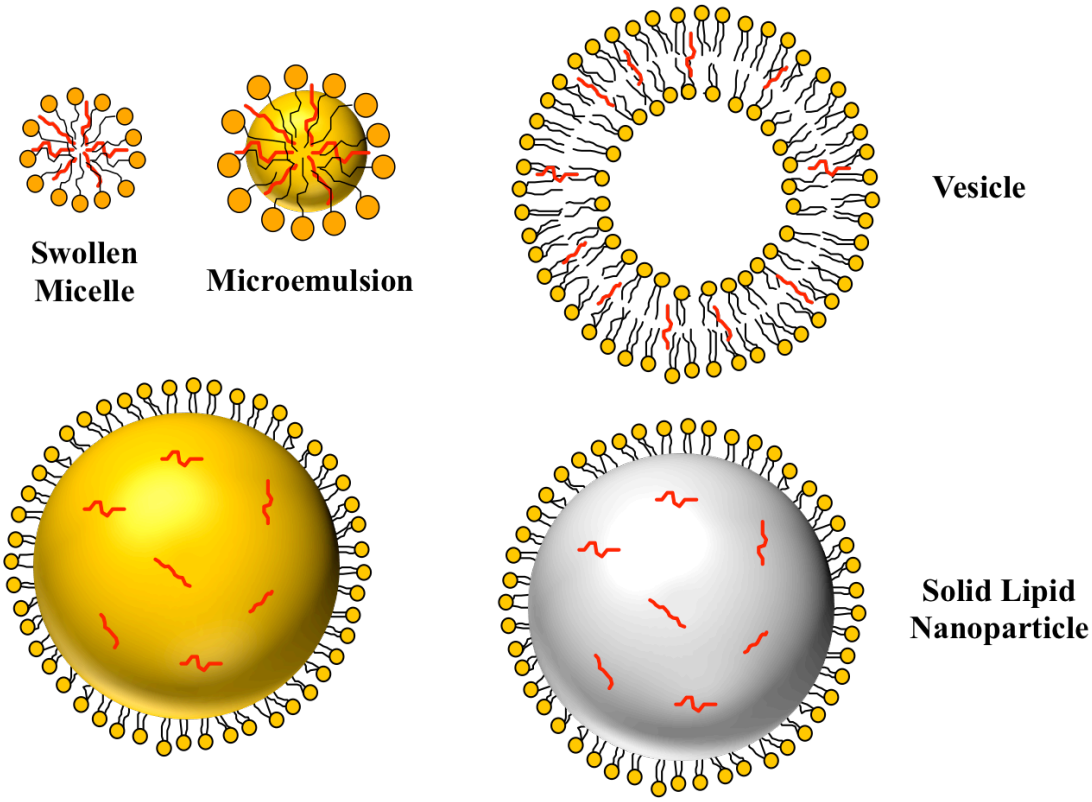

Figure 2-1 A variety of engineered lipid nanoparticles that are suitable for encapsulating and releasing lipophilic bioactive agents can be fabricated from food grade ingredient.

The term bioavailability is normally defined as the fraction of an ingested bioactive component that eventually reaches the systemic (blood) circulation in an active form [32]. There are a number of factors influencing the overall oral bioavailability (F) of an ingested lipophilic bioactive component: $F = F_M \times F_B \times F_A$. Here, FM is the fraction of the bioactive component that is not metabolized into an inactive state as its passes through the GIT. F_B is the fraction of the bioactive component that is released from the food matrix into the gastrointestinal fluids to become bioaccessible [33]. FA is the fraction of the bioaccessible bioactive component that is absorbed by the GIT and ends up in the systemic circulation. The major physicochemical and physiological processes that influence these parameters are highlighted below [34-37] (Figure 2-2):

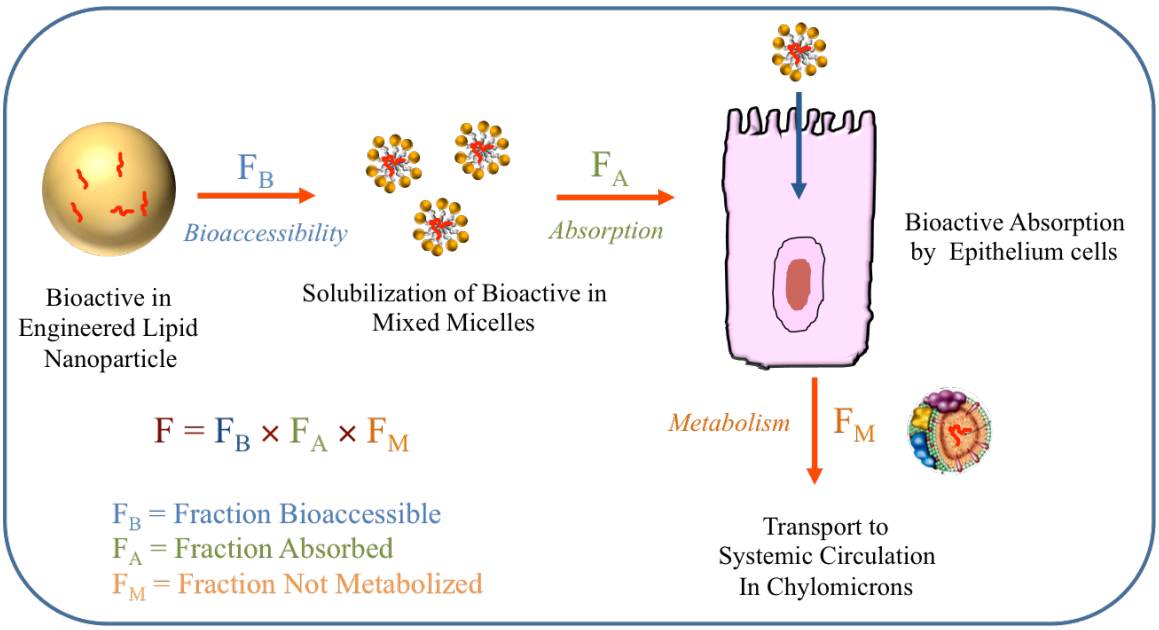

Figure 2-2 The overall oral bioavailability of a bioactive component in an engineered lipid nanoparticle depends on a number of processes that occur within the gastrointestinal tract, such as solubilization, absorption, and metabolism.

Metabolism (F_M): A bioactive component may undergo various types of biochemical or chemical transformation (metabolism) after it is ingested, which may alter its subsequent bioaccessibility, absorption, and bioactivity. These transformations may occur due to chemical reactions (e.g., hydrolysis by acid) or enzyme activities (e.g., lipolysis by lipases) in various regions of the GIT and other tissues (such as the mouth, stomach, small intestine, colon, enterocyte cells, lymphatic system, blood, liver, etc.).

Bioaccessibility (F_B): A highly lipophilic bioactive component needs to be released from the food matrix and solubilized within mixed micelles present in the small intestine before it can be absorbed. These mixed micelles consist of bile salts and phospholipids secreted by the body, as well as any lipid digestion products (i.e., monoacylglycerols (MAGs) & free fatty acids(FFAs)).

Absorption (F_A): The mixed micelles transport the solubilized lipophilic components across the intestinal lumen, through the mucous layer, and to the surface of the intestinal epithelium cells [38, 39]. The lipophilic components are then incorporated into the epithelium cells through various passive and/or active transport mechanisms [40].

The overall bioavailability of ingested lipophilic components can therefore be controlled by designing ELNs and food matrices that increase the fraction that is non-metabolized (F_M), bioaccessible (F_B), and absorbed (F_A). In principle, this goal can be achieved by manipulating the composition and structure of the engineered lipid nanoparticles. However, improved knowledge of the influence of specific

nanoparticle properties on the bioavailability of specific bioactive components is still needed.

2.2 Assembly of lipid nanoparticles outside the body: engineered lipid nanoparticles

ELNs with different compositions, structures, and physicochemical properties may be present within the colloidal-delivery systems designed to encapsulate lipophilic bioactives [18, 23, 28, 31, 41] (Figure 2-1). These ELNs can be fabricated from food-grade ingredients, such as those shown in Table 2-2. A brief overview of the most important types of ELNs found in food-based colloidal delivery systems is given below.

Table 2-1 Examples of structural components used to fabricate edible lipid nanoparticles suitable for delivering lipophilic bioactive components

Structural component	Examples of ingredients used
Lipophilic substances	Triacylglycerol oils (e.g., canola, corn, fish, medium-chain triglycerides, palm, peanut, soybean, sunflower oils), essential oils (e.g., carvacrol, lemon grass, oregano, thyme, thymol oils), flavor oils (e.g., lemon, lime, orange, peppermint oils), indigestible oils (e.g., waxes, hydrocarbon, paraffin, mineral oils)
Surface-active substances	Small-molecule surfactants (e.g., monoglycerides, diglycerides, Tweens, Spans, sugar esters), phospholipids (e.g., lecithin and lysolecithin), proteins (e.g., casein, gelatin, soy, and whey), polysaccharides (e.g., gum arabic and modified starch), solid particles (e.g., silica or titanium)

2.2.1 Fabrication of engineered lipid nanoparticles

Micelles. The lipid nanoparticles in micelle solutions are thermodynamically stable structures that are normally formed from amphiphilic molecules

("surfactants") that have a polar head group and a non-polar tail group [42, 43]. These surfactant molecules spontaneously self-assemble into micelles when they are dispersed in water above a certain concentration - the "critical micelle concentration" or CMC [44]. Surfactant molecules exist as monomers in aqueous solutions below the CMC, but they associate with each other and form micelles once this concentration is exceeded. The main driving force for micelle formation is the hydrophobic effect, i.e., the tendency for the system to minimize the thermodynamically unfavorable contact between non-polar groups and water [45]. The types of surfactant that form micelles in aqueous solutions tend to have a high hydrophilic-to-lipophilic balance (HLB) number [44, 45]. The non-polar tails of the surfactant molecules form the hydrophobic core of the micelle, whereas the polar head-groups form the hydrophilic shell that faces towards the water (Figure 2-1). Combinations of surfactants with different molecular characteristics (rather than a single surfactant) are often used to improve the formation, stability, or performance of micelle solutions. Lipophilic bioactive components can be incorporated into the hydrophobic interiors of micelles, and then the whole system if often referred to as a "swollen micelle" [46, 47]. Typically, swollen micelles have diameters within the range of 5 to 20 nm depending on their composition and the prevailing environmental conditions (such as temperature, pH, and salt concentration).

Micelle solutions containing lipophilic bioactive components are relatively straightforward to fabricate. Typically, the surfactant and bioactive component are mixed together and then added to an aqueous solution, which should lead to the spontaneous formation of swollen micelles. Alternatively, the surfactant and water

are mixed together first to form a micelle solution, and then the lipophilic bioactive component is added. Often it is necessary to heat and/or mechanically agitate the final solutions to ensure that all of the components are successfully incorporated into the micelles.

Microemulsions. In general, the term "microemulsion" refers to thermodynamically stable structures that contain surfactant, oil, and water molecules (such as oil-in-water, water-in-oil, and bicontinuous microemulsions) [45]. Oil-in-water (O/W) microemulsions are the most commonly used type for the delivery of lipophilic bioactive agents [45, 48-50]. These systems have very similar compositions, structures, and properties as swollen micelles and sometimes the terms "swollen micelles" and "microemulsions" are used interchangeably to refer to these systems. The two systems may be considered identical when the lipophilic bioactive component acts as the only oil phase. However, the oil phase in microemulsions may also consist of a mixture of a bioactive component and appropriate carrier oil. O/W microemulsions spontaneously form when certain combinations of surfactant, oil phase, and water are mixed together [45]. Sometimes, additional ingredients are also needed to facilitate their formation and stability, such as cosurfactants and cosolvents [45, 51, 52]. Like swollen micelles, microemulsions consist of a hydrophobic core comprised of oil molecules and non-polar surfactant tails, and a hydrophilic shell comprised of polar surfactant head-groups (Figure 2-1). Lipophilic bioactive components tend to be predominately present within the hydrophobic core of microemulsions, although any polar groups may protrude into the hydrophilic shell and water phase. Typically, microemulsions

have diameters in the range of 10 to 100 nm depending on their composition and environmental conditions. Microemulsions can be formed in a similar manner to swollen micelle solutions. Typically, the surfactant, bioactive, and any carrier oil components are mixed together and then added to the aqueous phase. The resulting solution may then need to be heated and/or mixed to ensure good dispersion of the different components [53]. Microemulsions are thermodynamically stable systems and should therefore form spontaneously, and remain stable provided the environmental conditions are not altered too much. Phase diagrams are often developed to determine the range of compositions and temperatures where a microemulsion will remain thermodynamically stable [48, 51].

Liposomes. Liposomes consist of one or more shells, with each shell consisting of two layers of surfactant molecules (a "bilayer") with their non-polar tail groups facing toward each other (Figure 2-1) [54]. A unilamellar liposome has a balloon-like structure consisting of a single bilayer shell, whereas a multilamellar liposome has an onion-like structure consisting of multiple concentric bilayer shells [55-57]. The building blocks of liposomes are surface active substances with intermediate HLB numbers and optimum curvatures close to zero, e.g., phospholipids [45]. This kind of surface-active substance tends to spontaneously form bilayer structures when dispersed in aqueous solutions. Liposomes typically have diameters in the range from about 25 to >1000 nm.

There are a number of different approaches to forming liposomes, including various solvent evaporation, surfactant depletion, and extrusion methods [55]. For example, in the solvent evaporation method, the phospholipids (and bioactive

component) are first dissolved in an organic solvent that is then placed within an appropriate container. The organic solvent is then removed by evaporation, which leaves a thin film of phospholipids and bioactive components on the surface of the container. An aqueous solution is then added to the container, which leads to the spontaneous formation of liposomes due to "peeling off" of the surfactant bilayers from the containing surface after hydration. In the extrusion method, the phospholipids, bioactive, and aqueous solution are mixed together in a container, and then the resulting mixture is passed through a homogenizer (such as a high pressure valve homogenizer or microfluidizer). It may be necessary to optimize preparation conditions to produce stable liposomes with relatively small dimensions, such as temperature, pH, ionic strength, and homogenizer operation conditions.

Nanoemulsions. The lipid nanoparticles in nanoemulsions have somewhat similar structures to those found in microemulsions [58, 59], consisting of a hydrophobic core comprised of oil molecules, and a hydrophilic shell comprised of surface active molecules (Figure 2-1). However, nanoemulsions are thermodynamically unstable colloidal dispersions, and will therefore tend to breakdown over time through a variety of different destabilization mechanisms, such as flocculation, coalescence, gravitational separation, and Ostwald ripening [60]. The long-term stability of nanoemulsions can be improved by incorporating stabilizers such as emulsifiers, weighting agents, ripening inhibitors, and texture modifiers [58, 59]. Emulsifiers are surface-active substances that adsorb to the droplet surfaces and form a protective coating that prevents their aggregation.

Weighting agents are dense hydrophobic substances that are incorporated into the oil phase to increase its density so that it is closer to that of the aqueous phase. Ripening inhibitors are hydrophobic substances with a very low water-solubility that are mixed with the oil phase to prevent Ostwald ripening through an entropy of mixing effect. Texture modifiers, such as thickening and gelling agents, are added to the aqueous phase to increase the viscosity or form a gel that can inhibit the movement of droplets.

Nanoemulsions may be formed using a variety of different methods that can be classified as either high-energy or low-energy methods [58, 59]. High-energy methods use mechanical devices ("homogenizers") capable of generating intense disruptive forces to breakup and mingle the oil and aqueous phases leading to the formation of ultrafine oil droplets in water. The most commonly used high-energy devices for preparing food nanoemulsions are high-pressure valve homogenizers, microfluidizers, and sonicators [58, 61, 62]. Low-energy methods rely on the spontaneous formation of ultrafine oil droplets in water when certain types of surfactant, oil, and water are mixed together under controlled conditions [63]. The most commonly used low-energy approaches are the phase inversion temperature (PIT), spontaneous emulsification (SE) and emulsion inversion point (EIP) methods. The food-grade emulsifiers that can be used to form nanoemulsions include small molecule surfactants, phospholipids, proteins and polysaccharides, whereas those that can used to form micelles, microemulsions or liposomes are usually only certain types of small molecule surfactants and/or phospholipids. The lipid nanoparticles in food-grade nanoemulsions typically have diameters in the range of 20 to 200 nm

[58, 61, 62], however, larger lipid particles may be present if conventional emulsions or used rather than nanoemulsions [64].

Solid Lipid Nanoparticles and Nanostructured Lipid Carriers. Solid lipid nanoparticles (SLN) and nanostructured lipid carriers (NLCs) are similar in structure to nanoemulsions (Figure 2-1), but the lipid core is either fully or partially crystalline [12, 65, 66]. SLNs and NLCs are typically formed from high melting point lipids using by a two-step process. First, a nanoemulsion is prepared at a temperature above the melting point of the lipid phase to ensure that it remains liquid throughout the homogenization process. Second, this nanoemulsion is cooled in a controlled fashion to a temperature below the melting point to promote crystallization of the lipid phase. SLNs and NLCs can also be formed using low-energy methods by spontaneously forming a nanoemulsion at high temperatures, and then cooling it to induce lipid crystallization. The morphology of the lipid nanoparticles in SLNs and NLCs may change appreciably after the liquid-to-solid transition of the lipid phase has occurred due to the physical constraints associated with packing lipid molecules within crystals [65, 67]. As do nanoemulsions, the particles in SLN and NLC suspensions typically have diameters in the 20 to 200 nm range, although larger particles may be present if conventional emulsions are used as templates rather than nanoemulsions. For convenience, the term SLN is used below to refer to both fully and partly crystalline ELNs.

2.2.2 Design of engineered lipid nanoparticle properties

The ELNs found in foods and beverages vary considerably in their compositions and structures depending on the type of ingredients and fabrication methods used in their production. The functional performance of colloidal delivery systems (such as stability, opacity, rheology and biological fate) is ultimately determined by their particle characteristics [68]. Consequently, colloidal delivery systems with different functional performances can be designed by carefully controlling the characteristics of the ELNs they contain, such as composition, structure, dimensions, interfacial properties, charge, and physical state. Methods of controlling the properties of various kinds of ELNs have been described elsewhere[1, 22, 49, 58, 69, 70].

2.3 Disassembly of ELNs within the gastrointestinal tract

After ingestion, ELNs may undergo numerous different disassembly processes during their passage through the various regions of the GIT; however, eventually they are usually reassembled into mixed micelles within the small intestine prior to absorption. The fraction of a lipophilic bioactive component incorporated into these mixed micelles is usually taken as a measure of its bioaccessibility (F_B).

2.3.1 Characteristics of the major regions of the gastrointestinal tract

The initial structure and dimensions of an ingested ELN depend on the type of ingredients and processing operations used to assemble it (Figure 2-1). ELNs

may be distributed in different matrices within different products: freely suspended in an aqueous solution (as in beverages and soft drinks); trapped within a biopolymer matrix (as in some deserts, sauces, and yogurts); trapped within a solid matrix (as in some dried spices, breads, and other cereal products). The initial environment of an engineered lipid nanoparticle may have a major effect on its subsequent biological fate after ingestion. For example, the food matrix may have to be disrupted or dissolved before the ELNs are released, which may determine the time and location that they interact with the gastrointestinal fluids [23, 71, 72]. After ingestion, ELNs experience a complex set of environmental conditions as they pass through the various regions of the GIT (Figure 2-3), which alters their composition and structure. The physiochemical and physiological characteristics of these different regions have been reviewed recently[24, 73, 74]; as such, we provide only a brief of overview here.

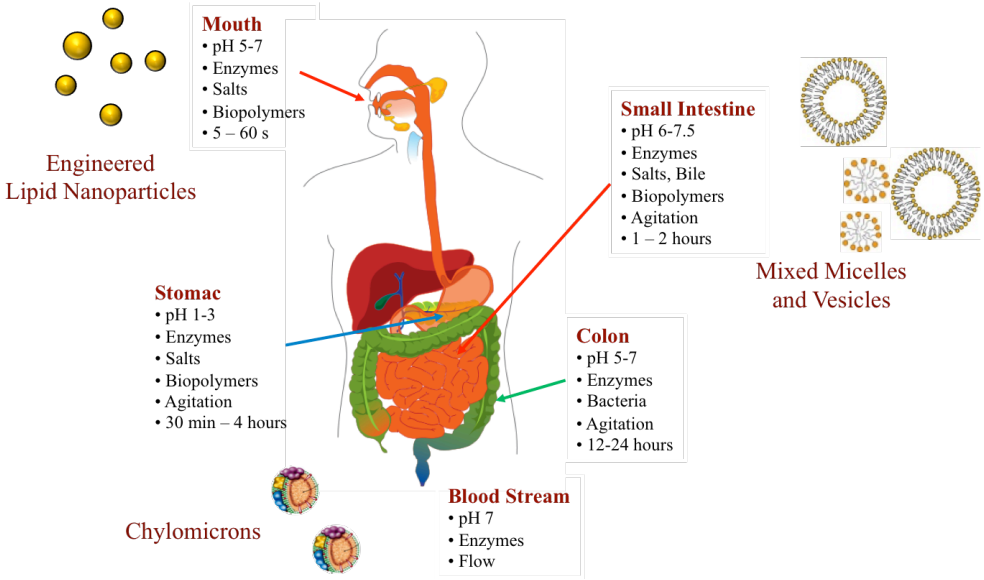

Figure 2-3 Schematic diagram of the physicochemical and physiological conditions in different regions of the human gastrointestinal tract and the different kinds of lipid nanoparticles.

Mouth. After entering the oral cavity, foods containing ELNs may undergo a variety of changes: mixture with saliva; dissolution, dispersion, and/or dilution; alterations in pH, ionic strength and/or temperature; exposure to digestive enzymes; interactions with oral surfaces; and exposure to complex fluid flow/stress patterns

Stomach. After being processed within the oral cavity, the ELNs are swallowed, pass through the esophagus, and enter the stomach. They are then exposed to relatively extreme conditions that may further alter their properties: low pH (1 to 3), high ionic strength (e.g., calcium and sodium salts), enzyme activity (e.g., proteases, amylases, and lipases), surface-active substances (e.g., phospholipids and proteins), and complex fluid flow/stress patterns.

Small Intestine. After leaving the stomach, the resulting material (chime) passes through a small valve (pylorus sphincter) and enters the small intestine, where it is further processed for absorption[75]. Any ELNs remaining in the chyme are mixed with small intestinal fluids that contain bile salts, phospholipids, lipases, proteases, bicarbonate, and other minerals. The presence of the bicarbonate causes the pH to rise to approximately neutral, which facilitates the action of the pancreatic enzymes, such as lipases, proteases, and amylases. These enzymes will break down any digestible components present, such as lipids, proteins, and starches. The hydrolysis of triacylglycerols (TAGs) leads to the formation of mixed micelles that can transport digested lipids and lipophilic bioactive components to the epithelial cells.

Colon: If all the components used to fabricate an ELN were fully digestible, then one would expect it to be digested and absorbed largely within the stomach and small intestine. However, if an ELN is fabricated from indigestible components (such as indigestible oils or fibers), then it may pass through these regions and enter the colon. The colon contains a variety of different microorganisms capable of metabolizing and utilizing dietary components, such as fats, proteins, carbohydrates, and dietary fiber[76].

2.3.2 Changes in particle properties in the gastrointestinal tract

After ingestion, the ELNs originally present within a food or beverage product usually change considerably as they pass through the different regions of the GIT as a result of their exposure to this complex physiological and physicochemical environment [71, 77-80]. There may be changes in the composition, structure, dimensions, charge, interfacial properties, and physical state of the lipid nanoparticles, all of which could greatly alter their biological fate [81]. Figure 2-4 shows an example of changes in the size and charge of ELNs initially stabilized by different kinds of lipid nanoparticles respond to changes in GIT conditions. A colloidal delivery system can then be designed to alter the biological fate of an encapsulated bioactive component in a desired manner, e.g., to increase its bioaccessibility, reduce its metabolism, or release it within a particular location of the GIT. This section gives a brief overview of the major physicochemical mechanisms responsible for the disassembly of ELNs in the GIT.

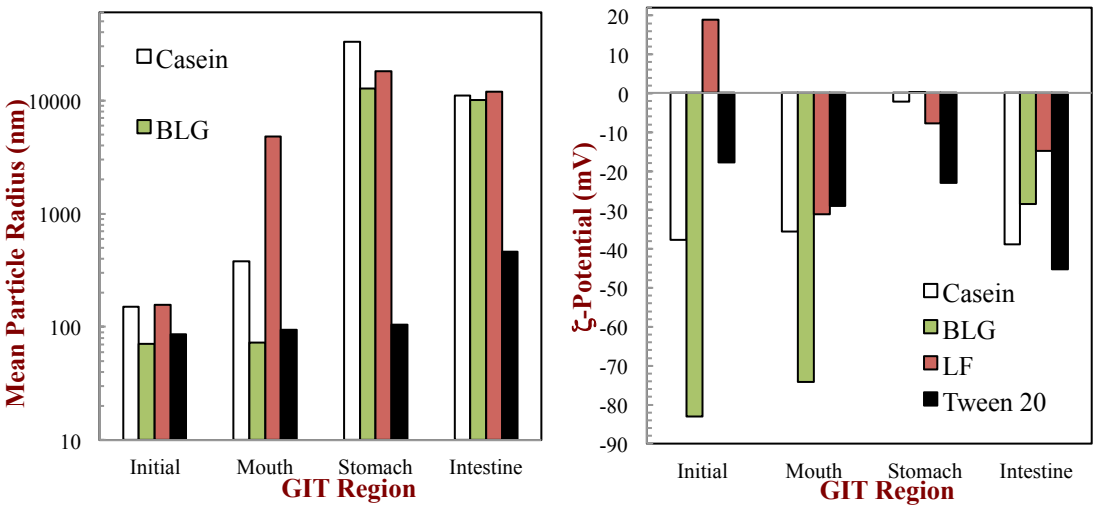

Figure 2-4 (a) Changes in the mean particle radius of colloidal dispersions initially containing lipid nanoparticles as they pass through different stages of the gastrointestinal tract (GIT): β-lactoglobulin (BLG), casein, Tween 20, lactoferrin (LF). (b) Changes in the particle charge (ζ-potential) of colloidal dispersions initially containing lipid nanoparticles as they pass through different stages of the GIT: β-lactoglobulin (BLG), casein, Tween 20, lactoferrin (LF).

Particle Structure. The structure of ELNs may change appreciably as they pass through the different regions of the GIT due to alterations in their environment, such as dilution, pH, ionic strength, temperature, surface active substances, polymers, biological surfaces, and enzymes. The ELNs originally present in a food or beverage may have a variety of different initial structures depending on the ingredients and method used to prepare them: swollen micelles; microemulsions; Nanoemulsions, SLNs, liposomes (Figure 2-1). The manner by which these structures are altered in the GIT depends on the initial organization of the components within the lipid particles. For example, micelles, microemulsions or liposomes may easily dissociate in the mouth or stomach after ingestion due to dilution or interaction with specific substances in the GIT (such as phospholipids,

bile salts, or minerals) [82]. However, indigestible nanoemulsions or SLNs may pass through the GIT with their hydrophobic cores largely intact (although their surface characteristics may change appreciably).

Particle Composition. The composition of engineered lipid particles may also change appreciably as they pass through the GIT, e.g., due to exchange of molecules with the surrounding media, or due to chemical or enzymatic degradation reactions. For example, triacylglycerol molecules within the hydrophobic core of a nanoemulsion droplet or SLN may be converted to FFAs, MAGs, and DAGs by gastric and pancreatic lipases in the stomach and small intestine, and then leave the droplet. Surface active substances in the shell of ELNs (such as proteins, phospholipids, or surfactants) may be hydrolyzed by digestive enzymes or they may be displaced by endogenous surface active molecules in the surrounding digestive fluids.

Particle Dimensions: A variety of different physiochemical mechanisms can change the dimensions of the particles [74, 83-87]: (i) flocculation – two or more particles associate with each other but keep their individual integrities; (ii) coalescence – two or more particles merge with each other and form a larger particle; (iii) partial coalescence – two or more partly crystalline particles fuse together to form a clump; (iv) Ostwald ripening – large particles grow and small ones shrink due to molecular diffusion of oil molecules through the aqueous phase; (v) digestion – particles shrink due to enzymatic degradation of their components and the subsequent release of digestion products (such as FFA, MAGs, or amino acids); (vi) solubilization –particles shrink due to transfer of some of the lipophilic

bioactive components or lipid molecules into the surrounding aqueous phase (Figure 2-5).

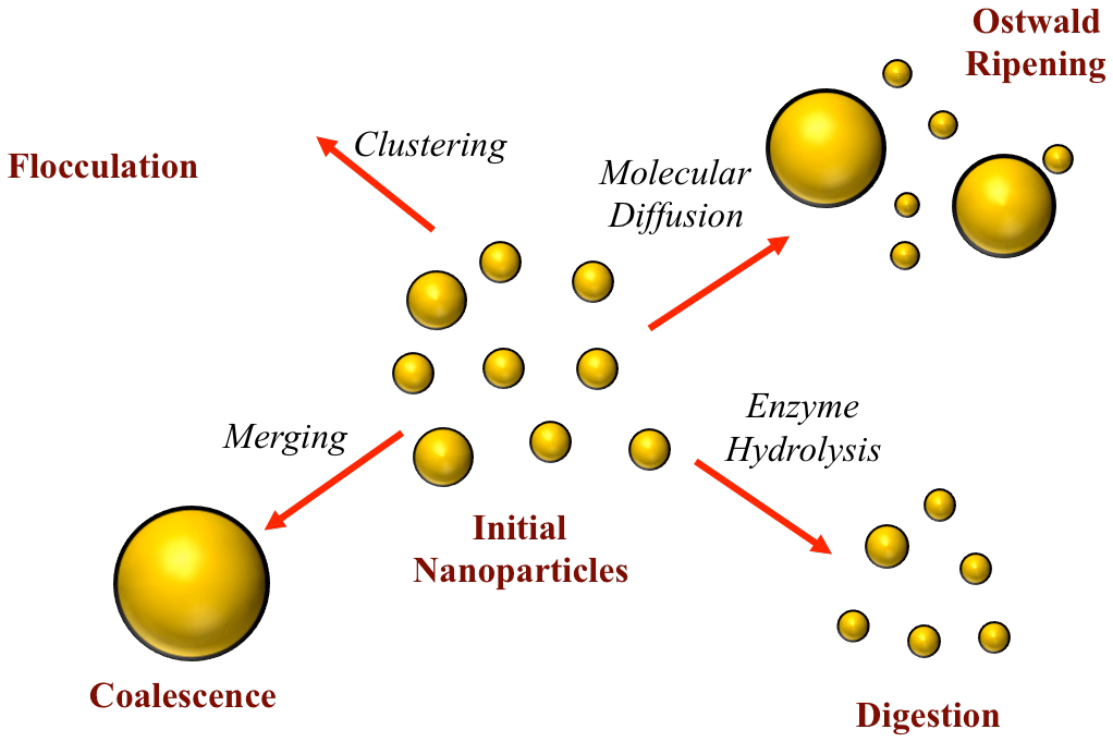

Figure 2-5 The dimensions and structure of lipid nanoparticles may change considerably as they pass through the gastrointestinal tract due to several different physicochemical processes.

Interfacial properties. The interfacial characteristics of ELNs may also be altered appreciably as they pass through the GIT due to the following: (i) competitive adsorption – surface active components within the gastrointestinal fluids may adsorb to the nanoparticle surfaces and displace some of the original surface active substances coating them; (ii) co-adsorption – surface active components within the intestinal fluids may adsorb to the nanoparticle surfaces and penetrate between the original surface active substances coating them; (iii) multilayer formation – certain substances within the gastrointestinal fluids may

adsorb on top of the original interfacial coating (e.g., charged polymers onto oppositely charged particles); (iv) digestion or degradation – some of the original surface active substances at the particle surfaces may be fully or partially digested or degraded due to the highly acidic conditions in the stomach or due to the presence of specific enzymes [88]. Numerous studies have reported that the interfacial characteristics of lipid nanoparticles can be appreciably altered as they pass through the different regions of the GIT [85, 89-94].

Physical state. The physical state of one or more of the components used to assemble an engineered lipid nanoparticle may change as it passes through the GIT. For example, the hydrophobic core of ELNs may be solid within a freezer or refrigerator during storage, but it may melt when it is exposed to elevated body temperatures. Conversely, the hydrophobic core of ELNs may be liquid within a hot food, but it may crystallize when it is exposed to cooler body temperatures. Crystalline lipophilic bioactive components that are fully dissolved within the TAG core of an engineered lipid nanoparticle, may precipitate when the TAG is digested and the bioactive component is released into the gastrointestinal juices [95]. Conversely, a lipophilic bioactive component that is initially crystalline within an ingested food product dissolve when it is exposed to gastrointestinal juices. All of these changes in physical state of an ingested component may alter their biological fate. Various studies have demonstrated the potential importance of the physical state of the lipid phase on the behavior of ELNs under simulated GIT conditions [80, 90, 96, 97].

2.3.3 Controlled disassembly of engineered of lipid nanoparticles

The disassembly of ELNs due to these different breakdown mechanisms can be controlled by altering their initial composition and structure. For example, nature of the hydrophobic core has a strong influence on partial coalescence, Ostwald ripening, digestion, and solubilization processes, whereas the nature of the hydrophilic shell has a strong impact on droplet digestion, flocculation, and coalescence. As mentioned earlier, fabricating the hydrophobic core from a digestible lipid may cause the lipid nanoparticles to be completely dissembled in the small intestine, whereas fabricating them from an indigestible liquid may leave them partly intact.

2.4 Assembly of lipid nanoparticles within the GIT: mixed micelles

One of the key events determining the bioavailability of lipophilic bioactive components within the GIT is the formation of colloidal structures called mixed micelles [25, 98]. Mixed micelles solubilize lipophilic bioactive components and transport them to the epithelium cells where they can be absorbed [3, 99]. In the absence of digestible lipids, simple mixed micelles are formed by the endogenous bile salts and phospholipids in the intestinal secretions [100]. In the presence of digestible lipids, complex mixed micelles are formed from lipid digestion products (MAGs and FFAs), bile salts, and phospholipids [24, 101, 102]. The term “mixed micelles” actually refers to a complex mixture of colloidal structures whose properties may change throughout digestion, such as micelles, vesicles, and liquid crystals [103]. Many of these structures have dimensions within the nanometer

range and can therefore be considered to be biological lipid nanoparticles. For example, micelles typically have diameters in the 3 – 20 nm range, whereas vesicles have diameters from 20 nm to > 1000 nm [103].

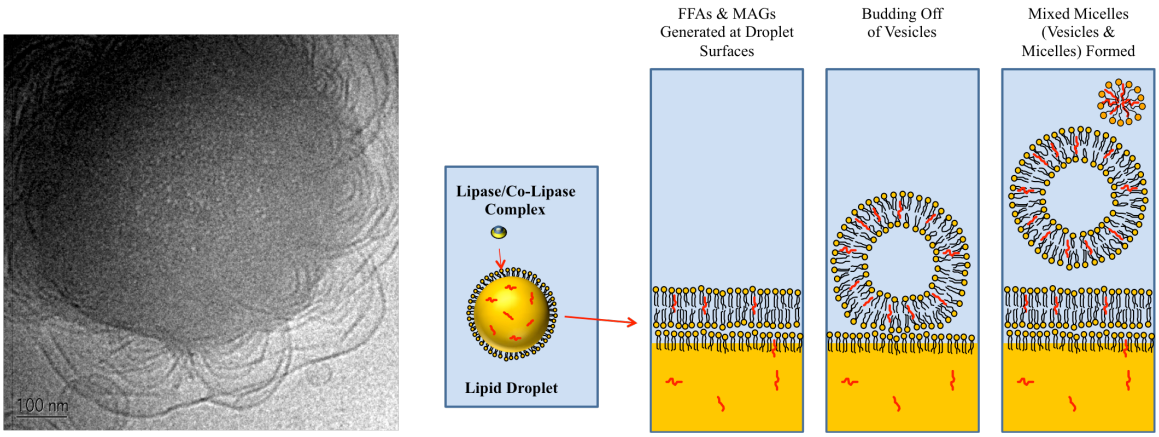

Figure 2-6 (*a*) Cryo-TEM image of an aspirate collected from human small-intestinal fluids after ingestion of a fatty meal. The image shows lipid bilayers forming at the surface of a fat droplet during digestion, which are believed to mix with bile salts and phospholipids to form mixed micelles. The images were kindly supplied by Professor Dimitris Fatouros from his article "Insights into Intermediate Phases of Human Intestinal Fluids Visualized by Atomic Force Microscopy and Cryo-Transmission Electron Microscopy ex Vivo" (Mu¨ llertz et al. 2012), with permission. (*b*) Highly schematic proposed mechanism for the formation of mixed micelles during lipid digestion. Surface-active substances may consist of a mixture of phospholipids, bile salts, FFAs, and MAGs and not just a single substance (as shown here). The structures formed may interact with other molecules to form mixed micelles. Abbreviations: FFA, free fatty acid; MAG, monoacylglycerol; TEM, transmission electron microscopy.

An electron microscopy study of the colloidal structures formed in the small intestine after lipid digestion (Figure 2-6a) suggests an interesting mechanism for the formation of mixed micelles [103]. The FFAs and MAGs generated at the surface of the lipid droplets during lipase digestion of TAGs form liquid crystalline bilayers, that bud off and form vesicles or micelles that move into the aqueous phase (Figure 2-6b). Presumably, lipophilic bioactive components are trapped within the bilayers that bud off and therefore end up within the mixed micelles phase. In practice, the

precise nature of the colloidal structures formed is likely to depend on the nature of the delivery system and food matrix ingested, as well as the physiological conditions within the person. After they are formed, the mixed micelles transport FFAs, MAGs, and bioactive lipophilic compounds from the lumen of the small intestine, across the mucus layer, and to the surface of the enterocyte cells (Figure 2-7). . Once they reach the apical side of the epithelium cells the FFAs, MAGs, and lipophilic bioactive components may be absorbed through various passive or active transport mechanisms [104].

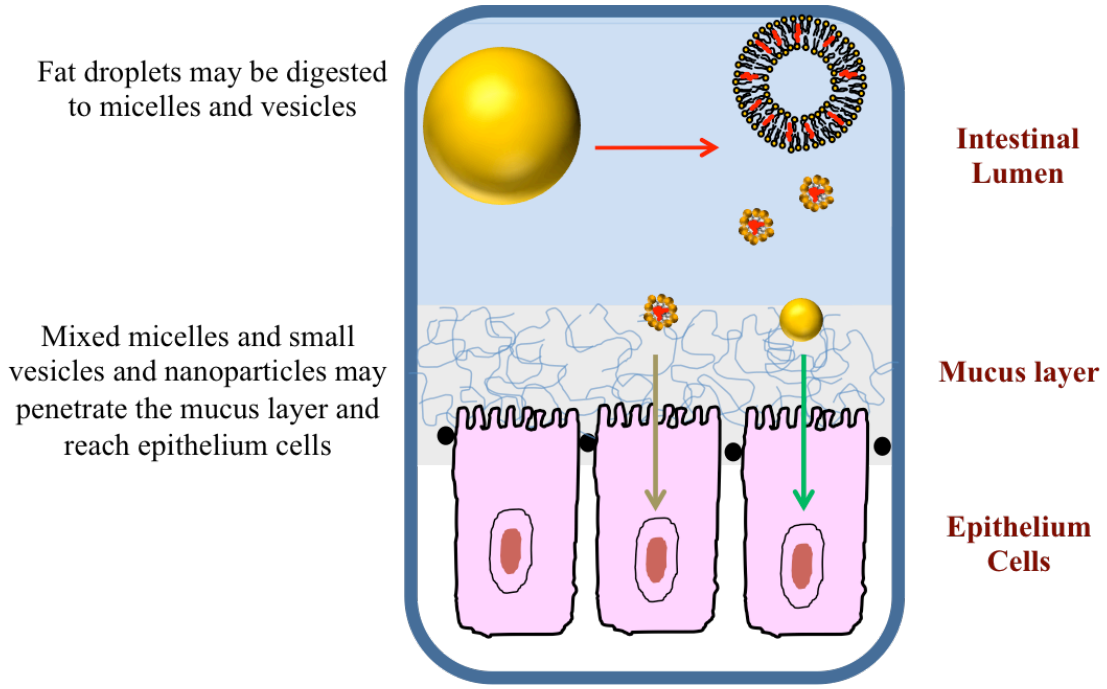

Figure 2-7 Lipid nanoparticles may penetrate into the mucus layer and become trapped (mucoadhesion) or transported across it. Nanoparticles that are not digested and that travel through the mucus layer may be directly adsorbed by the epithelial cells.

In the absence of lipid digestion products, the bile salts and phospholipids present within the intestinal fluids form simple mixed micelles [98]. Bile salts are

anionic surface-active substances that have fairly rigid plate-like structures, with one side being hydrophilic and the other side being hydrophobic [98]. Phospholipids are ionic surface active substances that have a polar head-group and two non-polar hydrocarbon tails. The structure of these two biological surface active substances is therefore quite different from that of most conventional food-grade surfactants that have a hydrophilic head group and a single hydrophobic tail. The main driving force for the formation of simple mixed micelles is the hydrophobic effect, but other interactions may also be important, such as hydrogen bonding [98]. It is proposed that simple mixed micelles have a disk-like shape with hydrodynamic diameters ranging from around 3.6 to 60 nm depending on their composition [105]. At relatively low lecithin-to-bile salt ratios relatively small micelles are formed (≈ 3.6 to 7 nm), but at high ratios relatively large micelles are formed (≈ 4.0 to 60 nm). Simple mixed micelles would tend to be present in the GIT under conditions where lipophilic bioactive components are ingested in the absence of fat or in the presence of indigestible fats. Simple mixed micelles can solubilize certain types of lipophilic bioactive components in foods, but they tend to be much less efficient than complex mixed micelles [106-108].

In the presence of lipid digestion products, the bile salts and phospholipids in the intestinal fluids interact with the FFAs and MAGs to form complex mixed micelles, which may adopt a variety of different structural organizations depending on the composition of the system, such as micelles and vesicles [103]. Micelles found in human intestinal fluids after ingestion of emulsified digestible fats have been reported to be relatively small (d ≈ 20 nm), whereas vesicles were reported to

be larger (d ≈ 20 to 150 nm). The main driving force for the formation of these structures is the hydrophobic effect, i.e., the tendency to reduce the contact area between non-polar groups and water [45].

In this section, we focus on the major factors that influence the composition, structure, and properties of this type of biological lipid nanoparticle, with an emphasis on how these factors can be controlled to improve the oral bioavailability of ingested lipophilic bioactive components.

2.4.1 Influence of molecular characteristics of ingested lipids on mixed micelle properties

A major way that the properties of mixed micelles can be manipulated is through altering the composition of the lipid phase that is ingested. Indeed, the solubilization capacity of mixed micelles is highly dependent on the type and amount of digestible lipids consumed with lipophilic bioactive components [109]. The simple mixed micelles formed in the absence of digestible lipids have relatively low solubilization capacities, whereas the complex mixed micelles formed in their presence have much higher solubilization capacities [99]. The structure, dimensions, and solubilization capacities of complex mixed micelles depend on the total amount of lipids consumed, as well as on the molecular characteristics of the fatty acid chains, such as chain length and degree of unsaturation [99].

The bioaccessibility of carotenoids has been reported to be higher for lipids containing long chain fatty acids (LCFA) than those containing medium chain fatty acids (MCFA), presumably because of differences in the solubilization capacity of the

mixed micelles formed [2]. The large hydrophobic carotenoid molecules may be able to fit into the large hydrophobic cores of mixed micelles formed by LCFA, but not the smaller hydrophobic cores formed by MCFA (Figure 2-8). However, for other types of lipophilic bioactive molecule (i.e., curcumin) the solubilization capacities of mixed micelles formed from MCFA and LCFA were found to be fairly similar [110], which may be because the bioactive molecules were small enough to be accommodated within both types of micelle.

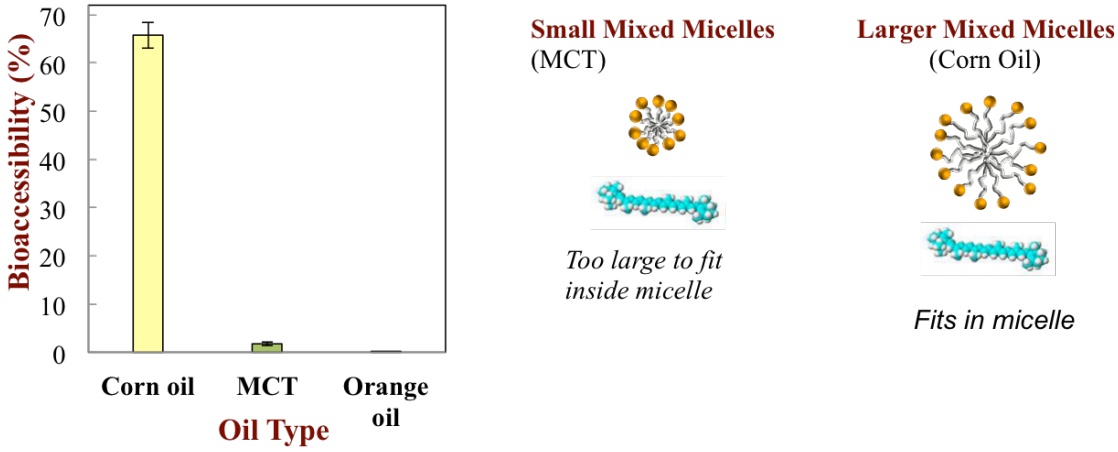

Figure 2-8 The bioaccessibility of a lipophilic compound is often influenced by the nature of the carrier oil. In this study, we examined the bioaccessibility of β-carotene encapsulated within nanoemulsions made from long-chain triglycerides (corn oil), medium-chain triglycerides (MCT), or an indigestible oil (orange oil). Data from Qian et al. (2012).

2.4.2 Influence of structural properties of engineered lipid nanoparticles on mixed micelle properties

Recent in vitro studies in our laboratory using corn O/W emulsions showed that the bioaccessibility of β-carotene increased with decreasing particle size, which was attributed to the faster and more extensive digestion of the triglycerides in the smaller droplets due to their greater surface areas(Figure 2-9). Another recent

study using soybean O/W emulsions also reported that the bioaccessibility of β-carotene increased with decreasing droplet size after in vitro digestion [111].

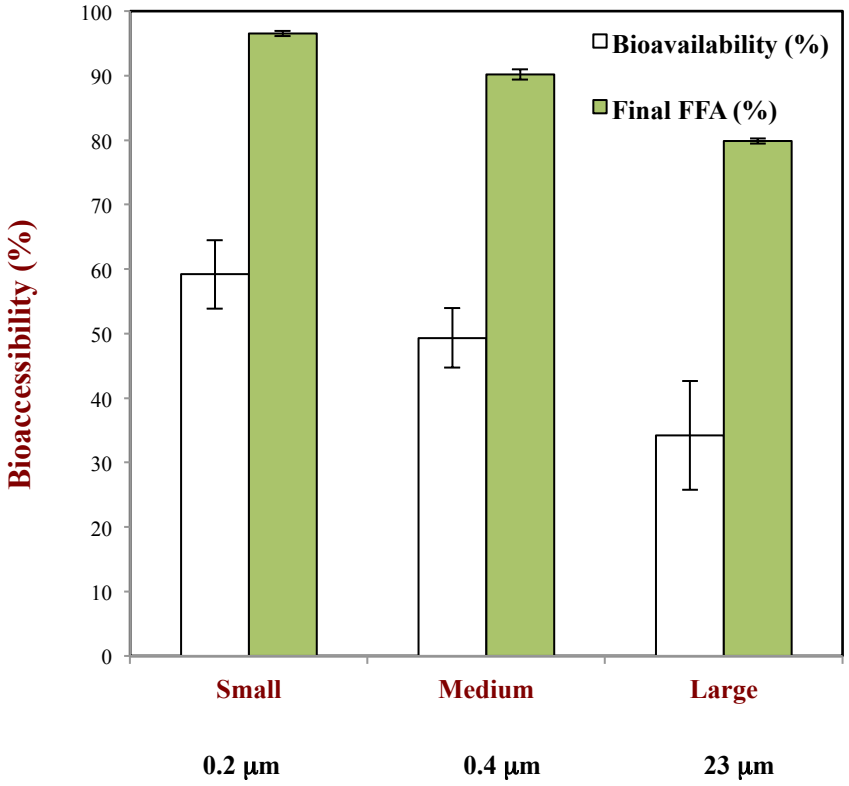

Figure 2-9 . Influence of the diameter of initial engineered lipid nanoparticles in corn oil-in-water nanoemulsions on the extent of fatty acid release and bioaccessibility of b-carotene after 2 hours digestion by lipase under simulated small intestine conditions. The initial mean droplet diameters were: large ($d_{43} \approx 23$ mm); medium ($d_{43} \approx 0.4$ mm); and small ($d_{43} \approx 0.2$ mm). From Silvia-Trujillo et al (2013).

Numerous researchers have also found that the rate and amount of fatty acid production during lipid digestion (and therefore the rate and extent of mixed micelle formation) increases as the droplet size decreases, which was attributed to an increase in the surface area of lipids exposed to the digestive enzymes [80, 112-114]. Nevertheless, other factors may also contribute to the influence of initial particle size on digestion, such as the concentration of free surfactant remaining in

the aqueous phase (since this can inhibit lipase absorption) [115] and alterations in interfacial structure (since this can affect the ability of lipase to reach the lipid phase) [116]. The kinetics of fatty acid production and mixed micelle formation has also been shown to depend on the physical state of the lipid phase in engineered lipid nanoparticles [97].

2.4.3 Influence of molecular characteristics of bioactives on mixed micelle properties

The ability of mixed micelles to incorporate lipophilic bioactive components is characterized by their solubilization capacity, which can be expressed as the bioactive component solubilized per unit mass of mixed micelles. The solubilization capacity of mixed micelles depends on the type and amount of digestible lipids consumed, as well as the molecular characteristics of the bioactive component. The colloidal structures present within mixed micelles have regions capable of solubilizing lipophilic bioactive molecules, e.g., the hydrophobic cores of micelles or bilayers of vesicles. If the bioactive molecules have dimensions smaller than these regions, then they are easily incorporated into the mixed micelle structure (Figure 2-8). However, if they have dimensions considerably larger than these regions, then they will not be solubilized easily and will have low Bioaccessibility. Recent studies have shown that curcumin can be incorporated easily into mixed micelles formed from MCFAs and LCFAs, which was attributed to its relatively small molecular dimensions[110]. However, β-carotene (which has considerably larger molecular dimensions than curcumin) can only be incorporated into mixed micelles formed from LCFAs (Figure 2-8)[2] .

Other recent studies have also reported that the transfer of lipophilic bioactive components from oil droplets to mixed micelles depends on the bioactives molecular characteristics [117]. In the absence of lipolysis (no lipase), the fraction of bioactives transferred into simple mixed micelles were relatively low: ≈ 2% for □-carotene; ≈ 1.5% for Coenzyme Q; ≈ 24% for vitamin D and ≈ 31% for phytosterols. On the other hand, in the presence of lipolysis (with lipase), the fraction of bioactive components transferred into complex mixed micelles were much higher: ≈ 80% for □-carotene; ≈ 90% for Coenzyme Q; ≈ 87% for vitamin D and ≈ 93% for phytosterols. An in vitro study also showed that the bioaccessibility of carotenoids dispersed in bulk oils after digestion by lipase was highly dependent on their molecular structure [118]: ≈ 89% for lutein; ≈ 49% for □-carotene; ≈ 37% for astaxanthin; and, ≈ 3% for lycopene.

2.4.4 Controlled assembly of mixed micelles

These studies clearly highlight the importance of the molecular structure of the bioactive components and of the mixed micelles in determining bioaccessibility. This knowledge can be used to tailor the design of ELNs so that they have specific characteristics (compositions, structures, and dimensions) that will form mixed micelles that will increase the bioavailability of specific lipophilic bioactive components.

2.5 Disassembly of mixed micelles within the GIT and absorption of bioactives

After they have been formed within the GIT there are a number of ways that mixed micelles may be broken down or their properties altered. In this section, we give a brief outline of some of the most important physicochemical or physiological mechanisms responsible for disassembly of mixed micelles within the GIT, and their ability to transport encapsulated components into the enterocytes.

2.5.1 Interactions with enterocytes

After being solubilized into mixed micelles and transported through the mucous layer the bioactive components and lipid digestion products are transferred into the enterocyte cells through various passive and active transport mechanisms [104, 119-121]. The precise mechanisms are still not fully understood, but it has recently been proposed that there are two major absorption mechanisms depending on the total amount of digested lipids present: (i) at low concentrations, FFA uptake is by a carrier-dependent (active) process; (ii) at high concentrations, FFA uptake is primarily by a carrier-independent (passive) process [122]. The active process at low FFAs concentrations may have developed so that animals could adsorb essential fatty acids required for survival even when the amount of lipids present in the diet is low [123], or it may play an important signaling/regulatory role that enables the body to adopt to subsequent processing of ingested lipids [124]. As mentioned earlier, it is believed that the lipophilic components within a mixed micelle (FFAs, MAGs, bioactives) are first released into the aqueous phase and then transported to the epithelium cells by molecular diffusion. Individual lipophilic molecules interact

with the apical side of the enterocyte cell membrane, then undergo a flip-flop mechanism within the membrane, and then are transported into the interior of the cell [120]. However, in principle, an entire micelle or vesicle containing bioactive components could be absorbed by an epithelium cell, or may fuse with the cell membrane [119, 125]. At present, the precise fate of mixed micelles at the epithelium cell surface is unknown [120, 126]. Overall, the fraction of a lipophilic bioactive component that is absorbed by the enterocytes is usually taken as a measure of its absorption (F_A).

The molecular characteristics of the initial lipid phase in a delivery system may play an important role in determining the rate and extent of the transfer of lipid digestion products and bioactives to enterocyte cells. In particular, using cell culture models, the chain length and degree of unsaturation of fatty acids have been shown to have an important influence on their absorption[127-129]. Some medium-chain fatty acids and acylglycerols have also been shown to improve the cell permeability, such as capric acid monocaprylin, and dicaprin [130]. A recent study of the influence of mixed micelle composition on the uptake of carotenoids by Caco-2 cells found that the absorption of □-carotene depended on the amount of FFAs, MAGs, phospholipids, and cholesterol present [131]. Another cell culture study using oily solutions as delivery systems showed that the absorption of carotenoids by Caco-2 cells after digestion in an simulated small intestine model depended on their molecular structure [118]. The fraction of carotenoids absorbed by the Caco-2 cells was ≈ 7.3% for lutein; ≈ 10.6% for beta-carotene; ≈ 7.7% for astaxanthin; and, ≈ 0% for lycopene.

2.5.2 Interactions with food components

The properties of mixed micelles may be altered due to their interactions with other components in the partially digested food matrix. Mixed micelles may interact with surfactants, which change their structures, compositions, and solubilization capacities [132, 133], and may therefore impact the bioavailability of any bioactive lipophilic components. Cationic biopolymers (such as chitosan, polylysine, or proteins) may bind anionic mixed micelles through electrostatic attraction causing them to precipitate, thereby trapping any encapsulated bioactive components [134-137]. Cationic mineral ions (such as calcium) present in the intestine may also bind anionic mixed micelles and cause them to precipitate as calcium soaps, thereby reducing the absorption of lipids and lipophilic bioactive agents [138-140]. The precise mechanisms that are important in a given situation will depend on the nature of the initial ELNsand the food matrix ingested. The dependence of mixed micelle properties on the presence of specific food components may prove to be a valuable means of controlling the bioavailability of lipophilic bioactive components.

2.6 Assembly of lipid nanoparticles within enterocytes: CMs

2.6.1 Chylomicron formation

After absorption, the biological fate of bioactive compounds depends on their molecular characteristics, as well as the nature of any co-absorbed lipid digestion products [7, 141-143]. More hydrophilic bioactive molecules travel across the

enterocytes and are released into the portal vein, which conducts blood containing the digested nutrients and bioactive agents to the liver for processing. These hydrophilic molecules may be transported as individual molecules, or they may be bound to other components (such as carrier proteins). Within the liver, bioactive components usually undergo substantial metabolism before entering the systemic circulation, which may cause them to lose some of their bioactivity before reaching their site of actions [99, 141, 143]. On the other hand, more lipophilic bioactive molecules are packaged into lipoprotein particles within the enterocyte cells, which then move into the lymphatic system where they are released directly into the systemic circulation without experiencing first-pass metabolism by the liver [120, 124, 144, 145]. The bioactivity of labile bioactive components may therefore be increased by targeting their transport to the lymphatic route rather than to the portal blood route (Figure 2-10). The transport route taken will therefore have a major impact on the chemical transformation (metabolism) of many lipophilic bioactive components (F_M).

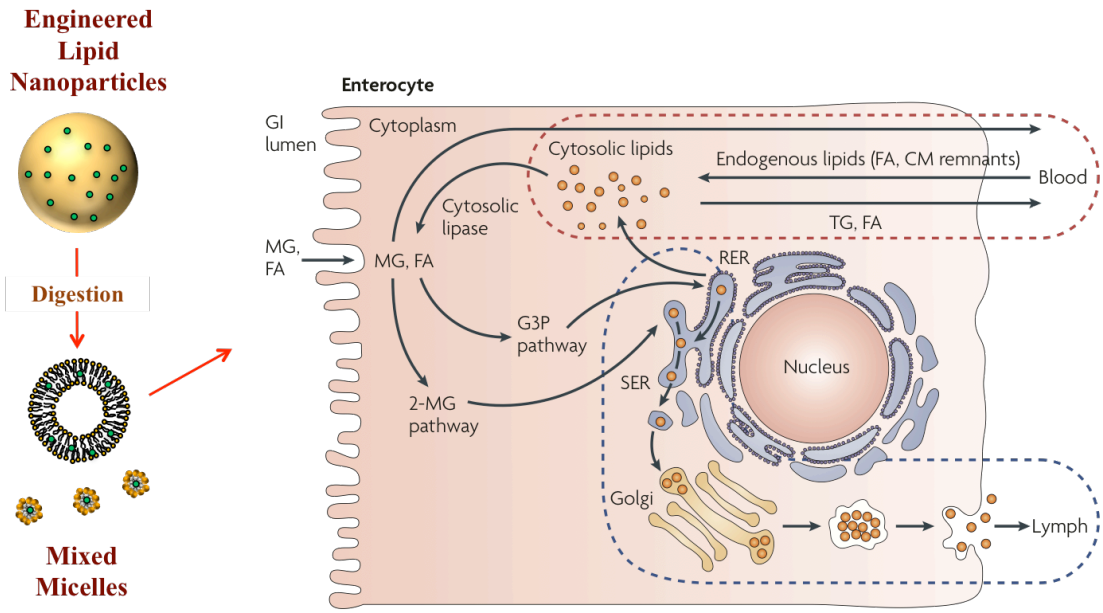

Figure 2-10 Lipophilic components may be transported by different pathways within the enterocyte depending on their molecular characteristics. After being transported across the apical membrane of the enterocyte, lipid digestion products (monoacylglycerides and fatty acids) can either diffuse across the enterocyte and enter the portal vein blood or be resynthesized into triglycerides. Part of figure (enterocyte cell) kindly provided by Professor Porter from his article "Lipids and Lipid-Based Formulations: Optimizing the Oral Delivery of Lipophilic Drugs" (Porter et al. 2007), with permission. Abbreviations: FA, fatty acid; MG, monoacylglyceride; RER, rough endoplasmic reticulum; SER, smooth endoplasmic reticulum; TG, triglyceride.

The nature of the lipoprotein particles formed within the enterocytes depends on the type and amount of lipid digestion products present [109, 146]. In the fed state (which are most important for food-based delivery systems), the predominant lipoprotein particles are CMs (CM) [122]. CMs consist of a lipophilic core (mainly TAGs, cholesterol and bioactive components) and a hydrophilic shell (mainly proteins and phospholipids). CMs can be distinguished from other forms of lipoproteins (such as very low-density lipoprotein (VLDLs), low-density

lipoprotein(LDLs), and high-density lipoproteins (HDL)) based on their physicochemical characteristics, such as density, size, and composition [147]. CMs have been reported to have densities < 960 kg m^{-3}, mean diameters between 72 and 1200 nm, and compositions of 80-95% TAG, 3-6% phospholipid, 2-4% cholesterol esters, 1-3% cholesterol, and 1-2% protein [147]. In addition, they may contain any highly lipophilic bioactive molecules that were taken up by the enterocyte cells. CMs are too large to directly enter into the portal vein; thus, they are transported via the lymphatic route [99, 148]. Figure 2-11 shows electron microscopy images of lipoprotein particles (presumably CMs and VLDLs) produced by Caco-2 cells in response to exposure to lipids (fatty acids and bile salt).

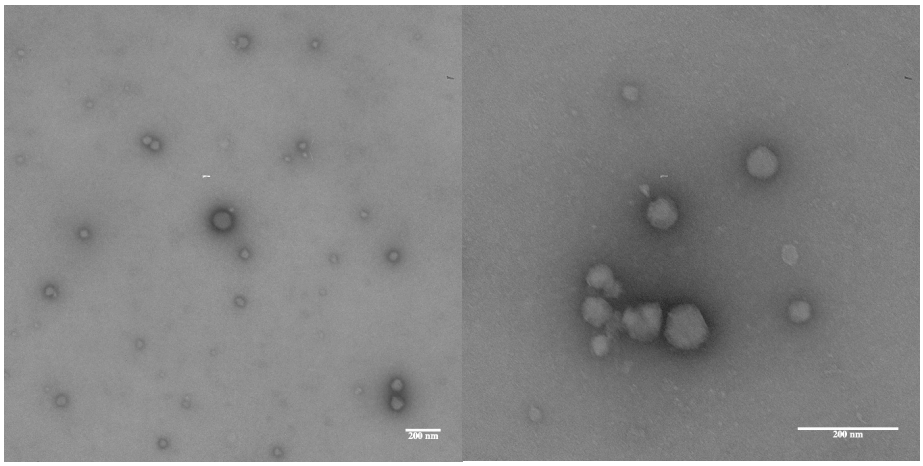

Figure 2-11 TEM images of lipoproteins (CMs and VLDLs) secreted by Caco-2 cell monolayers after incubation with oleic acid (*a*) and taurocholate acid (*b*) mixed micelles (1.6:0.5 mM) for 24 h (from authors' laboratory). Abbreviations: CM, chylomicron TEM, transmission electron microscopy; VLDL, very low-density lipoprotein.

The assembly of CMs within the enterocyte cells is still not fully understood, but considerable progress has been made in recent years due to the important role that they play in a number of chronic diseases [109, 120, 122, 124, 144]. A highly

simplified schematic diagram of the process is shown in Figure 2-10. Absorbed FFAs and MAGs absorbed are transported from the apical side of the enterocytes to the endoplasmic reticulum (ER), which may be mediated by the presence of fatty acid and monoacylglycerol binding proteins [124]. After reaching the ER, the FFAs and MAGs are reassembled into TAGs by specific classes of enzymes [124]. The TAGs formed accumulated within the phospholipid membranes of the ER, eventually causing them to split and release TAG droplets [122]. The subsequent formation of lipoproteins requires at least two major structural proteins: microsomal triglyceride transfer protein (MTTP) and apo-lipoprotein B48 (apoB) [124]. MTTP facilitates the transfer of the TAGs from their initial location within the ER bilayer to the apoB molecule. ApoB is very hydrophobic protein that is packaged into the TAG droplet to form lipoprotein particles. After formation these primordial lipoprotein particles undergo further changes within the enterocyte cells to form CMs, e.g., incorporation of additional lipids and protein [124].

2.6.2 Influence of molecular characteristics of bioactives on their lymphatic transport

Researchers in the pharmaceutical industry have identified the key characteristics of lipophilic molecules that determine their ability to be transported via the lymphatic system [99, 119, 141, 148, 149]. Two of the most important physicochemical characteristics of lipophilic molecules are their oil-water partition coefficient (log*P*) and oil solubility [150-152].

The log *P* value provides a measure of the relative affinity of a bioactive component for oil solubility is the maximum concentration of bioactive with a

log*P>5* and an oil solubility > 50 mg/L are considered to be highly lipophilic compounds that tend to be transported by the lymphatic rather than the portal blood route [141]. In reality, these two parameters do not accurately predict the behavior of many bioactive compounds and therefore more comprehensive systems have been developed for classifying them [153].

2.6.3 Influence of dietary components on chylomicron formation and properties

Different kinds of lipoproteins may be assembled within the enterocytes lining the small intestine depending on the nature of the food consumed. In the fed state (high fat), CMs are the major lipoproteins formed within the intestinal enterocytes. CMs have a structure somewhat similar to the oil droplets present in oil-in-water emulsions. They consist of a non-polar core that consists mainly of TAG molecules (85~92%) and solubilized bioactive components, and a more polar shell that consists of phospholipids (PL, 6~12%), cholesterol (1~3%) and proteins (1~2%, Apo B48, A-I, A-IV, and C's) [140, 149, 154]. The diameter of CMs typically ranges from around 75 to 1200 nm depending on the type and amount of lipids consumed. In the fasted state (low fat), very low density lipoproteins (VLDL) are the predominant lipoproteins formed in the enterocytes [155]. VLDL particles have smaller diameters (30 to 80 nm) than CM particles (75 to 1200 nm), and they contain lower amounts of TAG than CMs. Hence, the ability of VLDL to carry lipids or bioactive lipophilic compounds is more limited. It has been suggested that the assembly of intestinal CM and VLDL particles occurs by separate pathways [156, 157]. This assumption is based on differences in the relative amounts of CM and

VLDL produced in response to the presence of different co-ingested lipids [158] [156, 157].

The size and composition of CMs has been reported to depend on the type and amount of digestible lipids present within the digestion medium (Table 2-3). Consequently, the biological fate of bioactive components (lymph versus portal vein) may be directed by controlling the initial composition of co-ingested lipids in delivery systems. Researchers have reported that the mean diameter of CMs separated from the lymph of animals increased as the total amount of dietary fat (corn oil and butter) consumed increased [159]. However, the total number of CMs produced remained relatively constant as the dietary fat consumed increased, suggesting that individual CMs grew rather than more CMs being produced [160]. The composition of the proteins (apolipoprotein) adsorbed to the CMs surfaces was also found to be relatively insensitive to CM size [161]. The degree of unsaturation of the fatty acids in digestible lipids also influences the size of the CMs produced. At equivalent amounts, monounsaturated fatty acids (MUFAs) and polyunsaturated fatty acids (PUFAs) produce larger CMs than saturated fatty acids (SFAs) [162, 163]. MUFAs have been shown to increase the number of CMs secreted after a meal [164, 165]. Oleic and linoleic acids caused much greater secretion of CMs than steric and palmitic acids [166] (Table 2-3). However, some PUFAs have been shown to decrease postprandial TAG concentrations and the number of CMs produced compared to SFAs [167, 168].

Table 2-2 Summary of effects of different fatty acids on CM formation measured using Caco-2 cell models

Micelle solution	Secretion of Lipoproteins in the basolateral side			Reference
	Apo B Secretion*	TAG Secretion	Lipoprotein Density	
Oleic acid (C18:1)-TC	Increased or Decreased	Increased	CM/VLDL <1.006 g/ml,	[10]
Palmitic acid (C16:0)-TC	Unchanged	Unchanged	IDL/LDL 1.009 to 1.068 g/ml.	[164]
Linoleic acid (18:2)-BSA	Increased	Increased	CM/VLDL <1.006 g/ml	[166, 169]
Linolenic acid (18:3)-BSA	Increased Lower than C18:2	Increased, Lower than C18:2	CM/VLDL <1.006 g/ml	[3]
Stearic acid (18:0)-BSA	Increased, but not significantly	Unchanged	IDL/LDL, 1.009 - 1.068 g/ml.	[166]
Eicosapentaenoic acid (20:5, n-3)--TC	Unchanged	Decreased	CM/VLDL <1.006 g/ml,	[170]

In vitro studies using Caco-2 cells have also shown that the secretion of CMs after incubation with fatty acids depended on their degree of unsaturation: oleic acid (C18: 1) > linoleic acid (C18: 2) > linolenic acid (18:3) [166, 171]. Exposure of Caco-2 cells to eicosapentaenoic (C20: 5) acid has also been shown to reduce CM secretion [170] (Table 2-2). On the other hand, the lymphatic transport of a model lipophilic bioactive component (halofantrine) in a cannulated rat model was reported to decrease in the following order: C18: 2 > C18: 1 > 18:3 [172]. This study suggests that there is not always a simple correlation between the amount of CMs produced and the lymphatic transport of bioactive components.

Other studies suggest that the initial location of the fatty acid chains on the TAG molecule may also be important [173]. The size and number of CMs produced after administration of □-3 oils containing LCFA (L) and MCFA (M) in different sn-positions on the glycerol backbone were compared. This is important because when TAGs are digested by pancreatic lipase the fatty acids at the sn-1 and sn-3 positions are released as FFAs, whereas the one at the sn-2 position is released as part of a MAG. The presence of L-M-L led to more large-sized CMs being secreted than the presence of M-L-M [173]. Furthermore, when the M-L-M and L-M-L triacylglycerols were incorporated into lipid-based delivery systems, the lymphatic transport of a model lipophilic bioactive component (halofantrine) was higher for the L-M-L (≈ 27%) than the M-L-M (≈ 18%) [142]. Transportation of halofantrine to the lymph was also reported to be dramatically increased if co-administered with triglycerides containing long chain (C≥12) fatty acids than with those containing medium chain (8≤C<12) or short chain (C<8) fatty acids [174]. The fatty acids with shorter chain lengths were directly transported into the portal blood, while those with the longer chain fatty acids would re-esterified into triglycerides in the enterocyte and then incorporated into the core of CMs [7, 175]. Studies using Caco-2 cells have shown that co-administration of carotenoids with lipids that stimulate the formation of CMs lead to a higher concentration of carotenoids on the basolateral side [176].

The size of the CMs produced after ingestion of dietary lipids may also have an important effect on human health. Levy et al. suggested that larger CMs were removed more quickly that smaller ones [177]. In addition, the number of CM remnants formed is proportional to the number of CMs secreted (rather than their

total mass). Thus, the risk of atherogenic or cardiovascular diseases may be reduced by ingesting lipids that increase the size of CMs (loading more TG into every CM) since then there will be fewer CM remnants formed [81, 178].

2.7 Disassembly of CMs within the body

Ideally, one would like to know the complete biological fate of any ingested bioactive lipophilic component, e.g., where did it end up, how did it get there, how was its structure changed during transport, how long did it remain there, and what biochemical pathways did it alter? Some progress has been made in this area in the pharmaceutical industry, but knowledge of this area is relatively poor for lipophilic nutraceuticals. After CMs leave the enterocyte cells, they pass through the lymphatic system and are then released into the systemic blood circulation via the thoracic duct (near the neck) [109, 122, 141]. The properties of the CMs are then altered as they pass through the various regions of the body. Additional proteins (including apoC-II) adsorb to the surfaces of the CMs, whose role is believed to regulate their subsequent degradation by lipoprotein lipases in peripheral tissues [144]. TAGs in CMs undergo lipolysis in the systemic circulation, thereby delivering FFAs, MAGs, and possibly lipophilic bioactive components to the tissues (such as adipose tissue, mammary, heart, and skeletal muscle [179]. TAG hydrolysis causes the CMs to shrink in size, leaving a "chylomicron remnant" that is ultimately taken up by the liver [180, 181]. A link has been suggested between elevated CM levels in the blood after consumption of a fatty meal, and chronic diseases such as cardiovascular disease [182-184]. The nature of the TAGs within CMs may influence their ability to

promote these diseases, e.g., fatty acid chain length and degree of unsaturation [185]. Replacement of saturated fats with unsaturated fats has been advocated as a means of reducing the risk of cardiovascular disease, however, polyunsaturated fats may promote lipid oxidation thereby contributing to atherosclerosis, although this is still a matter of debate [186]. It may therefore be important to carefully design delivery systems so that they increase the bioactivity of encapsulated lipophilic components, but that they do not adversely affect health by promoting chronic diseases.

2.8. Potential advantages of controlling lipid nanoparticle assembly and disassembly

This review article has highlighted the relationship between the bioactivity of ingested lipophilic components and the fate of engineered and biological lipid nanoparticles within the human body. There are a number of potential advantages of specifically designing food-grade delivery systems that control the assembly and disassembly of lipid nanoparticles outside and inside the body [14, 29, 147]:

ELNs with different compositions and structures can be fabricated using food-grade ingredients and processing operations.

ELNs can be designed so that they are compatible with a variety of different food and beverage matrices: from transparent to opaque; from liquid to solid; from short to long shelf life.

ELNs can be designed so that they behave in a particular way within the GIT so as to increase the bioavailability of encapsulated beneficial lipophilic bioactive

agents. In particular, they can be designed to facilitate the incorporation of beneficial bioactive agents into mixed micelles and CMs.

Incorporation of a bioactive component within the hydrophobic core of CMs avoids first pass metabolism within the liver, and may also protect them from other unwanted metabolic reactions within the body, thereby increasing their bioactivity.

CMs are endogenous carriers of lipophilic substances within the human body, and therefore are not expected to elicit an immune response and should be cleared from the circulation by the reticulo-endothelial (RES) system normally used to clear particles from the system.

CMs have specific receptors on their surfaces, which potentially allow them to be targeted to specific sites within the body.

2.9. Conclusions

Nanotechnology has emerged as one of the most powerful tools for controlling the behavior of matters. It is finding increasing utilization within the food industry to improve food safety, quality, and healthfulness. Recently, there have been rapid advances in the fabrication and characterization of ELNssuitable for utilization within the food industry. In particular, lipid nanoparticles have been identified as powerful building blocks for the creation of delivery systems designed to encapsulate, protect, and release lipophilic bioactive food components (nutraceuticals) and drugs (pharmaceuticals). This review article has shown that ingested ELNs may be disassembled within the human GIT and reassembled into biological lipid nanoparticles (mixed micelles and vesicles) in the small intestine,

which are disassembled and reassembled into still other kinds of biological lipid nanoparticles in the enterocyte cells (CMs). Lipophilic bioactive components that are incorporated into CMs are transported into the systemic (blood) circulation via the lymphatic system, and therefore avoid first pass metabolism in the liver. The chylomicron - lymphatic pathway plays an essential role in improving the oral bioavailability of many lipophilic drugs, and may also be beneficial for the design of effective delivery systems for lipophilic nutraceuticals.

The extent of lymphatic transportation can be regulated by controlling the size, number, and composition of the CMs, which can in turn be regulated by controlling the properties of the ingested engineered lipid nanoparticles. Improved knowledge of the influence of the molecular characteristics of bioactive components, and the composition and structure of ELNs may lead to the rational design of lipid-based delivery systems for food and beverage applications. These delivery systems may be used to incorporate bioactive lipids into functional food products designed to improve human health and wellness.

CHAPTER 3

LITERATURE REVIEW: IMPROVING ORAL BIOAVAILABILITY OF NUTRACEUTICALS BY ENGINEERED NANOPARTICLE-BASED DELIVERY

3.1 Introduction

Nutraceuticals are foods and food constituents that provide health benefits beyond basic nutrition. Accumulating evidence has suggested that dietary consumption of nutraceuticals is associated with decreased risks of multiple chronic diseases. However, many nutraceuticals have poor oral bioavailability, which significantly lowers their efficacy as disease-preventing agents [3, 5, 187, 188]. An effective way to improve oral bioavailability of nutraceuticals is to utilize nanotechnology to encapsulate nutraceuticals in engineered nanoparticles (ENs)-based delivery systems [5, 6, 189].

3.2 Engineered nanoparticle-based delivery systems for nutraceuticals

Nanotechnology has become an important means of producing novel materials and structures for a wide range of applications within the food industry. Numerous ENs have been fabricated and tested for their potential use as delivery systems for nutraceuticals with the purpose of enhancing their health benefits through encapsulation, protection and/or controlled release of nutraceuticals [5, 187, 188]. Improving oral bioavailability of nutraceuticals has become a promising strategy to enhancing their efficacy in humans. Recently, considerable advances have been achieved in designing and manufacturing ENs to increase the oral

bioavailability of nutraceuticals. Generally, depending on the presence or absence of lipids as the major components of the delivery systems, ENs can be categorized as lipid-based or non-lipid-based (Table 3-1). Recent reviews have provided comprehensive descriptions of the manufacture and characteristics of different type of ENs suitable for food applications [5, 31, 81, 209-212]. This review elaborates the impact of ENs on oral bioavailability. It is noteworthy that, different from the ENs utilized in the pharmaceutical industry, ENs for food application has to be manufactured with 100% food-grade materials, such as edible lipids, proteins, carbohydrates, and surfactants, which has considerably increased challenges in creating effective delivery systems.

Table 3-1 ENs based delivery systems for improving oral bioavailability nutraceuticals.

	Delivery systems	Functional food components	Ingredients	Function sites	References
Non-lipid-based ENs	Biopolymric nanogels, antisolvent precipitation	Lipophilic compound (omega-3 fatty acids, CLA, oil soluble vitamins et al.)	Miscible solvents, biopolymers, surfactants	F_B	[72]
	Biopolymric nanoparticles	Omega-3/omega-6 polyunsaturated fatty acids	Water, dextrin	F_B&F_A	[190]
	Biopolymric nanoparticles	Curcumin	Water, β-cyclodextrin, modified starch, surfactant	F_B	[191]
	Organogel based	Curcumin	Water, organogel, surfactant	F_B&F_A	[192]

	nanoemulsion				
	Nanocomplex	Omega-3 fatty acids	Water, beta-lactoglobulin, protein	F_B	[193]
	Protein-based micelles	Vitamin D,	Water, surfactant (casein),	F_B & F_A	[194]
	Micelles	Curcumin	Water, surfactant	F_B & F_A	[195]
	Nano formulation	Co Q 10	Water, surfactant, glycerol,	F_B & F_A	[196]
Lipid-based ENs	Nanoemulsion	Lipophilic compound (Vitamin E, beta-carotene)	Water, oil, surfactant	F_B & F_A & F_M	[197-201],
	Nanoemulsion	Co Q10	Water, oil, surfactant	F_B&F_A & F_M	[202, 203]
	Liposome	Polyphenols (curcumin, resveratrol)	Water, phospholipids, cholesterol	F_B	[204]
	Nanoliposome	EGCG	Water, Phospholipids, cholesterol	F_B	[205]
	Nanoemulsion	Curcumin	Water, MCT, surfactant	F_B & F_A	[46]
	Solid lipid nanoparticles	Lipophilic compound (carotenoids, omega-3 fatty acids, phytosterols)	Oil, surfactant	F_A &F_M	[12, 206]
	Microemulsion	Curcumin	Water, surfactants, oil	F_B	[207]
	Micelles	Lycopene	Oil, water, lecithin, surfactant	F_B & F_A	[208]

3.3 Oral bioavailability of nutraceuticals

The oral bioavailability of a nutraceutical is defined as the fraction of the ingested nutraceutical that actually reaches the systemic (blood) circulation in an active form [213]. Only these nutraceuticals are available to be distributed to the tissues and organs where they can exert their beneficial health effects. For ingested nutraceuticals, there are a few barriers preventing them from reaching the systemic circulation in an active form, e.g. chemical instability during digestion, poor solubility in GI fluids, slow absorption from the GIT, and first-pass metabolism (Figure 3- 1). The oral bioavailability (F) of a nutraceutical encapsulated in ENs can be estimated by the following equation [5, 212]:

$$F = F_B \times F_A \times F_M$$

Here, F_B is the fraction of an ingested nutraceutical that survives passage through the upper GIT and that is released from the food matrix/ENs into the GI fluids, thereby becoming bioaccessible for absorption by enterocytes. FA is the fraction of the bioaccessible nutraceutical that is actually absorbed by the enterocytes and then transported to the portal blood or lymph (and into the systemic circulation). F_M is the fraction of absorbed nutraceutical that is in an active form after first-pass metabolism in the GIT and liver (and any other forms of metabolism). In the following sections, the effects of food-grade EN-based delivery systems on bioaccessibility, absorption, and first-pass metabolism of encapsulated nutraceuticals are discussed.

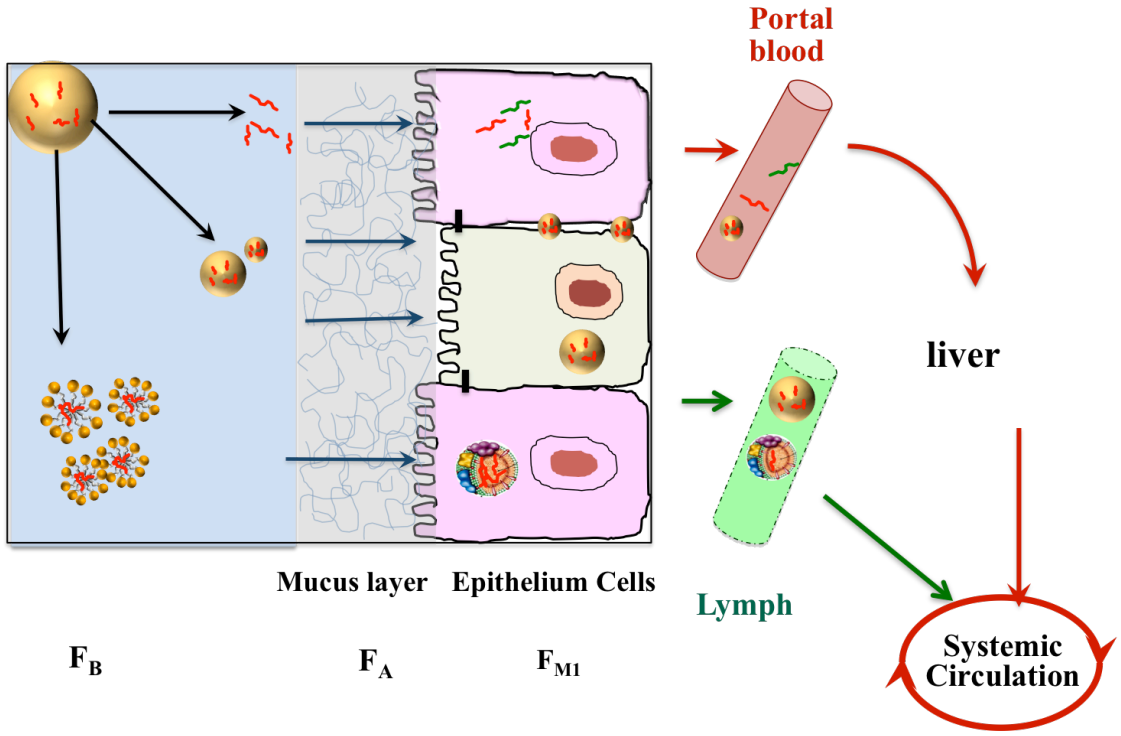

Figure 3-1 After digestion of different nanoparticels in the lumen, FFI may release, nanoparticles may not break down and for lipid based nanoparticles, FFI are trapped in the mixed micelles (F_A). Four absorption (F_A) routes include: released compound diffusion into enterocytes, nanoparticle paracellular absorption, M cell uptake via Peyer's patches and mixed micelle-chylomicron transportation. FFI and small size particels (<50nm) are transported into the potal vein. CMs and nanoparticles uptake by M cell enter into the lymph and avoid metabolism in the enterocytes (F_{M1}) and liver (F_{M2}).

3.4 Engineered nanoparticles enhance bioaccessibility of nutraceuticals

A nutraceutical is exposed to substantial changes in the composition, structure, and flow behavior of its environment during its passage through the upper GIT, i.e. mouth, stomach, and small intestine. These conditions may cause changes in the physical state, location, and chemistry of the nutraceutical, therefore decreasing its bioaccessibility. ENs has been developed to protect nutraceuticals from adverse GI conditions. For example, (−)-epigallocatechin gallate (EGCG), a

green tea polyphenol, is unstable under the pH conditions found in small intestinal fluids. Encapsulation of EGCG in nanoliposomes fabricated from phospholipids, cholesterol, and Tween 80 decreased its degradation in simulated intestinal fluids around 10-fold [205]. Nutraceuticals can also be encapsulated in solid lipid nanoparticles and biopolymer-based nanoparticles that can be designed to protect nutraceuticals from premature degradation and improve their stability in the GIT [190, 214]

To be bioaccessible to enterocyte absorption, a nutraceutical needs to be solubilized within the GIT. Highly lipophilic nutraceuticals, such as carotenoids and curcuminoids have low bioaccessibility due to their poor solubility in aqueous GI fluids. Lipid-based ENs, such as nanoemulsions and solid lipid nanoparticles, have frequently been used to enhance the bioaccessibility of lipophilic nutraceuticals. The nature of the carrier oil used to solubilize lipophilic nutraceuticals within lipid-based ENs has been shown to influence their loading capacity and bioaccessibility [198, 215]. After ingestion, the compositions, structures and physiochemical properties of nutraceutical-loaded ENs may be changed appreciably due to their exposure to different GIT conditions, e.g. their size, charge, physical state, and aggregation state [5]. The presence of digestible components (protein, lipid and surfactant) also play an important role in determining the biological fate of lipid-based ENs in the GIT, which in turn has a great impact on the bioaccessibility of nutraceuticals[5].

In the GIT, digestible carrier oils (mainly triglycerides) in ENs are hydrolyzed by lipases to produce free fatty acids and monoacylglycerols. These lipid digestion

products interact with bile salts and phospholipids in the lumen of the small intestine to form “mixed micelles” with complex structures (Figure 3-2A) [5]. Nutraceuticals encapsulated within ENs are transferred to the mixed micelles during the digestion process, which greatly enhances their bioaccessibility [102, 216, 217]. The type of carrier oils used in ENs is critical for the bioaccessibility of lipophilic nutraceuticals. Nanoemulsions containing mainly long chain triglycerides produced much higher bioaccessibility of vitamin E, β-carotene and Co-enzyme Q10 than those containing mainly medium chain triglycerides [198, 200, 202]. In contrast, nanoemulsions containing medium chain triglycerides has been shown to produce higher bioaccessibility of curcumin than those containing long chain triglycerides [110]. These findings suggest that the effects of different carrier oils on bioaccessibility are specific to different nutraceuticals; therefore, EN-based delivery systems should be specifically designed for particular nutraceuticals in order to effectively improve their bioaccessibility. The particle size of ENs can also influence nutraceutical bioaccessibility. Nanoemulsions with smaller particles have been reported to give a higher bioaccessibility of β-carotene than those with larger particles [217]. A potential explanation for this phenomenon is that smaller lipid particles generate mixed micelles more rapidly than larger particles during lipid digestion, which can increase the rate of transfer of the nutraceuticals from the particles to the mixed micelles. The surfactants used in oil-in-water nanoemulsions may have an impact on the bioaccessibility of encapsulated nutraceuticals. It was reported that the extent to which carrier triglyceride oil was digested in a simulated GI tract was positively correlated with the hydrophilic/lipophilic balance of the

surfactant and inversely correlated to the surfactant aliphatic chain length [218]. The difference in the oil digestion may lead to difference in the solubilization of nutraceuticals in mixed micelles, resulting in different bioaccessibility. Therefore, appropriate surfactants can be selected for specific nanoemulsions to offer higher bioaccessibility. Moreover, biopolymer-based non-lipid delivery systems can be used to enhance bioaccessibility by increasing solubility of highly lipophilic nutraceuticals [72]. For example, the solubility of curcumin in simulated intestinal fluids was significantly increased by encapsulating it in β–cyclodextrin and modified starch [191].

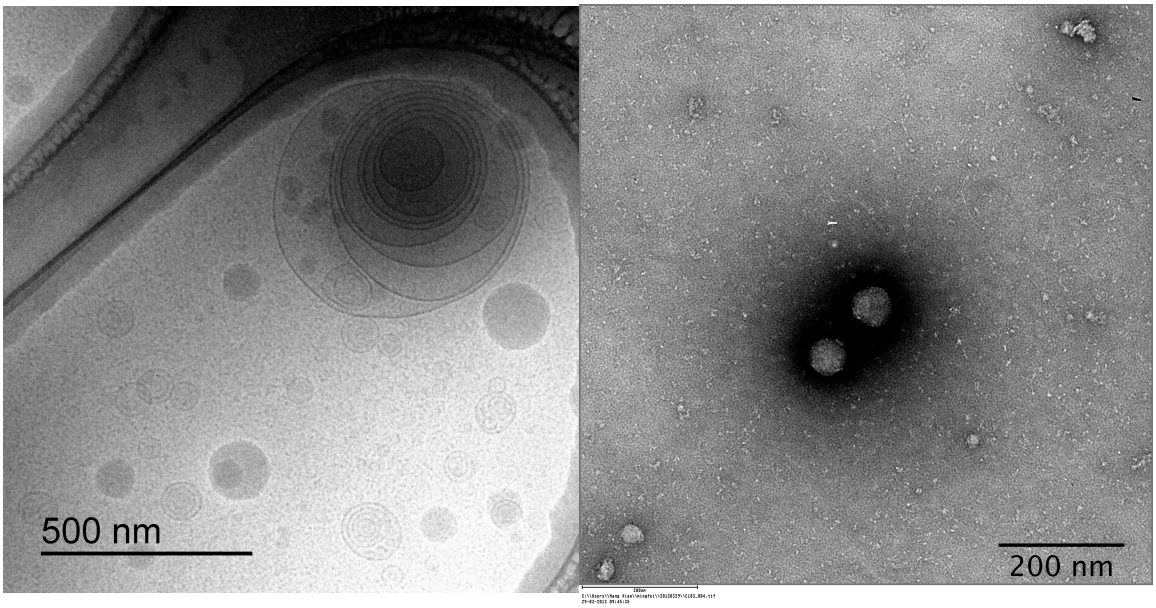

Figure 3-2 Cory-TEM image of mixed micelles and morphologies of CMs by TEM. Mixed micelles consist of linoleic acid and bile salts. Single layer, multiple layer and lipid crystal co-exist in the solution. Fatty acids in mixed micelles stimulate the formation of CMs.

3.5 Engineered nanoparticles enhance the absorption of nutraceuticals

The small intestine is the place where most nutraceuticals are absorbed after their oral ingestion [219]. Figure 1 depicts the major routes of absorption in the small intestine. Lipid-based ENs such as nanoemulsions have been frequently used to encapsulate lipophilic nutraceuticals such as β-carotene, curcumin, vitamin E, and Co Q10 to enhance their absorption [2, 110, 198, 200-203, 217, 220]. Mixed micelles (Figure 3-2A) generated after digestion of nanoemulsioins transport lipophilic nutraceuticals across the aqueous mucus layer, and make them available for absorption by enterocytes. Inside the enterocytes, lipophilic nutraceuticals are packaged into CMs (Figure 2B) due to their high lipophilicity [20, 141]. The CMs are lipid particles endogenously produced by the enterocytes using lipid components supplied by mixed micelles, such as free fatty acids, monoacyglycerols, and cholesterol [221]. Nutraceuticals associated with CMs are then transported to the lymphatic circulation system via a chylomicron-mediated pathway[5].

It has been shown that the presence of mixed micelles made from free fatty acids and bile acids greatly enhanced trans-enterocyte transport of lipophilic nutraceuticals, such as 5-hydroxylnobiletin, a flavonoid found in citrus fruits [221]. This enhancement in absorption was associated with production of chylomicron in the enterocytes stimulated by the mixed micelles. Moreover, the degree of saturation of fatty acids in mixed micelles is also an important factor influencing the absorption of nutraceuticals. For example, mixed micelles formed with oleic acid, linoleic acid, or linolenic acid were shown to have different effects on trans-enterocyte transport of 5-hydroxylnobiletin [4]. Mixed micelles formed with oleic acid resulted in much

higher trans-enterocyte transport of 5-DN than mixed micelles formed with linoleic acid or linolenic acid (Figure 3-3).

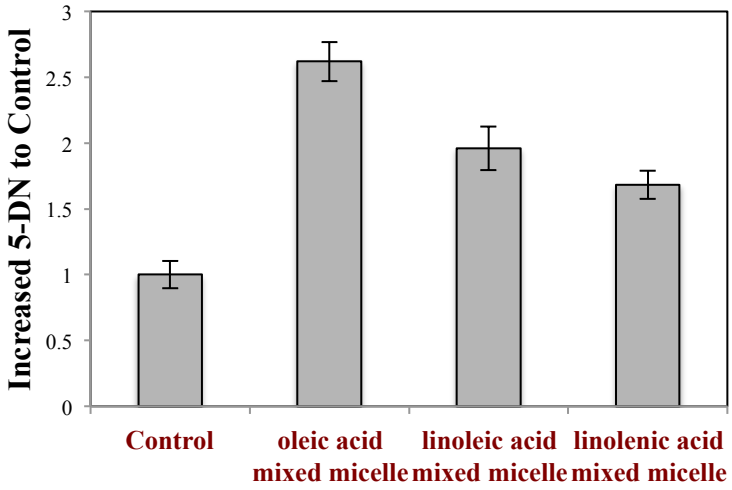

Figure 3-3 Increased trans-enterocyte transport of 5-hydroxylnobiletin in Caco-2 cell monolayer by incorporation it in oleic acid, linoleic acid and linolenic acid mixed micelles compared to Control (considered as "1" fold).

After passage through the upper GIT, it is possible for nutraceuticals to remain trapped inside non-digested nanoparticles, rather than being released [214]. The nutraceutical-ENs may then be paracellularly transported to the portal blood via tight junctions, or taken up by M cells via Peyer's patches and then secreted into the lymph [214]. Certain substances can modulate the structure and integrity of intestinal epithelial cells, such as EDTA (opens intracellular tight junction seals), chitosan (causes separation of tight junction components), surfactants (disturb the integrity of the plasma membrane), and free fatty acids (enhance plasma membrane permeability) [222]. These substances can therefore be incorporated into delivery systems to enhance the absorption of nutraceuticals [196, 223]. For digestible ENs, encapsulated nutraceuticals can be released and solubilized within the intestinal

fluids, and then taken up by the enterocytes via passive diffusion or active transport [28]. Eventually, these nutraceuticals may be transported directly to the portal blood or through the chylomicron-mediated lymphatic transport.

3.6 Engineered nanoparticles decrease first-pass metabolism of nutraceuticals

First-pass metabolism (also known as first-pass elimination) is a process during which a nutraceutical is metabolized by a wide array of enzymes present mainly in the gut and liver (Figure 3-1). The result of first-pass metabolism is that only a fraction of the ingested nutraceutical reaches the systemic circulation unchanged, which leads to a decreased oral bioavailability. ENs can be designed to help nutraceuticals bypass first-pass metabolism and thus increase their bioavailability. Lipid-based ENs, such as nanoemulsions, have been used to bypass liver metabolism by promoting intestinal lymphatic transport of lipophilic nutraceuticals[5]. As mentioned above, nanoemulsions promote chylomicron-mediated transport of nutraceuticals from enterocytes to the lymphatic circulation. Subsequently, lymph carries chylomicron-associated nutraceuticals to the systemic circulation via the subclavian vein without passing through the liver, thus avoiding first-pass metabolism in the liver (Figure 3-1) [3]. ENs can also protect nutraceuticals from first-pass metabolism in enterocytes. For example, ENs can increase paracellular transport of nutraceuticals by altering the integrity of tight junctions [216, 222, 223]. Paracellularly absorbed nutraceuticals are not subject to metabolism by intracellular enterocyte enzymes, and may therefore have higher bioavailability. ENs that promote chylomicron-mediated transport of nutraceuticals,

such as nanoemulsions, may also decrease first-pass metabolism in the enterocytes. This is because that nutraceutical associated with the CMs may have less chance to interact with metabolizing enzymes within the cell in comparison to nutraceuticals freely present in the cytoplasm of enterocytes [4, 216]. Moreover, the carrier oil type of nanoemulsions plays an important role in the first-pass metabolism of nutraceuticals in the enterocytes. For example, olive oil-based nanoemulsion resulted in a minimal metabolism of pterostilbene (an important phenolic nutraceutical found in blue berries) in enterocytes, whereas flaxseed oil-based nanoemulsion led to an extensive metabolism of pterostilbene [216]. In order to provide guiding principles for rational design of ENs to decrease first-pass metabolism, more mechanistic investigations are needed to establish the relationship between the different characteristics of ENs and their effects on first-pass metabolism of specific nutraceuticals.

3.7 Conclusions

Accumulating research has demonstrated that food-grade engineered nanoparticles can be utilized to improve the oral bioavailability of nutraceuticals, which may enhance their potential health benefits in humans. More systematic mechanistic investigations are needed to elucidate the relationship between the particle characteristics of ENs and their impact on the biological fate of nutraceuticals. Improved knowledge in this area would provide a solid scientific foundation for the rational design of novel EN-based delivery systems to improve the efficacy of nutraceuticals.

CHAPTER 4

ENHANCED LYMPHATIC TRANSPORT OF POLYMETHOXYFLAVONE BY MONO-UNSATURATED LONG- CHAIN FATTY ACIDS

4.1 Introduction

Many bioactive compounds that may promote human health are highly lipophilic molecules [3], such as oil-soluble vitamins, carotenoids, polyunsaturated triacylglycerols, and flavonoids [11]. However, the potential health benefits of these compounds are limited because of their relatively low oral bioavailability after oral administration, which is mainly attributed to their low aqueous solubility [12]. Research with pharmaceuticals and nutraceuticals has shown that the oral bioavailability of lipophilic molecules can be greatly enhanced by co-administration with certain digestible lipids, especially those containing long chain triglycerides [1, 102, 167, 171]. For instance, the uptake of Vitamin E was significantly improved if it was consumed with a certain amount of oil during a meal [224].

Triacylglycerols (TAGs) are the main source of digestible lipids within the human diet, and act as a solvent for any lipophilic bioactive molecules that are ingested. After ingestion, TAGs pass through the gastrointestinal tract and are hydrolyzed by gastric and pancreatic lipase to form monoacylglycerols (MAG) and free fatty acids (FFA) [24]. These lipid digestion products then combine with phospholipids and bile salts in the small intestine to form “mixed micelles” that are

capable of solubilizing and transporting lipophilic bioactive molecules to the enterocytes where they are absorbed[225].

Usually, consumption of a fat rich meal promotes the assembly and secretion of lipoproteins (such as CMs) inside the intestinal epithelial cells [10]. CMs are essential for the transport of dietary fat and lipophilic compounds into the systemic circulation. Structurally, CMs are biological nano- or micro-particles that consist of a triglyceride-rich core surrounding by a layer of phospholipids, cholesterol and proteins [109]. Lipids and bioactive lipophilic compounds that are incorporated into CMs are transported via the lymphatic circulation rather than the portal vein circulation, thus avoiding first-pass metabolism in the liver, which can increase the bioavailability of certain compounds [141, 226]. However, not all bioactive components follow the lymphatic way. The molecular characteristics of the lipid digestion products and bioactive components play an important role in determining the rate and extent of this process. For example, unsaturated TAGs that contain more oleic acids were found to be more efficiently incorporated into lipoproteins than saturated TAGs [227]. Moreover, highly lipophilic compounds that have high oil-water partition coefficients and high TAG solubility are more likely to be transported by the lymphatic system than less lipophilic compounds [226].

An intestinal cell line derived from human colorectal carcinoma (Caco-2 cells) is widely used as a model for studying the intestinal synthesis and secretion of lipoproteins [228]. Caco-2 cells can form a monolayer on cell culture membranes ("transwells") that mimics the human intestinal tract, which offers considerable advantages in the rapid screening of the influence of different dietary components

on the absorption process [164, 228]. However, it should be noted that the phosphatidic acid pathway is considered to be the primary way that triglycerides are resynthesized in Caco-2 cells, whereas the monoglyceride pathway is the primary way in human intestinal cells [229], which may lead to some differences in the results obtained by in vivo and in vitro studies.

In our study, we evaluated the effect of fatty acids on the transport of 5-hydroxy-6, 7, 8, 3', 4'-pentamethoxylflavone (5-ND) across the monolayer of enterocytes using the Caco-2 cell model. 5-ND is a poorly water-soluble compound extracted from citrus fruit (Figure 4-1), which has previously been shown to inhibit the growth of multiple human cancer cells [230, 231]. Our central hypothesis is that the bioavailability of 5-ND can be increased by stimulating the formation and secretion of CMs by co-administering with model lipid digestion products (oleic acid). The results of this study are useful for the rational design of delivery systems for bioactive lipophilic components, such as nutraceuticals and pharmaceuticals.

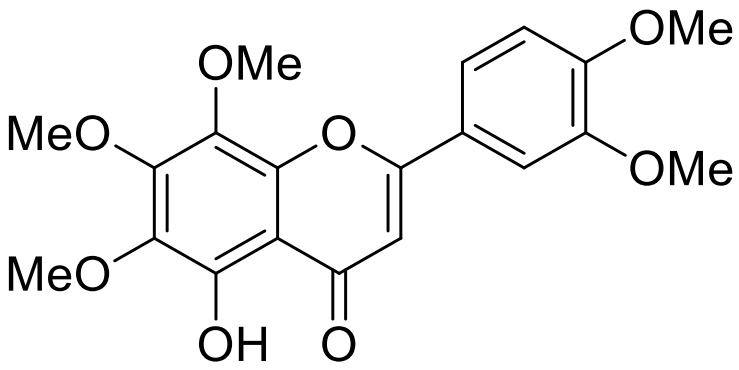

Figure 4-1 Molecular structural of 5-hydroxy-6, 7, 8, 3', 4'-pentamethoxylflavone (5-ND) – a bioactive flavonoid with a low water solubility

4.2 Materials and methods

4.2.1 Materials

The following products were purchased from Sigma Chemicals (St. Louis, MO): OsO_4, oleic acid (OA), taurocholic acid (TC), phosphatungstic acid (PTA) and OptiprepTM density gradient medium. All other chemicals and solvents of analytical grade were from Fisher Scientific (Pittsburgh, PA).

4.2.2 Cell culture

Caco-2 cells (passage 45~55) were maintained in the complete Dulbecco's modified essential medium (DMEM), containing high glucose, 10% fetal bovine serum (FBS), 1% antibiotic and 1% amino acids. The transepithelial electrical resistance (TEER) was measured at 37 °C using the Millicell® ERS-2 epithelial voltammeter (World Precision Instruments, Sarasota, FL). TEER values at 37 ºC were around 260 Ω/ cm^2. Cell monolayers with TEER values below 165 Ω/ cm2 were discarded[10]. For absorption experiments, the Caco-2 cells were seeded at a concentration of 3×10^5 cells/mL on transwells (Corning Inc., MA, USA) with permeable polyester filters (3 μm pore size and 4.67 cm^2 surface area). The medium was changed every other day for 3 weeks to induce differentiation of Caco-2 cells. Before the start of the fatty acids treatments, the cells were incubated for 4 h with serum-free complete medium. Cells were then incubated with 2.0 mL of the complete media containing different treatments on the apical side. The basolateral side contained 2.0 mL of serum-free complete medium.

4.2.3 Preparation and characterization of oleic acid- sodium taurocholate micelles

Fatty acids micelles were prepared according to a method described previously [10, 164], with some modifications. Oleic acid-sodium taurocholate mixed micelles (OA: TC = 1.6: 0.5 mM) were formed using the following procedure. A 10 mM TC solution was formed by dissolving an appropriate amount of TC into 1 mL of PBS. OA was then added to the TC solution drop-by-drop and mixed by swirling over night at room temperature to ensure complete homogenization. The solution was then filtered using a 0.22 μm filter (EMD Millipore, USA). The particle diameter (Z-average) and charge (□-potential) were measured using a combined dynamic light scattering/particle electrophoresis instrument (NanoZS, Malvern Instruments, Malvern, UK). Samples were with complete DMEM. The prepared OA-TC solutions were then stored at -20 ºC prior to use.

4.2.4 Basolateral 5-ND levels determination

Caco-2 cell monolayer was incubated with different samples for 1, 2, 4, 8 and 24 h in the apical side. After each incubation period, 100 □L of medium was collected from the basolateral side, and 100 □L of fresh complete medium without FBS was added back to the basolateral side. 5-ND in the samples was extracted twice with ethyl acetate and the organic solvent was evaporated using rotary evaporation (SAVANT speedvac, Thermo Fisher Scientific, Pittsburgh, PA). The resulting residue was dissolved into 100 μL mobile phase for HPLC analysis. The 5-ND concentration was determined as we described previously using a HPLC system

(CoulArray®, Chelmsford, MA, USA) equipped with a multi-channel electrical conductivity detector (Model 6210, CoulArray®, Chelmsford, MA, USA) [232].

4.2.5 Cellular levels of 5-ND

After the cells were incubated with different treatments for 24 hours, the Caco-2 cell monolayer was washed with PBS twice, and then 1 mL of trypsin-EDTA solution was added. Until all the cells were suspended, 1 mL of complete media (containing 10% FBS) was used to neutralize the trypsin. The suspension was harvested by pipette and cells were collected by centrifugation (240 rcf, 1 min). The cells were then quickly washed with ice-cold PBS and re-suspended with 1 ml ice-cold PBS. Cellular 5-ND was extracted by sonicating with 30% methanol. After centrifugation at 1700 rcf for 15min, the resulting supernatants were collected for HPLC analysis. Protein levels in each sample were determined using a Bicinchoninic Acid (BCA) Kit (Sigma Chemicals, St Louis, MO), with serum albumin as the standards.

4.2.6 Isolation of lipoprotein particles

Lipoproteins including CMs secreted by Caco-2 cell monolayers were isolated by density gradient ultracentrifugation [164]. After the cells had been incubated with the samples for 24 h, the medium in the basolateral side was collected and transferred to a tube containing saline EDTA [233]. The solution was then mixed with optiprep (60% iodixanol) at the ratio of 4:1(v/v). 9% iodixanol-PBS solution was prepared and gently transferred to the ultracentrifuge tube (Seton, USA).

Appropriate amount of 12% iodixanol-medium solution was slowly injected to the bottom of the ultracentrifuge tube. The lipoproteins were separated by centrifuging at 28,000 rpm for 3 hours in a SW40 rotor (Beckman Coulter, Indianapolis, IN) at 20 ºC. The top 1 mL (d < 1.006 g cm-3) was collected for further analysis, which has previously been reported to contain CMs (CM) and very low-density lipoproteins (VLDL) based on the density (d) of this fraction.

4.2.7 Dual staining of lipoproteins for TEM

Samples were mixed 1:1(v/v) with 4% OsO_4 and fixed for 2 to 5 min before application to a carbon film. Excess sample was removed from the film. A negative stain (1% PTA) was then placed on the surface of the carbon film. After 3 to 5 min, the excess stain was washed by distilled water. The grid was then viewed in a transmission electron microscope (JEOL 100s, Tokyo, Japan).

4.2.8 Statistical analysis

All experiments were carried out at least three times using freshly prepared samples and the results are reported as the calculated mean and standard deviation of these measurements. The difference among samples were analyzed by ANOVA with significance level of $p<0.05$.

4.3 Results

4.3.1 Characterization mixed micelle solutions

In previous studies, bovine serum albumin (BSA) has been widely used to bind free fatty acids and facilitate their delivery to Caco-2 cells [234, 235]. However, more recent research suggested that this may not be a realistic model for cell culture studies, since BSA promotes the assembly of VLDL, whereas bile salts (such as taurocholic acid or TC) promote the formation of CMs[10]. Bile salts are known to play an important role in the digestion and absorption of lipids within the gastrointestinal tract (GIT), and therefore we used TC rather than BSA in this study to better mimic GIT conditions [10]. Under in vivo intestinal conditions, fatty acid delivery to enterocytes is via mixed micelles that contain bile salts; hence OA-TC micelles were prepared. Figure 4-2 shows the OA-TC solution both in PBS buffer and diluted with DMEM for treatment. The solutions formed are optically transparent or only slightly turbid, and were found to contain an even distribution of small particles with diameters ranging from about 5 to 250 nm as determined by both TEM and Zetasizer (Figure 4- 2). The size of these particles suggests that they were most vesicles rather than micelles, since micelles tend to have diameters below about 10 nm. The particles in the mixed micelle solution were found to have a negative charge by particle electrophoresis measurements (= -53.45±0.45mV mV), which can be attributed to the presence of ionized fatty acid and TA molecules, i.e., -COO- groups.

A

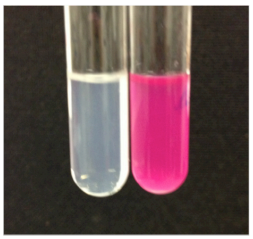

B

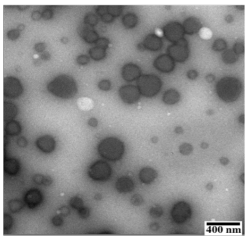

C

Zeta potential	Average size	PDI
-53.45±0.45mV	41.025±0.675	0.364±0.029

D

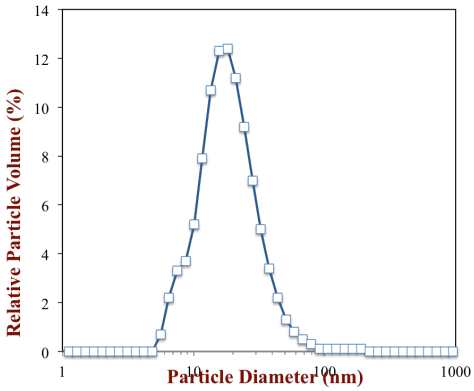

Figure 4-2 Characterization of OA-TC micelle solution (OA and TC were mixed at the ratio of 1.6: 0.5mM):A. OA-TC solution in the PBS (left) and DMEM (right) separately; B. Transmission electron microscope of OA-TC micelle solution; C. Zeta potential, Size and PDI of the OA-TC micelle solution; D. Size distribution based on volume%.

4.3.2 Effect of oleic acid on the integrity of Caco-2 monolayers

Before samples were applied onto Caco-2 cells, the integrity of each well was checked. The TEER values were initially about 260 ± 65 Ω/cm2 (Figure 4-3A), which is indicative of good monolayer integrity. Confluent monolayers were then incubated with 5-ND -OA-TC, 5-ND-TC and 5-ND samples separately for 24 h. The TEER values were measured after 1, 2, 4, 8 and 24 h to evaluate the influence of the samples on the integrity of the cell monolayers. The results showed that the integrity of the Caco-2 cell monolayers did not change appreciably with time during incubation of each of the samples. Moreover, after cells were treated with TC or OA+ TC, there was no obvious difference compared to the control group. This demonstrates that at the concentrations used in this study, OA, TC or 5-ND did not adversely influence the integrity of the Caco-2 cells.

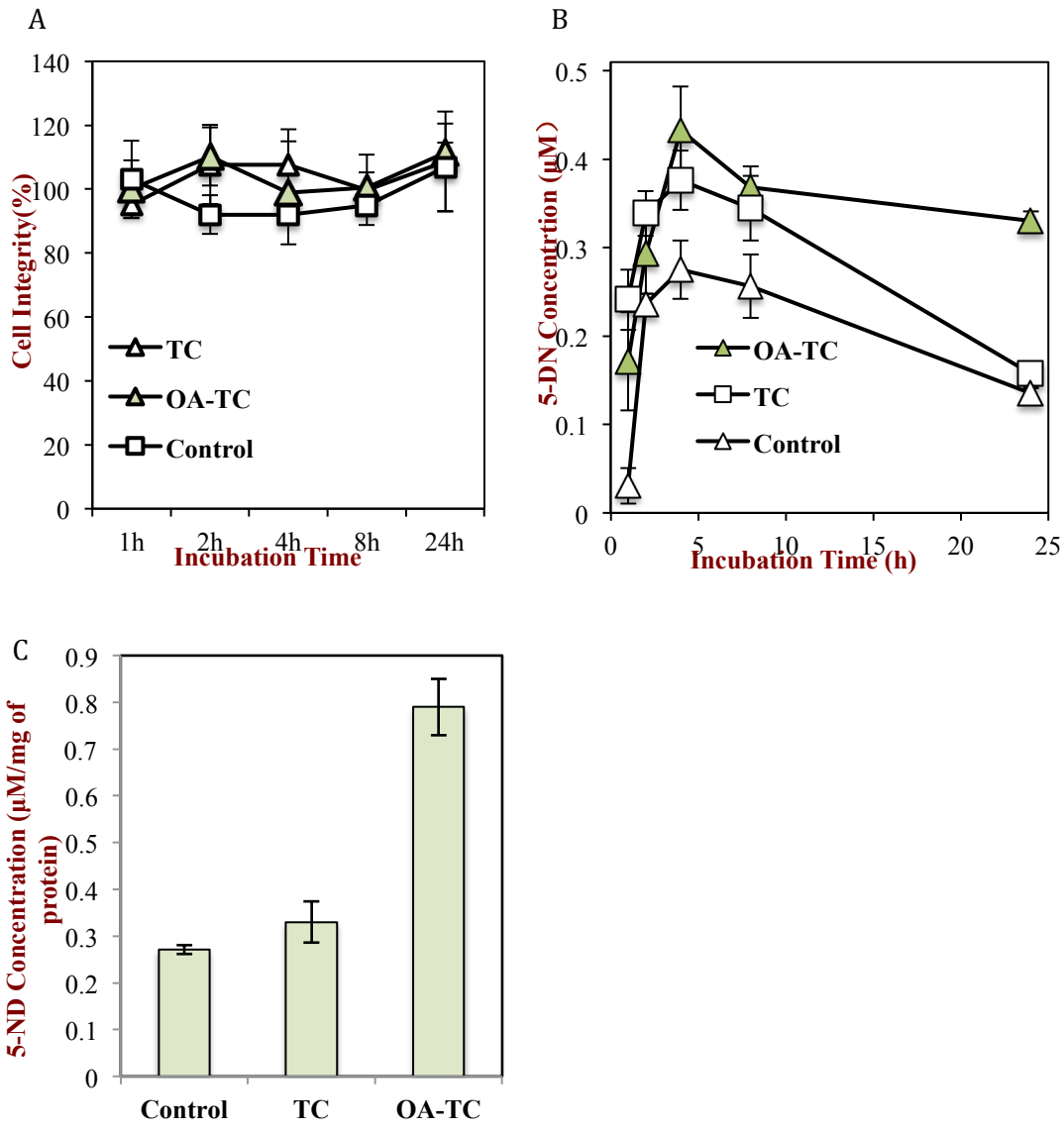

Figure 4-3 Caco-2 cell monolayers exposed to treatments of 1.6 mM OA+0.5 mM TC + 5μM 5-ND, 0.5 mM TC + 5 μM 5-ND, as well as 5 μM 5-ND. Data represent mean ± SD for n=3 experiments: A.TEER was measured at 0h, 1h, 2h, 4h, 8h and 24h. Data represent mean ± SD for n=3 experiments; B. Determination of the concentration of the 5-ND in the basolateral side at 0h, 1h, 2h, 4h, 8h and 24h; C. Cellular accumulation of 5-ND after 24h.Different letters indicate statistical difference among the three groups at the given time point ($P<0.05$).

4.3.3 Transportation of 5-ND across Caco-2 monolayers

We then examined the secretion of 5-ND within the basolateral side of the Caco-2 transwells. Cells were incubated with 5 μM 5-ND, 5-ND-TC and 5-ND-OA-TC separately. The concentration of 5-ND in each well was then measured after 1, 2, 4, 8 and 24 h of incubation. A relatively rapid increase of the 5-ND concentrations in the TC group was observed (Figure 4-3B). Previously, bile salts have been reported to modulate the tight junction and barrier function of Caco-2 monolayers [236]. During the first 2 hours, we observed that the concentration of 5-ND in each group increased rapidly and that the OA-TC mixture improved the absorption of 5-ND without reducing the TEER. At 4 hours, the uptake and secretion of 5-ND in all these groups reached a peak with the OA-TC group having the highest concentration. The 5-ND concentration decreased during incubation from 8 to 24 h, especially for the control group and the TC group, while the OA-TC group did not decline much. Overall, at the 24 h, the accumulated basolateral level of 5-ND was increased about 3-fold in the presence of the OA-TC solution compared to the control, while no difference between TC and the control groups was observed.

4.3.3 Intracellular levels of 5-ND

After incubation for 24 h with different samples, the Caco-2 cells were collected for analysis of the remaining intracellular 5-ND. The level of 5-ND in the OA-TC treated cells was about 3-fold higher than the control (Figure 4-3C). The 5-ND levels in the TC group were similar to that of the control, which suggests that the presence of TC facilitated the transport of 5-ND through the junctions in the

monolayer without improving their uptake by the Caco-2 cells. These results illustrate that the transport of 5-ND into the cells occurs more rapidly and to a greater extent when co-administrated with OA-TC solution.

4.3.4 Formation and secretion of CMs

In this section, we examined whether chylomicron formation was stimulated by the presence of the fatty acids, since CMs are believed to facilitate the transport of bioactive compounds. Electron microscopy was used to detect the presence of lipoproteins in the basolateral side of the Caco-2 cells after 24 hours incubation with OA-TC solutions. Colloidal particles with mean diameters in the range 20 to 150 nm were observed using this method (Figure 4- 4). Based on previous studies, particles with diameters > 70 nm can be considered to be CMs, whereas those with diameters < 70 nm can be considered to be VLDLs [237]. When Caco-2 cells were incubated with the same concentration of 5-ND in the absence of OA-TC mixed micelles, we did not observe any CMs.

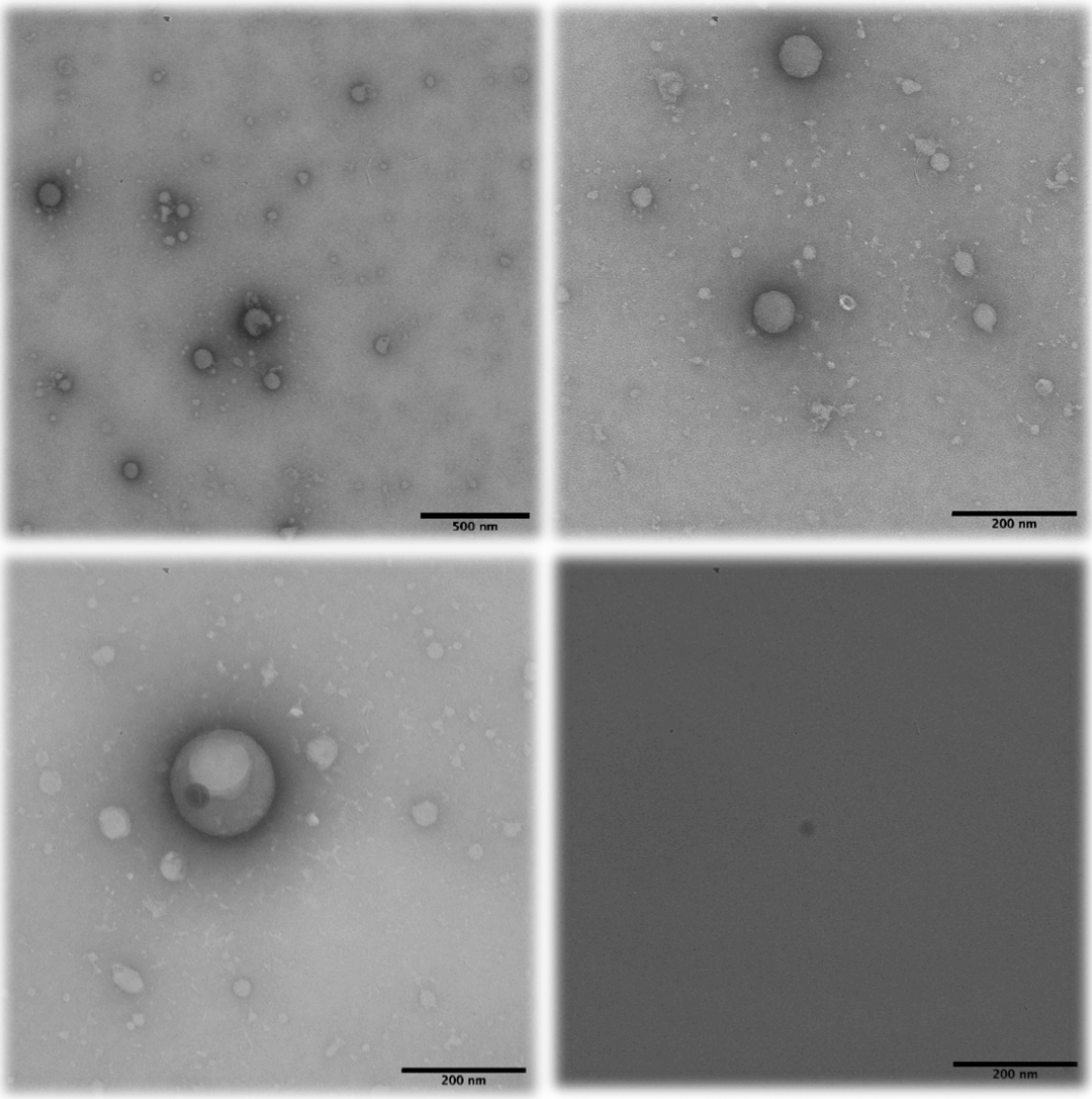

Figure 4-4 Transmission electron microscope (TEM) of lipoproteins (CMs)
A, Lipoproteins; B, Small CMs; C, Large CMs; D, Control.

4.3.5 Size distribution of lipoproteins

Image analysis was used to determine the particle size distribution of the lipoproteins measured by electron microscopy (Figure 4-5). This information was then used calculate the fraction of particles that were CM (≈30%) and VLDL (≈70%),

which corresponds to a VLDL-to-CM ratio of about 7:3. Less than 5% of the particles had diameters below 30 nm.

4.4 Discussion

The Caco-2 cell line is widely accepted as a reliable model for studying the intestinal absorption of lipids and lipoprotein production. We used this model to study the influence of a model fatty acid digestion product (oleic acid) on the absorption and transport of a highly lipophilic bioactive compound (5-ND). Oleic acid is a monounsaturated fatty acid that is commonly present in the lipid phase of foods. Our results showed that the presence of mixed micelles containing oleic acid and taurocholic acid (OA-TC) increased the cellular absorption and transport of 5-ND (Figure 4-3B and Figure 4-3C). We also showed that the presence of OA-TC stimulated the production of lipoproteins, such as CMs and VLDL (Figure 4-4), which would account for the observed effects.

Bioactive lipophilic molecules that are incorporated into CMs are transported into the systemic circulation *via* the lymphatic system, rather than the portal vein, thereby bypassing first-pass metabolism [7]. Previous researchers have identified that oleic acid is able to stimulate synthesis of both apo-B lipoproteins and triglycerides without damaging the monolayer of Caco-2 cells [10, 166]. Since oleic acid is highly hydrophobic, it was necessary to mix it with bile salts (TC) so as to form stable colloidal dispersions that could be applied to the Caco-2 cells. We showed that OA: TC mixed micelle solutions was almost transparent and that they contained relatively small colloidal particles, which were probably vesicles (Figure

4-2). Previous studies suggest that TC may also enhance the expression of apo-B by enterocytes [10]. All experiments in the present study were therefore performed using a molar ratio of 1.6:0.5 OA-to-TC, since this has previously been shown to stimulate maximum amounts of apo-B production in CM fractions [228].

The transepithelial electrical resistance (TEER) is widely used as a means to determine the cell-to-cell integrity of cell culture monolayers. Previous studies showed that the TEER of Caco-2 cell monolayers significantly decreased after being exposed to 5 to 30 mM of oleic acid for 180 minutes [238]. However, our results exhibited little influence of oleic acid on TEER for any of the three treatments studied. This may be related to the relatively low concentrations of OA and TC used in the present study. Our results also demonstrated that 5-ND did not change the integrity of the Caco-2 cell monolayers when used at a concentration of 5 □M.

The presence of TC improved the transport of 5-ND across the cells compared to the control (Figure 4-3B), which can be attributed to its ability to enhance the permeability of the cell monolayer. Nevertheless, the accumulation of 5-ND within the Caco-2 cells was not higher than the control (Figure 4-3C). In addition, the amount of 5-ND present in the basolateral side noticeably decreased at longer incubation times. This may be associated with the metabolism of 5-ND as previously demonstrated in our laboratory[239]. The presence of oleic acid in the mixed micelles appeared to have a transport-enhancing effect: there was an increase in cellular accumulation relative to the control (Figure 4-3C) and an increase in the rate and extent of basolateral 5-ND (Figure 4-3B). One reason is that OA and TC form

mixed micelles (vesicles) that can incorporate 5-ND, thus increasing its solubility and transport within the aqueous phase.

The formation of CMs by the Caco-2 cells was confirmed using electron microscopy (Figure 4-4). Lipoproteins with particle diameters ranging from about 20 to 150 nm were found in the basolateral side of the Caco-2 cells (Figure 4-5), with about 30% of them being CMs and 70% VLDL particles. The presence of these lipoproteins would account for the observed increase in 5-ND transport across the cells. Previous studies have also illustrated that different types of fatty acids affect the number and size of the CMs formed, such as the saturation extent and the chain length [172, 240]. In addition, encapsulation of 5-ND within lipid nanoparticles may improve its bioavailability by inhibiting its metabolism within and outside the cells. We intend to carry out further studies in this area in future.

4.5 Conclusions

In summary, this in vitro study showed a 3-fold enhanced transport of polymethoxyflavones across Caco-2 cells in the presence of model mixed micelles. We postulate that the OA-TC mixed micelles (vesicles) solubilize 5-ND in the apical medium, which facilitates the intracellular uptake of 5-ND by the enterocytes. The presence of oleic acid within the cells stimulates the secretion of CMs that incorporate the lipophilic 5-ND molecules. Chylomicron formation may increase the bioavailability of lipophilic compounds such as 5-ND in a number of ways: (i) increasing the amount that is transported across the cells; (ii) protecting them from metabolism within the cells; (iii) preventing first-pass metabolism in the liver. This

research provides a strong base for further studies on the design of colloidal delivery systems that can increase the bioavailability of lipophilic compounds in foods.

CHAPTER 5

CONTROLLING THE GASTROINTESTINAL FATE OF NUTRACEUTICAL-ENRICHED LIPID NANOPARTICLES: FROM MIXED MICELLES TO CHYLOMICRONS

5.1 Introduction

It is widely recognized that current treatment options for many types of cancer need to be improved. Intravenous delivery of anti-cancer drugs is often painful, inconvenient, and burdensome for patients. In addition, it has been associated with an acute hypersensitivity reaction in patients due to the presence of solubilizers in the drug delivery systems [241, 242]. Oral administration of drugs is therefore considered to be a more convenient and desirable delivery route for patients [243]. However, many pharmaceuticals are so highly lipophilic that they have relatively low oral and variable bioavailability [3, 11]. Hence their potential beneficial health effects are not fully realized due to their poor absorption by the human body. In addition, there is increasing interest in preventing cancer through intake of natural anticancer components present within the diet, i.e., nutraceuticals. Nutraceuticals must be delivered via the oral route as part of foods and beverages, but they may also have poor or variable oral bioavailability, which decreases their potentially beneficial bioactive effects. An effective way to enhance the oral bioavailability of lipophilic bioactive compounds is to encapsulate them within delivery systems containing digestible lipids [3, 14, 244].

Triacylglycerols (TGs) are the most common form of digestible lipid used in lipid-based delivery systems, with over 95% of them being digested in the human

gastrointestinal tract (GIT) [245]. After ingestion, TGs are hydrolyzed by digestive enzymes (lipases) in the stomach and small intestine to form free fatty acids (FFA) and monoacylglycerols (MGs) [245] . These lipid digestion products interact with biological surfactants secreted by the body (phospholipids, bile salts, and cholesterol) to form various nanostructured assemblies collectively known as "mixed micelles" [225, 246]. These mixed micelles have hydrophobic regions capable of incorporating lipophilic bioactive agents. The mixed micelles can then travel through the intestinal lumen, across the mucus layer, and to the apical side of the epithelium cells, where they release their contents for absorption by various passive and active transport mechanisms [247].

After absorption by the epithelium cells, the biological fate of lipophilic molecules depends on their molecular characteristics as well as that of any co-absorbed lipid digestion products [3, 141]. For example, after intracellular trafficking, medium-chain or short-chain fatty acids (MCFAs or SCFAs) directly enter into the portal vein, while long-chain fatty acids (LCFAs) are incorporated into CMs and then transported to the lymph, thus avoiding first metabolism in the liver [101]. A chylomicron (CM) is a biological lipid nanoparticle assembled in the epithelium cells that consists of a hydrophobic core containing TGs and lipophilic bioactives, and a hydrophilic shell consisting of phospholipids and proteins [164].

Previous studies have reported that the formation and properties of CMs depend on the nature of the fatty acids entering the epithelium cells. Monounsaturated fatty acids (MUFAs) and polyunsaturated fatty acids (PUFAs) were found to produce larger CMs than saturated fatty acids (SFAs)[164]. Oleic (C18:1)

and linoleic (C18:2) acids were also reported to promote greater secretion of CMs than steric (C18:0) and palmitic (C16:0) acids [248]. Studies have also shown that the bioavailability of ingested bioactive components depends on the nature of the fatty acids they are ingested with [163, 248]. However, there is not always a close correlation between the bioavailability of lipophilic bioactive agents and the nature of the CMs formed. For example, oleic acid was found to stimulate the formation of larger and more numerous CMs than linoleic acid, but the lymphatic transport of a lipophilic bioactive component (halofantrine) was reported to be higher for linoleic acid than oleic acid [163, 248]. This means that there is not always a simple correlation between the production of CMs and the lymphatic transport of bioactive components.

Our previous research using a Caco-2 cell culture model demonstrated that mixed micelles, consisting of oleic acid and sodium taurocholate, increased the lymphatic transport of an encapsulated lipophilic bioactive agent (polymethoxyflavone) by promoting its incorporation into CMs [249]. The purpose of the current study was to examine the influence of fatty acid type (C18:1, C18:2, C18:3) on the formation and structure of mixed micelles , lipid droplets and CMs, as well as on the incorporation of a bioactive lipophilic agent into the CMs. This study is particularly important as polyunsaturated fatty acids are finding increasing utilization in the human diet because they have been associated with various health benefits, such as protection against coronary heart disease and stroke as well as anticancer effects[250] [251-254]. The knowledge gained from this study could be

used to rationally design lipid-based delivery systems with improved efficacy by oral administration.

5.2 Materials and methods

5.2.1 Materials

The following products were purchased from Sigma Chemicals (St. Louis, MO): 4%OsO_4, oleic acid (C18:1), linoleic acid (C18:2), linolenic acid (C18:3), taurocholic acid (TC), Sulfatase from Heli pomatia, phosphatungstic acid (PTA) and OptiprepTM density gradient medium. All other chemicals and solvents were of analytical grade and were obtained from Fisher Scientific (Pittsburgh, PA). Apolipoprotein B (Apo B) human Elisa kit was purchased from Abcam (Cambridge, MA).

5.2.1 Cell culture preparation

Caco-2 cells (passage 55~65) were cultured in complete Dulbecco's modified essential medium (DMEM) containing high glucose, 10% fetal bovine serum (FBS), 1% antibiotic, and 1% amino acids. For experiments, cells were seeded at 3×105 cells/mL on transwells (Corning Inc., MA, USA) containing polyester filters (3 □m pore size and 4.7 cm^2 surface area) and grown for 21 days. The transepithelial electrical resistance (TEER) was then measured at 37 °C using a Millicell® ERS-2 epithelial voltammeter (World Precision Instruments, Sarasota, FL). Data are expressed as Ω×cm^2. Before the start of different fatty acid treatments, Caco-2 monolayers were washed and incubated for 4 h with serum-free complete medium as described previously [249].

5.2.2 Model mixed micelle preparation

Model mixed micelles containing different types of fatty acids were prepared using a method described previously [249]. Three types of model mixed micelles were prepared: oleic acid-sodium taurocholate (C18:1-TC); linoleic acid-sodium taurocholate (C18:2-TC) and linolenic acid- sodium taurocholate (C18:3-TC), with the same fatty acid-to-TC molar ratio of 1.6:0.5. A known amount of fatty acids was added to a TC solution and then mixed with a sonicator at around 4 ºC. The solutions were then swirled overnight under a nitrogen atmosphere before being stored at -20 ºC prior to use. The particle diameter (Z-average) and charge (-potential) were measured using a combined dynamic light scattering/particle electrophoresis instrument (Nano ZS, Malvern Instruments, Malvern, UK). Samples were diluted with DMEM solution prior to measurement.

5.2.3 Determination of 5-DN and its metabolites

Caco-2 cells were incubated with C18: 1-TC-5-DN, C18: 2-TC-5-DN, C18: 2-TC-5-DN and 5-DN separately. Aliquots of basolateral solution (100 μL) were collected at 1, 2, 4, 8 and 24 h, and replaced with similar amounts of DMEM solution each time. The apical solution and the cells were also collect after 24 h. 5-DN and its metabolites (5, 3'-dihydroxy-6, 7, 8, 4'-tetramethoxylflavone (5,3’-DHTMF) and 5, 4'-dihydroxy-6, 7, 8, 3'-tetramethoxylflavone (5,4’-DHTMF)) in the samples were extracted twice with ethyl acetate and the organic solvent was evaporated using rotary evaporation (SAVANT speedvac, ThermoFisher Scientific, Pittsburgh, PA). Same samples were also incubated with certain amount of sulfatase solution in

water bath to release the conjugated metabolites before being extracted by ethyl acetate. The resulting residue was then dissolved into 100 μL mobile phase for HPLC analysis. The 5-DN concentrations were determined using a HPLC system (CoulArray®, Chelmsford, MA, USA) equipped with a multi-channel electrical conductivity detector (Model 6210, CoulArray®, Chelmsford, MA, USA) [232].

5.2.4 Isolation characterization of lipoprotein by TEM

Lipoproteins secreted in the basolateral side were isolated by density gradient ultracentrifugation [164]. The basolateral preserved in saline EDTA was mixed with optiprep (60% iodixanol) at the ratio of 4:1(v/v). Then 9% idoixanol-PBS was layered on top. The lipoproteins were separated by centrifuging at 28,000 rpm for 3 hours in an ultracentrifuge (SW40 rotor, Beckman Coulter, Indianapolis, IN) at 20 ºC. The top 1 mL (d < 1.006 g cm-3) was collected for further analysis. Dual staining of lipoproteins was used for transmission electron microscope (TEM, Philip, tecnai 12) with 4% OsO4 and then 1% PTA. The grid was then viewed in the TEM.

5.2.5 Apolipoprotein B analysis.

The medium in the basolateral side was collected and centrifuged at 2000 g for 10 minutes to remove debris. Supernatants were collected and concentrated in Vivaspin tubes and then stored at -20 °C for use. Cells in the tranwells after 24 h treatment were rinsed and scraped into a tube with 5 ml cold PBS containing 0.5M EDTA. The suspension was then centrifuged at 1000 rpm for 10 min at 4 °C and the supernatant was collected. The cells were then lysed to release the proteins and the

supernatant was collected after centrifugation at 13000 rpm for 30 min at 4 °C. Apo B was detected using a specific ELISA kit (ab108807, UK).

5.2.6 Transmission Electron microscopy.

Transmission electron microscopy (TEM) was used to visualize intracellular changes in lipid structure and distribution within Caco-2 monolayers. Cells were exposed to different treatments for 24 h before being fixed and prepared for electron microscopy according to Leonard et al[255]. Sections were then examined in the transmission electron microscope.

5.2.7 Statistical analysis.

All values are expressed as mean±standard deviation (SD) unless stated otherwise. The difference among samples were analyzed by ANOVA with significance level of $p<0.05$.

5.3 Results

5.3.1. Morphologies of mixed micelles.

The mean diameter mixed micelles was around 60 nm and their electrical charge (zeta-potential) was around -50 mV for each type of mixed micelle. As shown in Figure 5-1, simple micelles, uni-lamellar vesicles, bi-lamellar vesicles, and multi-lamellar vesicles coexisted in all the mixed micelle systems formed. These structures have previously been shown to increase the solubility of lipophilic compound in

intestinal fluids[256, 257]. Interestingly, the degree of unsaturation of the initial fatty acids did not have a major impact on the nature of the mixed micelles formed.

A

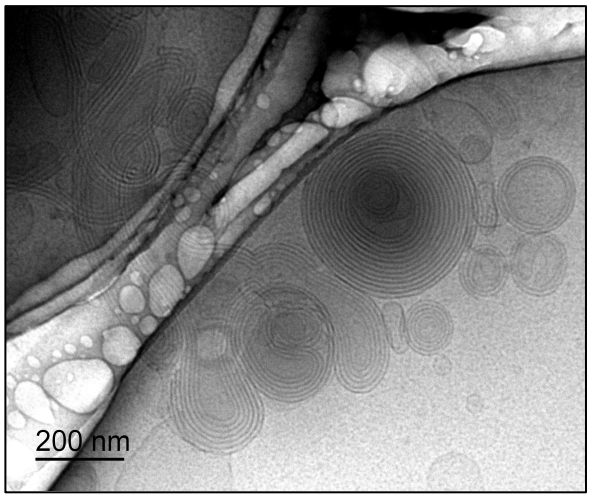

B

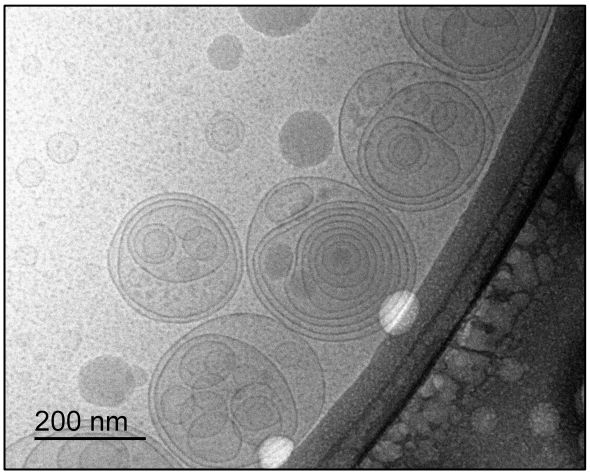

C

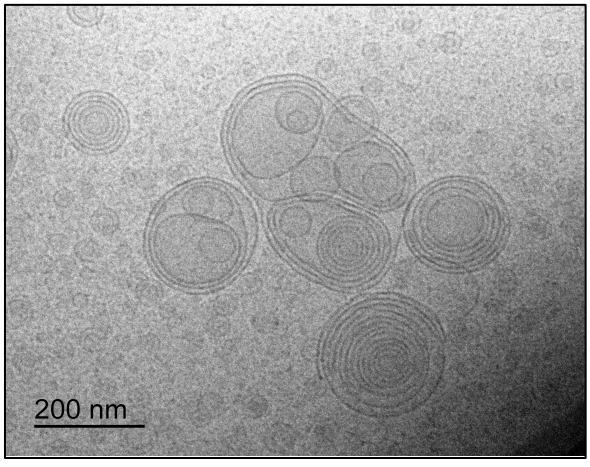

Figure 5-1 Morpholgies of C18: 1-TC-5-DN (A), C18: 2-TC-5-DN (B) and C18: 3-TC-5-DN (C) mixed micelle by cryo-TEM.

5.3.2. Transport of 5-DN

Caco-2 cell monolayers were incubated with model mixed micelles containing different types of unsaturated fatty acids. A fixed volume of media in the basolateral side was collected after 1, 2, 4, 8 and 24 h' incubation, and replaced with a similar volume of FBS-free complete DMEM. 5-DN and its metabolites in the DMEM were then extracted and analyzed by a method we used previously [239]. The basolateral concentration of 5-DN was around 7-fold higher than the control for the mixed micelles containing C18: 1, and around 4-fold and 3-fold higher for the mixed micelles containing C18: 2 or C18: 3 (Figure 5-2A). During the first hour, the level of 5-DN in all the fatty acid treated groups significantly increased compared to the control, with the largest increase being for the C18: 1 samples (Figure 5-2A). From 2 to 8 h, a steep increase in the amount of 5-DN absorbed occurred in all groups including the control group. After 24 h, the 5-DN concentrations decreased appreciably for the control group, but remained relatively constant for the samples containing unsaturated fatty acids. We hypothesized that this decrease in 5-DN occurred due to metabolism within the Caco- 2 cells, and therefore we measured the concentration of the metabolites formed (Figures 5-2B & 2C). A significant increase in the levels of 5,3'-DHTMF and 5,4'-DHTMF were detected in the control group indicating that some metabolism of 5-DN had indeed occurred. On the other hand, far less metabolites were found in the samples containing the unsaturated fatty

acids. Moreover, we found nearly half of the metabolites are conjugates (Figures 5-2B & 2C).

A

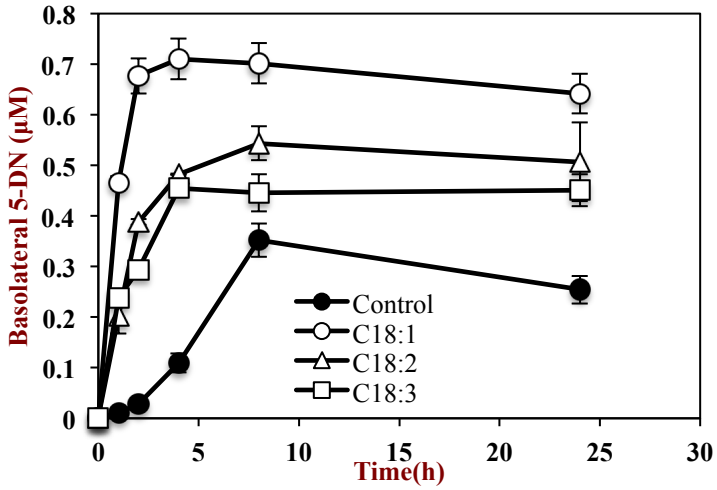

B

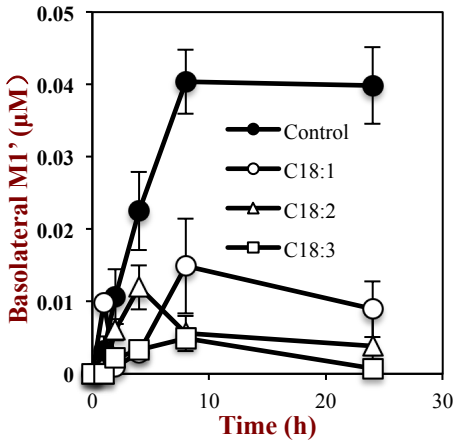

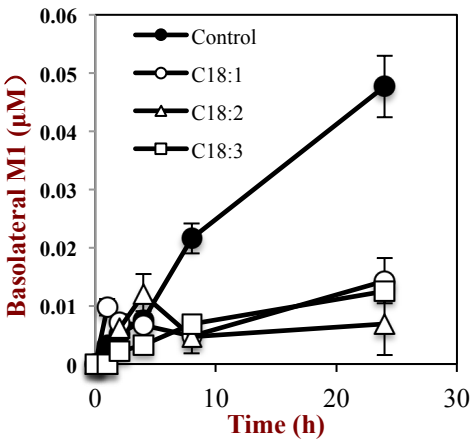

C

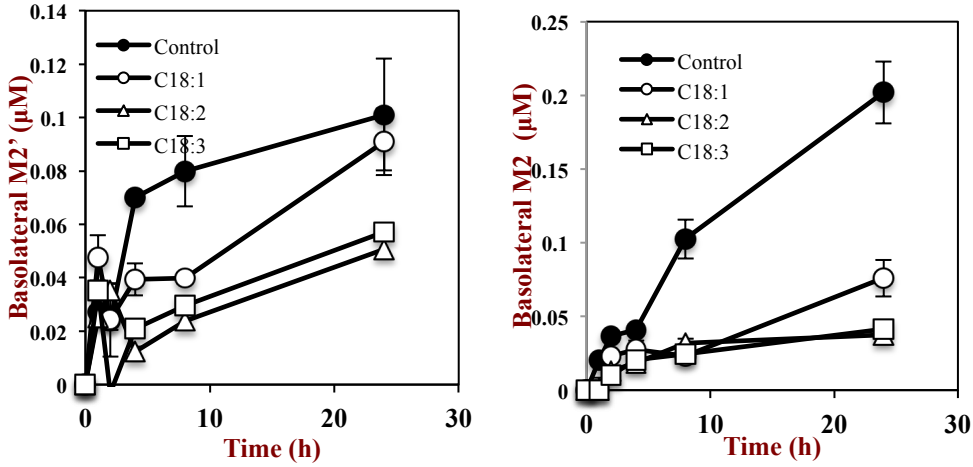

D

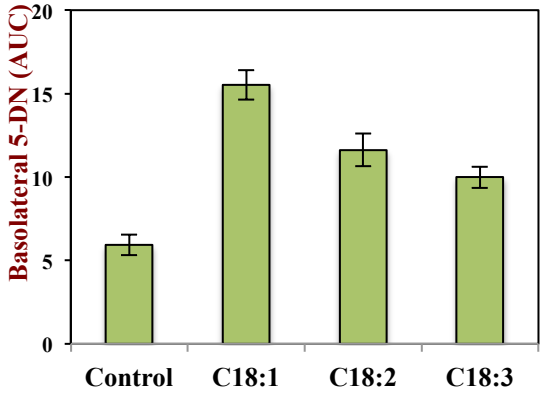

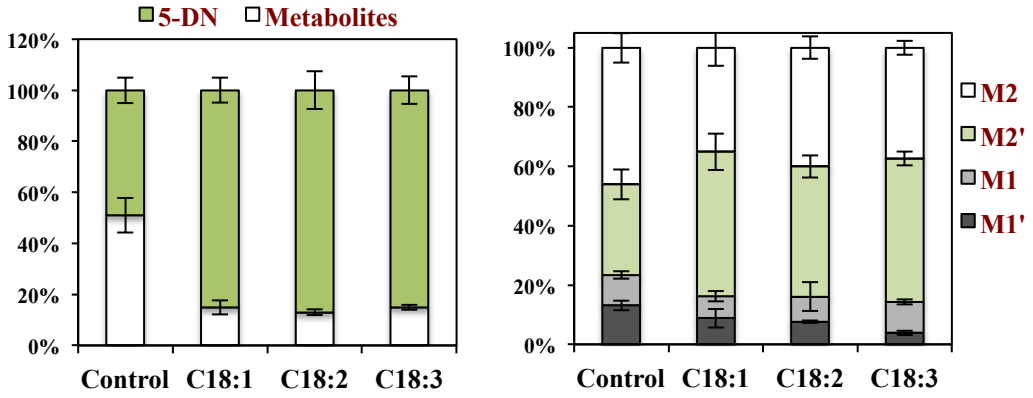

Figure 5-2 Determination of the concentration of the 5-DN and its metabolites (5,3'-DHTMF and 5,4'-DHTMF) in the basolateral side at 1h, 2h, 4h, 8h and 24h: A.Levels of 5-DN; B. Levels of (5,3'-DHTMF) (conjugates & non-conjugates); C. Levels of 5,4'-DHTMF (conjugates & non-conjugated). D. Percentage of metabolites. Data represent mean ± SD for n=3 experiments. Different letters indicate statistical difference ($P<0.05$).

5.3.3 Apical and intracellular levels of 5-DN

The apical levels of 5-DN were also detected after 24 h incubation to provide a measure of how much was not transported into the cells. The remaining concentration of 5-DN in the apical cell decreased in the following order: control > C18:3 > C18:2 > C18:1 (Figure 5-3A). These results show that mixed micelles increased the uptake of the lipophilic bioactive agent into the cells, and that the extent of the increase grew as the degree of unsaturation decreased. The level of the metabolites 5,3'-DHTMF and 5,4'-DHTMF and their conjugated form in the apical solution were also measured after incubation (Figure 5-3B). No significant differences were found between the mixed micelle groups and the control group, which suggests that metabolism mainly occurs within the cells rather than in the apical solution.

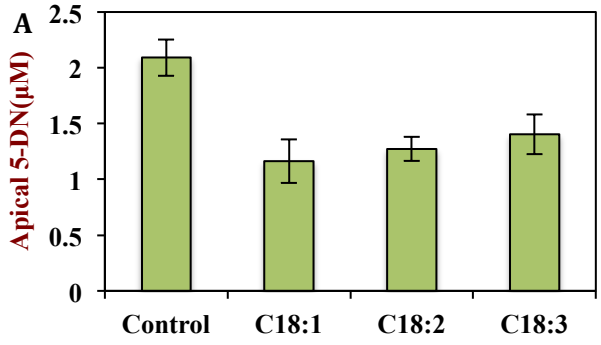

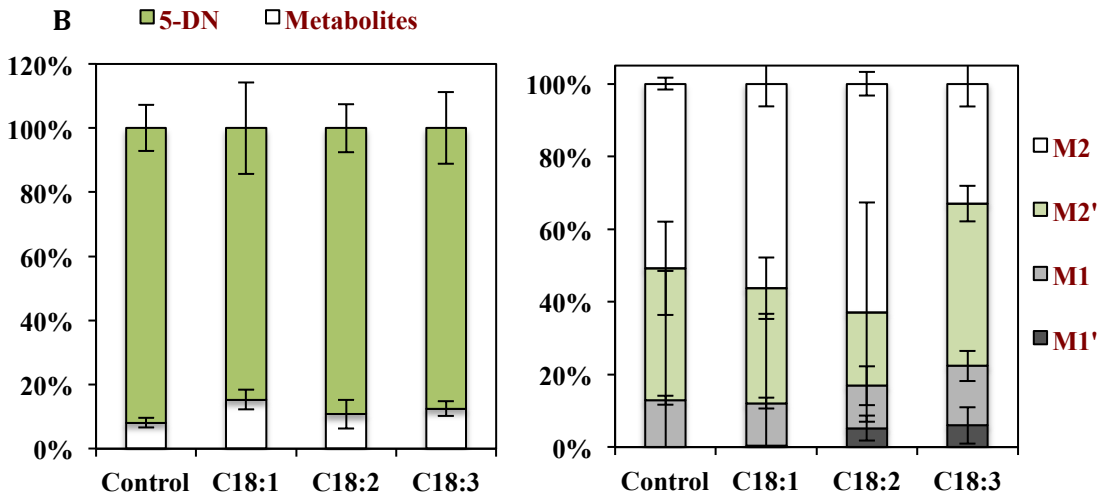

Figure 5-3 Levels of 5-DN (A) and its metabolites (B) remaining in the apical side of the transwells after 24h's incubation of C18: 1-TC-5-DN, C18: 2-TC-5-DN, C18: 3-TC-5-DN and Control (5-DN). Data represent mean ± SD for n=3 experiments. . Different letters indicate statistical difference ($P<0.05$). "NS" represents no significant difference between groups.

The intracellular levels of 5-DN after incubation with different formulations are shown in Figure 5-4. Significant differences were found between the mixed micelle group and the control (Figure 5-4A). Moreover, the metabolism of the 5-DN also decreased when it was incorporated into the mixed micelles (Figure 5-4B). Among the experimental groups, the mixed micelles containing oleic acid (C18:1) exhibited the most effective enhancement of 5-DN absorption.

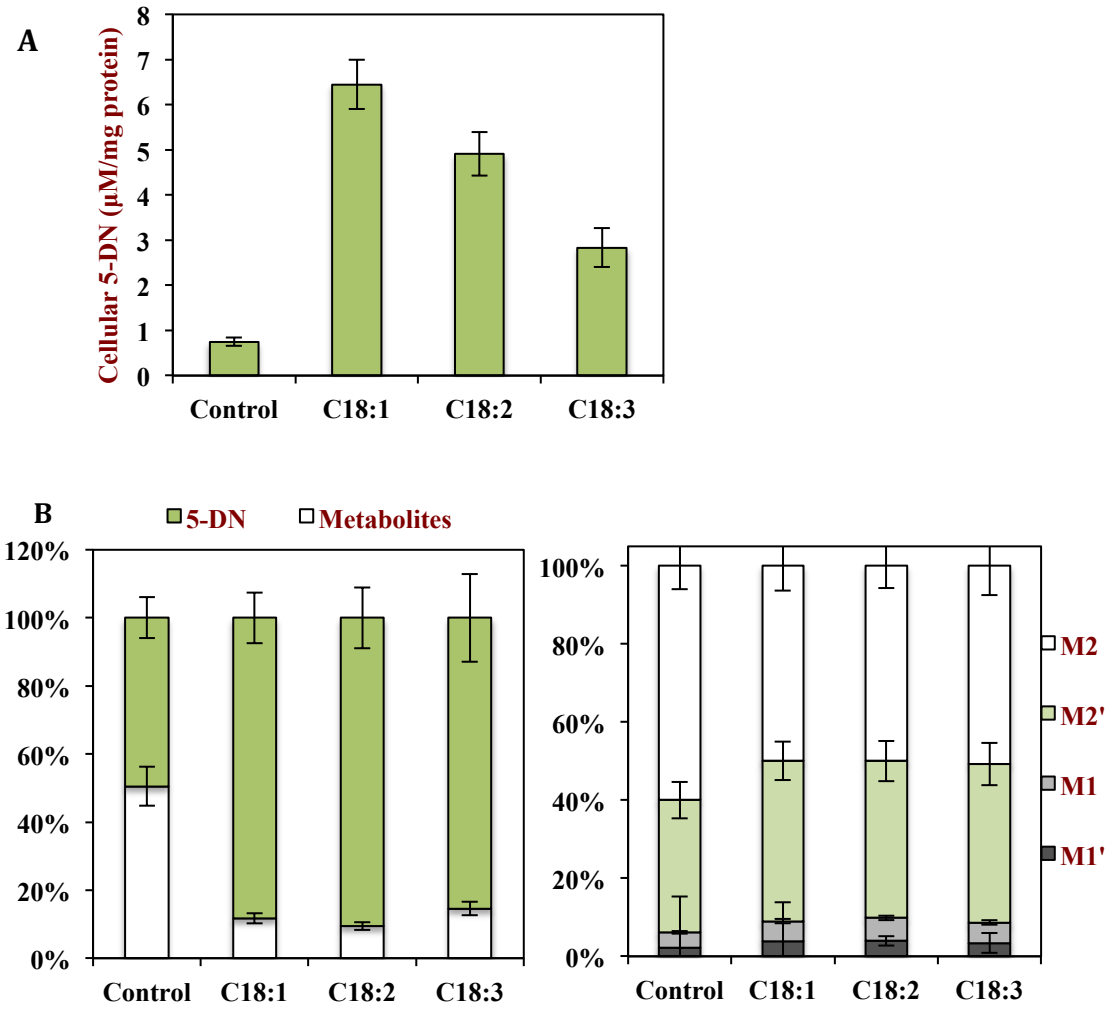

Figure 5-4 Cellular levels of 5-DN (A) and its metabolites (B) after 24h's incubation of C18: 1-TC-5-DN, C18: 2-TC-5-DN, C18: 3-TC-5-DN and Control (5-DN). Data represent mean ± SD for n=3 experiments. Different letters indicate statistical difference ($P<0.05$).

5.3.4 Biological nanoparticles formation

We examined whether the degree of unsaturation of the fatty acids affected the formation and secretion of lipoprotein particles, such as CMs. Previous studies have demonstrated that unsaturated fatty acids are more potent at stimulating the formation and secretion of large lipoprotein particles than saturated fatty acids [166]. Studies have also shown that monounsaturated fatty acids (C18:1) are more

effective at promoting chylomicron or very low density lipoprotein formation than polyunsaturated fatty acids (C18:2 and C18:3) [171]. TEM was used to observe the morphology of the lipoproteins secreted by Caco-2 cell model after different treatments, as well as to observe changes in the morphology of the Caco-2 cells (Figure 5-5). Viable enterocytes were observed in all the groups with mature microvilli as well as the presence of cytosolic lipid droplets in the mixed micelle groups. Cytosolic lipid droplets, with diameters around 1 to 4 μm, have been considered to be important contributors to the control of postprandial triglyceridemia as their lipid content will be ultimately transported from the epithelium cells as CMs[258]. After 24 h, the cells incubated with mixed micelles containing C18: 1 and C18: 2 formed more numerous and larger sized lipid droplets than those incubated with mixed micelles containing C18: 3.

For the control sample, there was little evidence of the formation of large numbers of lipid droplets within the Caco-2 cells, or secretion of lipoproteins (Figure 5-5). All mixed micelles promoted the formation of lipid droplets and lipoproteins, but the samples containing C18: 1 stimulated the formation of larger ones than those containing C18: 2 or C18: 3. Image analysis was used to determine the particle size distribution of the lipoproteins measured by electron microscopy (Figure 5-5). Based on previous studies, particles with diameters from 75 to 1200 nm can be considered to be CMs, whereas those with diameters from 30 to 80 nm can be considered to be VLDLs [141]. The volume of large lipoproteins was more than 80% of the total particles after C18: 1 treatment versus 60% for either C18:2 or

C18:3. This result suggests that more CMs were formed for the monounsaturated mixed micelles than for the polyunsaturated ones.

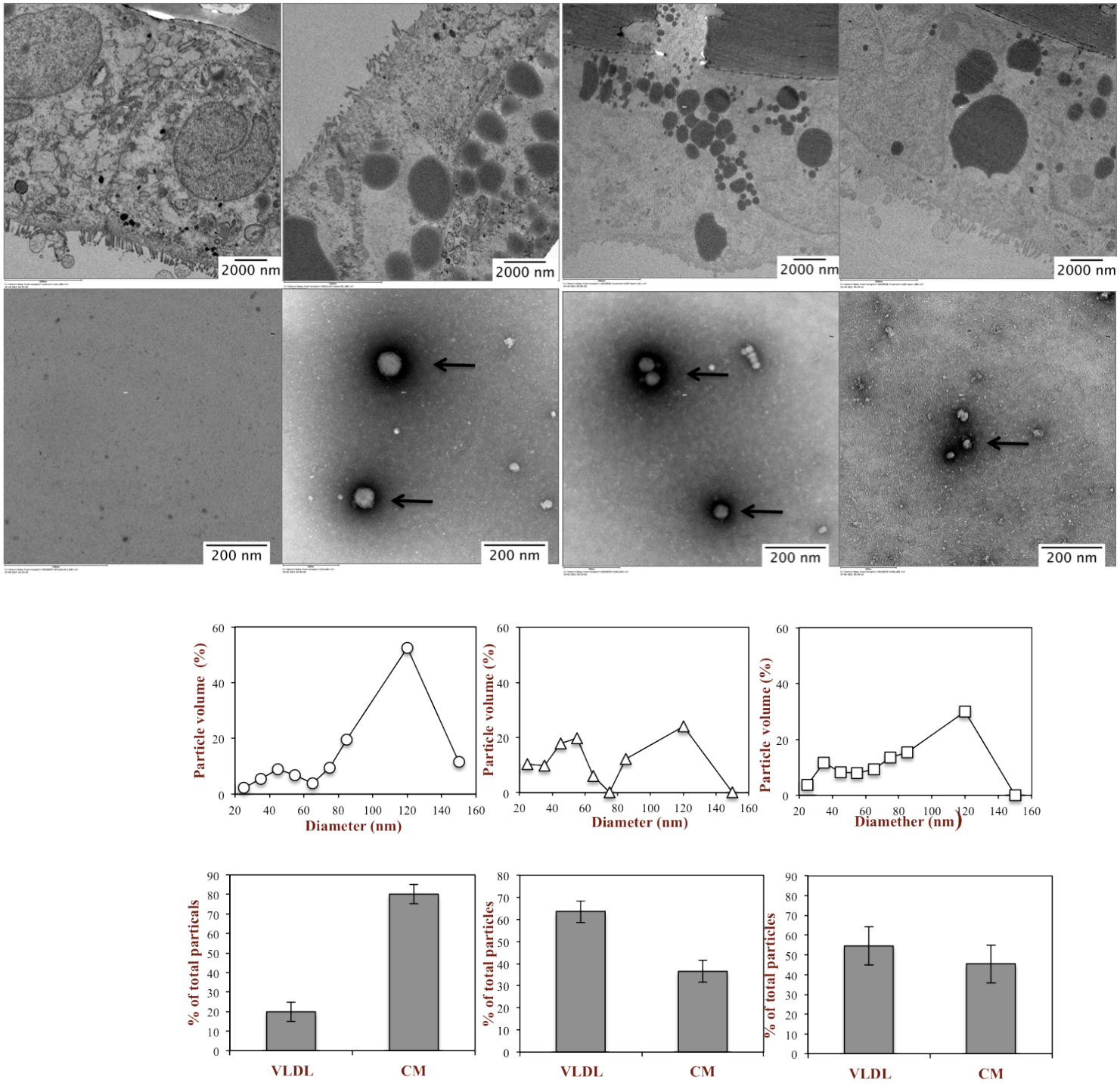

Figure 5-5 Morphology of mixed micelles, lipid organelles in Caco-2 monolayers and secreted CMs after incubation of different unsaturated fatty acids base mixed

micelles for 24h by TEM. Size distribution of lipoproteins secretion by the Caco-2 monolayer is analyzed.

5.3.5 Apolipoprotein B determination.

Apo B secretion in both the cellular and basolateral side was determined after the cells were exposed to the control or to mixed micelles containing different unsaturated fatty acids. Notably, all the mixed micelle groups increased Apo B secretion compared to the control in the basolateral side. However, the cells treated with C18: 3 showed a lower secretion of Apo B than the cells exposed to C18:1 or C18:2 (Figure 5-6A). Moreover, we also observed that all three fatty acids increased the cellular Apo B level, with the C18: 1 sample being the most effective (Figure 5-6B).

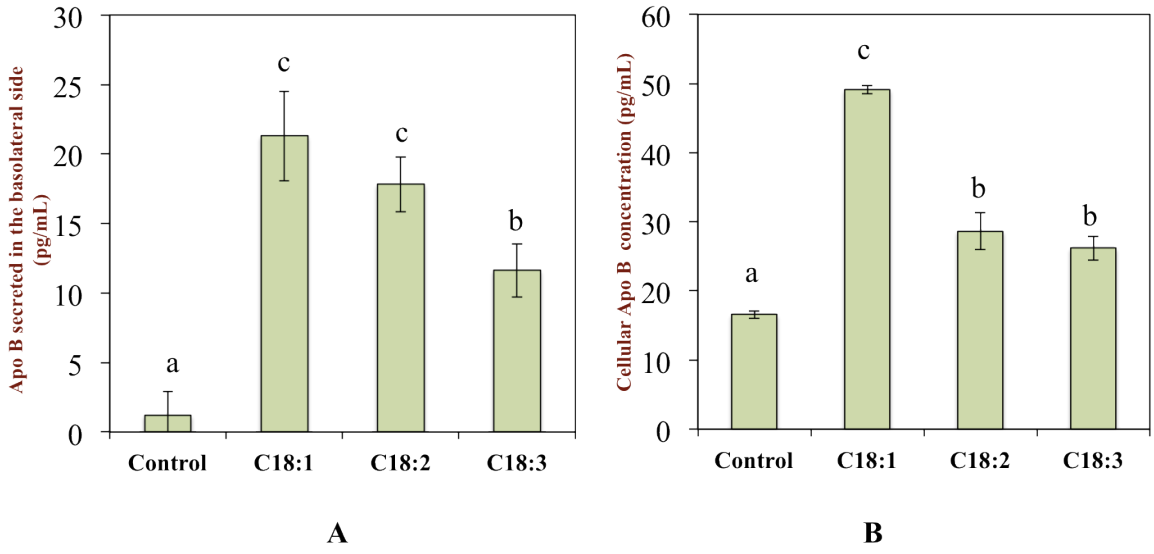

Figure 5-6 Basolateral and cellular Apo B concentration were detected after cells were incubated with different groups by ELISA kit. Data represent mean ± SD for n=3 experiments. Different letters indicate statistical difference ($P<0.05$)

5.4 Discussion

In this study, we have examined the influence of unsaturated fatty acid type on the formation of mixed micelles as well as the absorption, metabolism, and lipoprotein incorporation of 5-DN using a Caco-2 monolayer model. In addition, we have examined the influence of fatty acid type on the morphologies and levels of lipid droplets and lipoproteins formed by Caco-2 cells.

Our previous research found that co-administration of C18: 1 with 5-DN increased the bioavailability of this lipophilic nutraceutical. Our current study showed that both C18: 2 and C18: 3 can also enhance the absorption of 5-DN and its incorporation into CMs (Figure 5-2). In addition, these fatty acids did not have an appreciable impact on monolayer integrity (Figure 5-1), which suggests that there was little damage to the cell monolayer and the tight junctions [259]. Having said this, we did observe a slight decrease in the TEER value after 24h incubation with mixed micelles containing C18: 3. Previous studies have reported that n-3 fatty acids can enhance tight junction permeability [260], which may account for the slight decrease observed in our study. Hence, a slightly higher fraction of 5-DN may have been able to pass through the tight junctions for this sample, thereby avoiding exposure to enterocyte enzymes, which are responsible for the metabolism of 5-DN.

All three unsaturated fatty acids increased the transport of 5-DN into and across the Caco-2 cells compared to the control, with the C18: 1 sample being the most effective (Figures 5-2A & 2B). This effect was attributed to the fact that the fatty acids formed mixed micelles that enhanced the solubility of the lipophilic bioactive component in the aqueous apical solution, and because they promoted the

formation of biological lipid nanoparticles (CMs and VLDL) that can transport the bioactive compounds across the cells. In addition, the extent of metabolism of 5-DN was reduced when it was incorporated into CMs when compared to the control. This result suggests that 5-DN trapped within the hydrophobic interior of lipid droplets or CMs is partially protected from the metabolic enzymes in the cytosol of the cells. These results demonstrated that unsaturated fatty acids improved the absorption and transport of 5-DN, as well as inhibiting its metabolism by formation of lipid droplets or lipoproteins (Figure 5-5).

The mixed micelles formed by different fatty acids contained colloidal particles with single layer or laminar structures. These particles have hydrophobic regions that can solubilize 5-DN, thereby increasing its solubility within gastrointestinal fluids and enhancing its absorption from the small intestine. Electron microscopy indicated that all of the enterocytes had mature microvilli, and that cytosolic lipid droplets were formed within them when they were incubated with mixed micelles containing unsaturated fatty acids (Figure 5-5). These lipid droplets have previously been reported to be the result of fusion of oil droplets formed during triacylglycerol biosynthesis [261, 262]. The dimensions and amount of lipid droplets formed depended on the unsaturation of the fatty acids in the mixed micelles: C18:1 promoted the formation of a relatively high amount of lipid droplets, which had diameters around 1 to 4 μm; C18:2 promoted the formation of a similar amount of lipid droplets but they had smaller dimensions; C18:3 led to the formation of fewer lipid droplets but with some relatively large ones (Figure 5-5). We also found that the morphologies of the lipoproteins secreted by the model epithelium cells

depended on fatty acid type. The dimensions of the lipoproteins produced in the presence of C18: 1 and C18 2 were significantly larger than those produced in the presence of C18:3 (Figure 5-5). Previous studies have also highlighted the efficacy of C18: 1 for stimulating the formation and secretion of CMs [263]. While C18: 3 resulted in lower chylomicron production and faster clearance in the blood based on the in vivo experiments [264]. The formation of CMs is also associated with the enterocyte-based metabolism of 5-DN, since the incorporation of 5-DN in lipoproteins will avoid it being exposed to metabolic enzymes on the smooth endoplasmic reticulum (SER) [7, 265].

The detection of Apo B within the cells and on the basolateral side indicated that lipoproteins were assembled in the cells and transported out of them (Figure 6). The amount of Apo B produced decreased as the degree of unsaturation of the fatty acids increased, which is indicative of decreasing amounts of CMs being formed as the number of double bonds in the fatty acids increases. Previous studies have also reported that unsaturated fatty acids are capable of elevating Apo B secretion by Caco-2 cells [166], with polyunsaturated fatty acids being less effective [170]. As a result, the metabolic fate and distribution of these compounds within the human body may be changed. After the CMs are excreted into the lymph, they will directly enter the systemic circulation instead of undergoing first pass metabolism in the liver. Usually, it takes a few hours of circulation in the blood before chylomicron clearance [264]. This may allow these biological nanoparticles to interact with tumors through the “enhanced permeability and retention” (EPR) effect, since nano-sized particles have been shown to be more efficacious in animal models of cancer

[266]. The possibility of using lipoproteins, such as LDL and HDL, as a strategy for combating cancer has recently been highlighted [243]. CMs as natural nanoparticles that move through the systemic circulation may also be potential carriers of anticancer agents also. Based on our research, we can control the behavior of CMs by regulating the fatty acids composition in the oral delivery system or food matrix.

5.5 Conclusion

In conclusion, our study has shown that a long chain monounsaturated fatty acid (C18: 1) was most effective at improving the bioavailability of a lipophilic nutraceutical (5-DN). This increase in bioavailability was attributed to two effects: (i) an increase in the amount of 5-DN transported across the cells; (ii) a reduction in the amount of 5-DN that underwent metabolism. Polyunsaturated fatty acids (C18:2 and C18:3) also increased the bioavailability of this nutraceutical, but were slightly less effective than the unsaturated one (C18:1). This study provides important information for the creation of lipid-based delivery systems designed to increase the oral bioavailability of lipophilic compounds in foods and drugs. Since these are "natural" nanoparticles in the body, it may also provide a new route for cancer therapy or diagnosis.

CHAPTER 6

DESIGN OF NANOEMULSION-BASED DELIVERY SYSTEMS TO ENHANCE INTESTINAL LYMPHATIC TRANSPORT OF LIPOPHILIC BIOACTIVES: INFLUENCE OF OIL PHASE TYPE

6.1. Introduction

Many nutraceuticals found in foods are highly hydrophobic substances with low oral bioavailability, such as carotenoids, curcuminoids, and flavonoids [1, 267]. For this reason, the potential health benefits of these nutraceuticals may not be fully realized. In the pharmaceutical area, it is well established that ingestion of hydrophobic drugs as part of lipid-based delivery systems or in conjunction with lipid-rich foods enhances their oral bioavailability [3], especially those drugs that have high permeability in the small intestine [268]. Several physicochemical and physiological factors have been identified as important in determining the overall oral bioavailability of hydrophobic substances: bioaccessibility; absorption; and transformation [4]. Lipids enhance the solubilization of hydrophobic bioactives in the gastrointestinal fluids by forming mixed micelles consisting of bile salts, phospholipids, fatty acids, and monoacylglycerols [5, 6]. They may also enhance the subsequent absorption of hydrophobic bioactives by altering cell membrane permeability. Finally, the presence of co-ingested lipids may alter the absorption route of nutraceuticals by stimulating the formation of chylomicrons within the epithelium cells [3, 6, 7]. These chylomicrons can incorporate highly lipophilic

molecules and transport them into the systemic circulation via the lymphatic pathway, thereby avoiding first pass metabolism in the liver.

Recently, nanoemulsion-based delivery systems have been developed to encapsulate lipophilic bioactive components and to improve their oral bioaccessibility [23, 269, 270]. For example, in vitro studies using a simulated gastrointestinal tract have shown that the bioaccessibility of curcumin, □-carotene, and vitamin E can be greatly increased by delivering them in well-designed nanoemulsions [110, 198, 200]. The functional properties of nanoemulsion-based delivery systems can be tuned by changing their structures and compositions. Typically, the oral bioavailability of lipophilic bioactive components is highest when they are encapsulated in lipid droplets with smaller dimensions [212, 271]. The nature of the lipid carrier oil has also been shown to play a fundamental role in determining bioavailability. Indigestible lipids (such as orange oil) reduce the bioaccessibility of hydrophobic bioactives in the GI tract because they may not release them, and because they do not contribute to the formation of mixed micelles. Delivery systems containing short or medium chain triglycerides (SCTs or MCTs) may be readily digested, but they may still give low bioaccessibility because they do not form mixed micelles with a high solubilization capacity [71]. On the other hand, delivery systems containing long chain triglycerides (LCT) may be digested and form mixed micelles that can solubilize lipophilic bioactives, thereby leading to a high bioaccessibility. In addition, LCTs are more effective than SCTs or MCTs at stimulating the formation of chylomicrons within the epithelium cells, which

facilitates absorption via the lymphatic route (rather than the portal vein) and reduces first pass metabolism.

Most previous research on utilizing lipid-based delivery systems in the food science area has focused on improving the stability of bioactive components within foods, or on increasing their bioaccessibility in the GI tract. Studies on designing nanoemulsions to enhance bioactive absorption and reduce bioactive transformation are still rather limited. In this article, we therefore investigated the effect of lipid phase properties (MCT versus LCT) on digestion, bioaccessibility, and absorption of 5-DN using an in vitro digestion model combined with a Caco-2 cell monolayer model. We used sodium caseinate as an emulsifier since it is widely used to stabilize emulsions in the food industry [14]. The results of this study will facilitate the rational design of nanoemulsion-based delivery systems for incorporating lipophilic nutraceuticals into functional foods and beverages.

6. 2. Materials and Methods

6.2.1. Materials

Osmium tetroxide (4% OsO_4), phosphatungstic acid (PTA), Nile red, fast green, pepsin from porcine gastric mucosa, lipase from porcine pancreas pancreatin, casein (sodium salt), and Optiprep™ density gradient medium were obtained from Sigma Chemicals (St. Louis, MO). Apolipoprotein B (Apo B) human Elisa kit was purchased from Abcam (Cambridge, MA). 5-DN was extracted from citrus fruit in our laboratory. Medium chain triglycerides (MCT) were purchased from Coletica (Northport, NY). Canola oil, purchased from a local supermarket, was used as an

example of long chain triglycerides (LCTs). All other chemicals and solvents were of analytical grade and were obtained from Fisher Scientific (Pittsburgh, PA). Double distilled water was used for the preparation of all solutions and emulsions.

6.2.2. Determination of oil phase fatty acid composition

LCT and MCT were analyzed using a gas chromatograph equipped with flame ionization detector (GC-17A; Shimadzu corporation, Kyoto, Japan) using DB-23 column (30 m × 0.25mm i.d., 0.25 μm, Agilent technologies, J.W. Scientific, Santa Clara, CA, USA). Heptadecanoic acid (C17:0) was used as an internal standard.

6.2.3. Emulsion preparation

An oil phase was prepared by dissolving 5-DN in an appropriate carrier oil (MCT or LCT). An aqueous phase was prepared by dispersing emulsifier (1% sodium caseinate) in aqueous buffer solution (10 mM sodium phosphate, pH 7.0). Oil-in-water emulsions were prepared by blending the oil and water phases together using a high shear mixer and then passing them through a high pressure homogenizer (Microfluidizer, Microfluidics, Newton, MA, USA) for 3 passes at 15,000 psi.

6.2.4. Simulated gastrointestinal tract model

Each emulsion sample was then passed through a three-step simulated gastrointestinal tract model, which includes a mouth, gastric, and small intestine stage. Simulated saliva fluid (SSF), gastric fluid (SGF), and intestinal fluid (SIF) were prepared as described previously [267]. The particle size, charge (□-potential), and morphology were detected at each stage by dynamic light scattering and

electrophoretic mobility (Nano-ZS, Malvern Instruments, Malvern, UK) and confocal laser scanning microscopy (CLSM). For CLSM, 1 mL samples were stained with 1% Nile Red and Fast Green (fluorescent dye) for detection according to the method reported by Li et al [272]. The digested samples were finally centrifuged at a speed of 5000 g for 10 min to obtain the mixed micelle layer. The bioaccessibility of 5-DN was estimated using the following equation as described previously [200]:

$$Bioaccessibility = \frac{C_{micelle}}{C_{Total}} \times 100\%$$

6.2.5. Cell culture model

Caco-2 cells, passage 40 to 50, were maintained in complete Dulbecco's modified essential medium (DMEM), containing high glucose, 10% fetal bovine serum (FBS), 1% antibiotic, and 1% amino acids. For experiments, cells were seeded at 4.5×105 cells/well on transwells. The medium was changed every other day for 3 weeks to induce differentiation of Caco-2 cells. The transepithelial electrical resistance (TEER) was measured at 37°C using a Millicell® ERS-2 epithelial voltammeter.

After cells were treated with different samples for 1, 2, 4, 8 and 24 h, 100 μL of media from the basolateral side was collected, and each time 100 μL of complete medium was immediately added back to the basolateral compartment. The 5-DN in the collected samples was extracted twice using ethyl acetate to achieve high recovery and the organic solvent was evaporated (SAVANT speedvac system). The resulting residue was dissolved in 100 μL mobile phase for HPLC analysis. For

determination of the intracellular levels of 5-DN after 24 h, the Caco-2 cell monolayer was washed with ice-cold PBS twice to stop the treatment, and the cells were collected. The intracellular DMN was isolated by sonication and then centrifugation. The levels of DMN in the supernatant were analyzed by HPLC.

6.2.6. Transmission electron microscopy

The morphology of the Caco-2 cell monolayer was determined by TEM (Philips, Tecnai 12) Cells were exposed to different treatments for 24 h before being fixed and prepared for electron microscopy according to Leonard et al [273]. Chylomicrons were collected and detected using the same method described previously [274].

6.2.7. Detection of Apo B expression

The medium in the basolateral side was collected and centrifuged at 2000g for 10 minutes to remove debris. Supernatants were then collected and concentrated in Vivaspin tubes and then stored at -20 °C for use. Apo B was detected using a specific ELISA assay (ab108807, UK).

6.3. Results and discussion

6.3.1. Fatty acids composition

Previous studies have shown that digestible lipids play an important role in promoting the intestinal absorption of lipophilic nutraceuticals [5]. For example, the bioavailability of carotenoids from salads is much higher when they are ingested

with full-fat rather than reduced-fat salad dressings [275]. The presence of LCT (corn oil) in foods was shown to greatly enhance the oral bioavailability of coenzyme Q10 [271]. However, the impact of digestible lipids on bioaccessibility depends on their composition. The bioaccessibility of β-carotene and Vitamin E were shown to be higher when they were co-ingested with LCT rather than MCT [267, 276], whereas the bioaccessibility of curcumin was reported to be higher for MCT than LCT [110].

To evaluate the effect of fatty acid type on the in vitro digestion and absorption of 5-DN, we selected canola oil as a representative LCT. Canola oil is commonly consumed food oil that is rich in oleic acid [277]. A gas chromatographic analysis of the oil phases utilized in this study showed that the canola oil contained around 60% oleic acid ($C_{18:1, n-9}$), with almost 95% total unsaturated long chain fatty acids and only 5% saturated ones (Figure 6-1). Conversely, the MCT used consisted primarily of medium chain saturated fatty acids: 60% octanoic acid ($C_{8:0}$) and 40% capric acid ($C_{10:0}$) (Figure 6- 1).

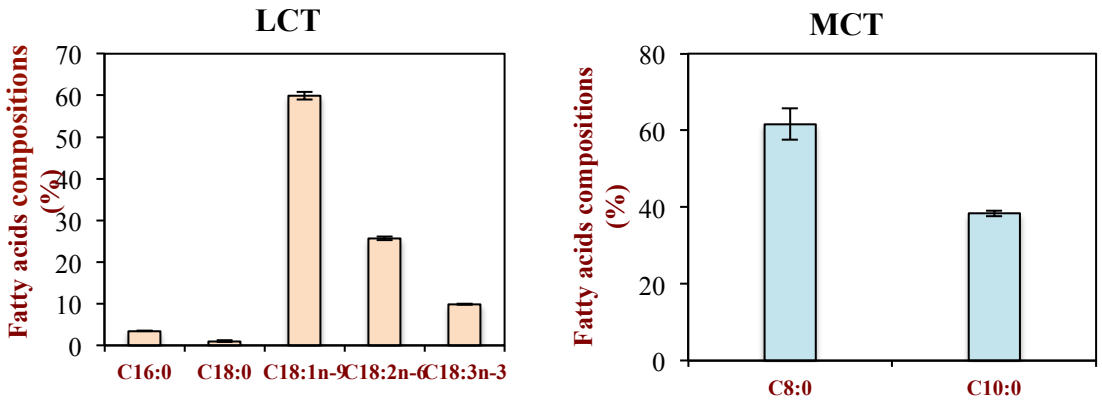

Figure 6-1 Fatty acids composition of LCT and MCT by GC.The ratio of fatty acids with different length and saturation were characterized.

6.3.2. Properties of initial emulsions

Nanoemulsion-based delivery systems were prepared using either LCT or MCT as the carrier oil phase, and sodium caseinate as an emulsifier (Table 6-1). This amphiphilic protein was selected as an emulsifier because it is widely used in the food industry to stabilize emulsions [87]. In addition, studies have shown that sodium caseinate has little impact on the integrity or absorption characteristics of Caco-2 cell monolayers, in contrast to other widely used food-grade surfactants, such as Tween 20 or 80 [278-280].

Initially, the nanoemulsions contained droplets with relatively small mean particle diameters (170 to 180 nm) and high negative charges (-39 to -43 mV) with their properties not being strongly dependent on oil type (Table 6-1). The relatively small size and anionic nature of the droplets can be attributed to the adsorption of caseinate molecules to their surfaces during homogenization. The caseinate molecules provide a negative charge because the protein is above its isoelectric point (pI ≈ 4.6) under neutral pH conditions. The droplets in the original nanoemulsions are prevented from aggregating with each other because of a relatively strong electrostatic and steric repulsion associated with the adsorbed caseinate layer.

Table 6-1. Composition, particle size and Z-potential of MCT emulsion and LCT emulsion

Emulsion Composition	**Particle Size (nm)**	**Z-potential (mV)**
Canola oil 4%wt, salt caseinate 1%, PBS 95%, 5-DN 1mM	178.2±1.2	-43.3±0.8

MCT oil 4%wt, salt caseinate 1%, PBS 95%, 5-DN 1mM	172.8±0.6	-39.4±0.5

6.3.3 Impact of carrier oil on gastrointestinal fate of emulsified lipids

After the emulsions were made, they were passed through oral phase, gastric phases and small intestine phase of the gastrointestinal model. After exposure to each phase, the particle size (Figure 6-2 A), charge (Figure 6-2B) and structural organization (Figure 6-2 C) were measured. Finally, bioaccessibility of 5-DN in the mixed micelle phases formed by digestion of the delivery systems was determined (Figure 6-2 D).

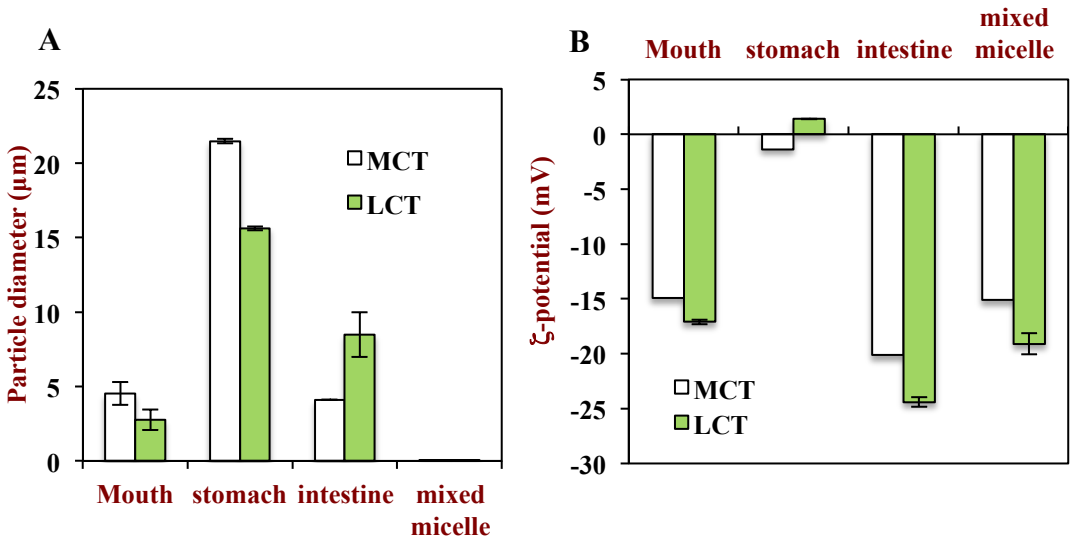

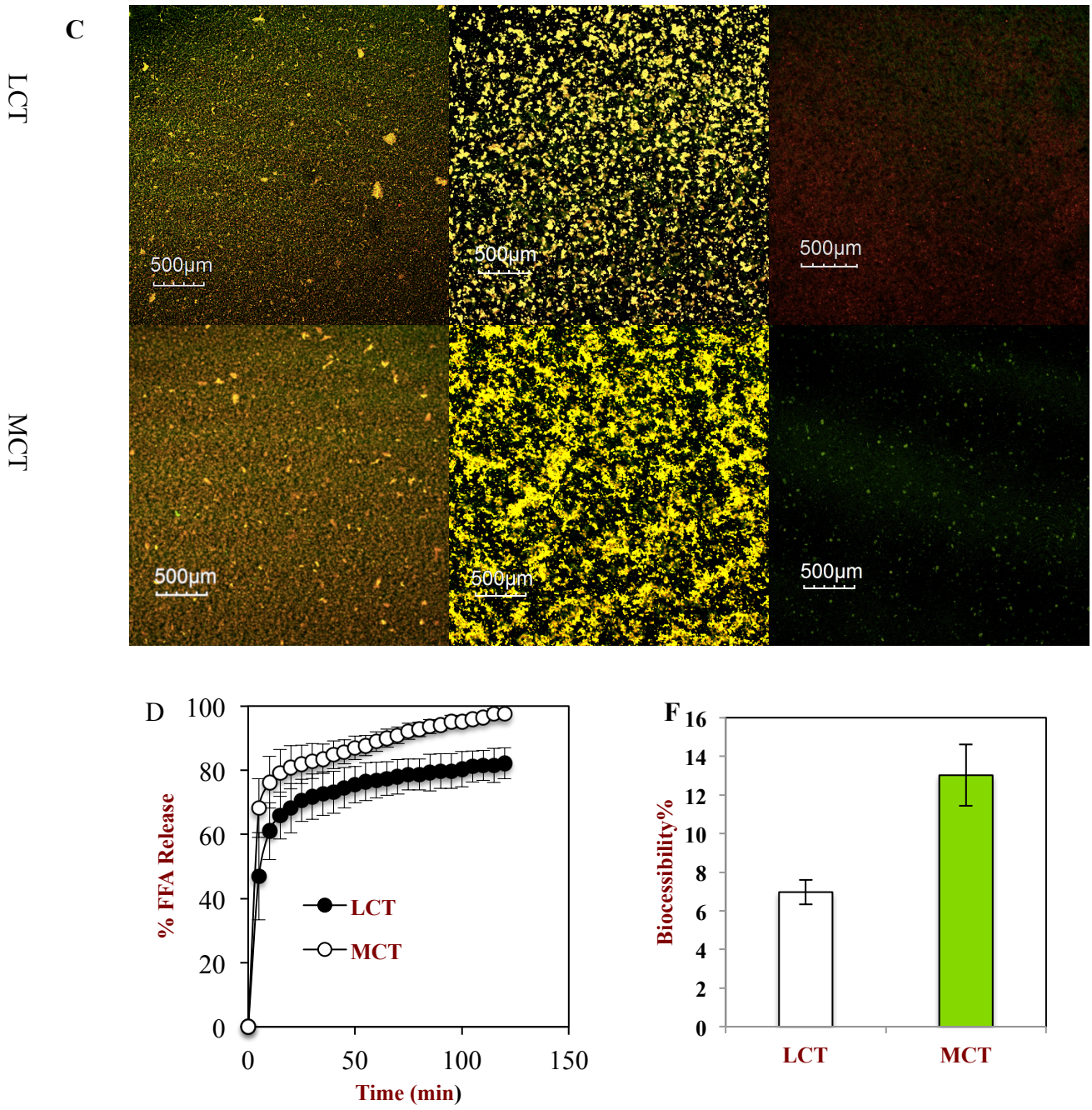

Figure 6-2 Particle size, z-potential and morphology changes during simulated GI digestion are shown in (A), (B), and (C) in three in vitro digestion stages: mouth, stomach and small intestine. The release of free fatty acids (FFA) shows in (D) and (F) displays the bioaccessibility of 5-DN in canola oil based emulsion and MCT based emulsion separately. Samples stained with Nile Red (for oil) and Fast Green (for protein). "Yellow" stands for the merged color.

Oral stage: The freshly prepared nanoemulsions were mixed simulated saliva fluids and then agitated for 10 minutes at 37°C. A few floccules were observed in the microscopy images of both emulsion-saliva mixtures after this stage, and there was an appreciable increase in the mean particle diameter determined by light scattering, which indicated that appreciable droplet aggregation had occurred. Previous studies suggest that flocculation may occur within the mouth due to bridging or depletion flocculation promoted by mucin [281]. There was also an appreciable change in the electrical characteristics of the droplets after exposure to the oral conditions, which may have been due to adsorption of anionic mucin molecules to their surfaces.

Gastric Stage: After exposure to the mouth stage, the resulting "bolus" was mixed with simulated gastric fluids and incubated for 2 hours. There was evidence of extensive droplet aggregation after exposure to the gastric stage, as demonstrated by the large increase in mean particle diameter in the light scattering measurements and heterogeneous structures observed in the microscopy images. There are a number of reasons for the aggregation of the protein-coated oil droplets under gastric conditions. First, there is a substantial change in the pH and ionic strength of the aqueous solution surrounding the lipid droplets, which may reduce the electrostatic repulsion between them. Second, the proteins adsorbed to the oil droplet surfaces may be hydrolyzed by pepsin, which will reduce their effectiveness at stabilizing the droplets by altering interfacial thickness, charge, or hydrophobicity [87]. Third, the mucin from the simulate saliva may have promoted depletion or bridging flocculation. Previous studies have also reported that caseinate-coated oil

droplets are highly prone to droplet aggregation under simulated gastric conditions [272]. The electrical charge on the emulsions was relatively low after exposure to the gastric environment, which can be attributed to the high ionic strength (which causes electrostatic screening) and the low pH (which should cause the proteins to become cationic). The fact that the droplets did not have a high positive charge under the acidic conditions in the stomach suggests that anionic species adsorbed to their surfaces, such as mucin.

Small Intestinal Stage: The digesta resulting from exposure of the nanoemulsion-based delivery systems to the small intestinal stage contained relatively large negatively charged particles (Figure 6- 2). The nature of these anionic particles cannot be ascertained from the light scattering, ?-potential or microscopy measurements, but they may have been undigested oil droplets, micelles, vesicles, protein aggregates, or insoluble calcium soaps. Triacylglycerols (TAGs) are converted into free fatty acids (FFAs) and monoacylglycerols (MAGs) in the presence of pancreatic lipase, bile salts, and calcium. The rate and extent of this process can be monitored by automatic titration of the free fatty acids produced using the pH-stat method (Figure 6-2D). There was an initial rapid increase in FFAs during the first 5 minutes, followed by a more gradual increase after that until a relatively constant final value was reached. The samples containing MCT appeared to be digested slightly faster and more extensively than those containing LCT. This may have been due to the fact that medium chain FFAs are more readily dispersible in aqueous solutions than long chain FFAs, and are therefore rapidly removed from the droplet surfaces. On the other hand, long chain FFAs may accumulate at the

droplet surfaces, thereby inhibiting the ability of lipase to further digest the remaining TAGs [282].

The bioaccessibility of 5-DN was calculated from measurements of its concentration in the mixed micelle phase and digesta (Figure 6-2F). The bioaccessibility of 5-DN was significantly higher for MCT than for LCT. This may have been because there was slightly more digestion for the MCT nanoemulsion that for the LCT one, and therefore more 5-DN may have been released from the droplets and more mixed micelles may have been formed to solubilize it [5]. Previous studies have shown that the bioaccessibility of carotenoids is much higher in the mixed micelles formed by LCT than those formed by MCT. This difference may have been due to the fact that carotenoids are much larger and more hydrophobic molecules than 5-DN. As a result, carotenoids cannot easily be accommodated within mixed micelles formed from medium chain FFAs, but 5-DN molecules can.

6.3.4. Impact of carrier oil on 5-DN transport in Caco-2 cell monolayer

The mixed micelle phases were then applied to Caco-2 cell monolayers to determine the absorption and transport properties of 5-DN. In vivo animal studies have shown that 5-DN may be transformed into its metabolites (5,3'-didemethylnobiletin and 5,4'-didemethyl-nobiletin) by phase I and phase II enzymes in the cytoplasm of the gut epithelium cells [283, 284]. Hence, the concentration of 5-DN and its metabolites in the basolateral side of the Caco-2 cells were periodically measured over a 24h period, and the apical and intracellular levels were also determined after 24 h incubation.

Figure 6-3A shows the results of transport 5-DN in mixed micelles from the apical side to the basolateral side of the Caco-2 cells. For the first 2h, there was a dramatic increase of 5-DN for both groups. The ratio of 5-DN transport to the basolateral in the LCT group was about 2-fold of that in the MCT group after 24 h, i.e., 52% and 25%, respectively. Only around 20% of the transported 5-DN was metabolized for the LCT group, while almost 60% was metabolized for the MCT group. We hypothesize that the cause of this difference may be related to the formation of cytosolic oil droplets and chylomicrons in the Caco-2 cells. After absorption by enterocytes, 90% of long-chain FFAs are believed to be assembled into triglycerides, stored in oil droplets or packaged into chylomicrons, and then transported out of the cell into the lymphatic system [108, 285]. However, only a relatively small fraction of medium-chain FFAs (8 to 13%) are packaged into chylomicrons [285]. Hence, long-chain FFAs are more efficient at forming chylomicrons than medium-chain ones. For highly lipophilic components like 5-DN, the chylomicron-lymph route is an important absorption pathway [108]. Normally, 5-DN may be converted into its metabolites in the cytoplasm of the enterocytes. However, when 5-DN is located within cytosolic oil droplets or chylomicrons it will avoid exposure to the enzymes in the aqueous phase that normally promote its metabolism. The reason that the 5-DN was more stable to metabolism in the LCT group may therefore be because it is better protected in this group (see next section).

More 5-DN remained in the apical of the Caco-2 cells for the LCT group than for the MCT group after 24 h incubation (Figure 6-3B). For both groups, less than 10% percent of the 5-DN was converted to metabolites in the apical side, and there were

no significant differences between the groups. On the other hand, intracellular metabolites were much higher for the MCT group than the LCT group, with the metabolite level being about twice that of the remaining 5-DN level for the MCT group (Figure 6-3C). As mentioned earlier, we hypothesize that 5-DN was incorporated into cytosolic lipid droplets and chylomicrons in the Caco-2 cells thereby avoiding exposure to the metabolic enzymes in the cytoplasm[286]. In order to confirm this hypothesis, the change in cell morphology and chylomicron secretion was measured for the different lipid phases.

A

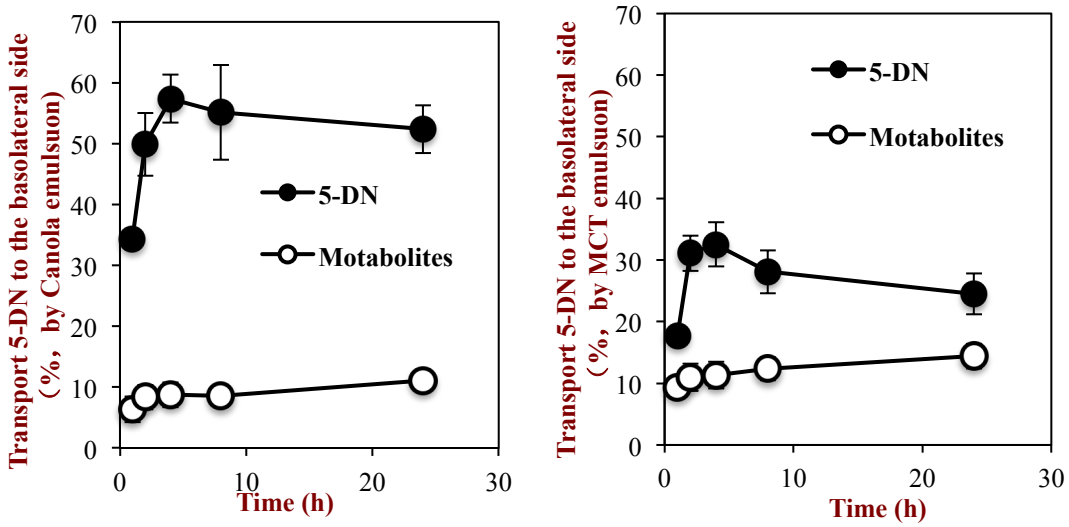

B

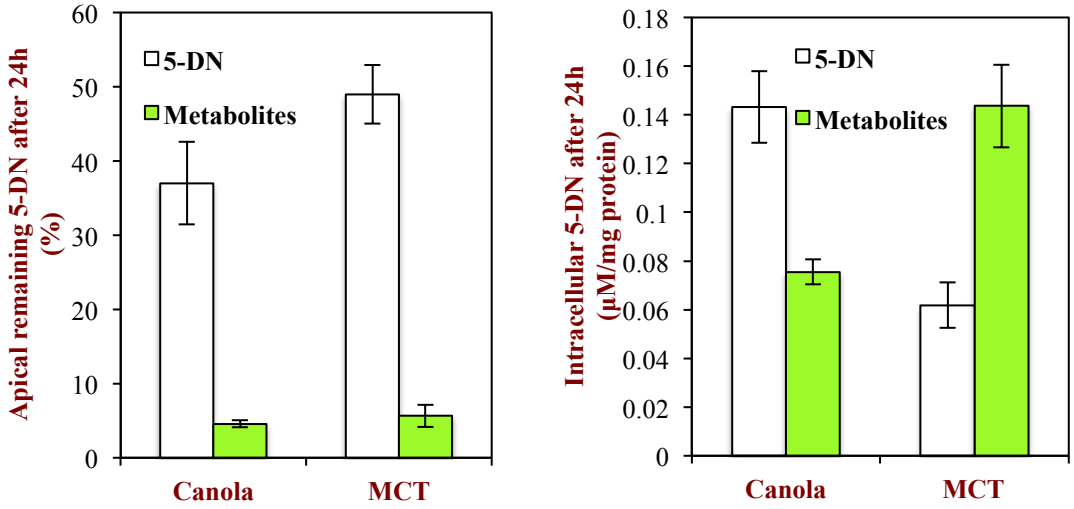

Figure 6-3 Transport of 5-DN in mixed micelles (Canola oil based & MCT based) from apical side to basolateral side in Caco-2 cell monolayer. Figure (A) shows the process of 5-DN and its motabolites being transported to the basolateral side. Figure (B) and (C) show apical /intracellular remaining 5-DN and its metabolites after 24h incubation.

6.3.5.Impact of oil type Caco-2 morphaology and chylomicron secretion

After 24 hours incubation, basolateral media were collected and centrifuged to isolate the chylomicrons, and the level of Apo B in the solutions was measured. The solution was then dual stained according to a previously described method to obtain TEM images [274]. The morphologies of the treated Caco-2 cell monolayers were also characterized by TEM (Figure 6-4).

The morphology of cells incubated with mixed micelles collected after digestion of LCT nanoemulsions (Figure 6-4A) and MCT nanoemulsions (Figure 6-4B) was compared. Previous studies have shown that some dietary fats may affect the lipid composition of the microvillus membrane of enterocytes[287]. However, no significant difference in cellular morphology was observed in the current study, with the microvilli in both groups appearing numerous and mature after 24 h incubation.

Numerous large cytosolic lipid droplets and lipoproteins were observed in the enterocytes incubated with LCT nanoemulsions (Figures 6-4B&C), whereas fewer lipid droplets and lipoproteins were observed after incubation with the MCT ones (Figure 6-4E&F). Measurement of the basolateral ApoB levels also indicated that more lipoproteins were produced in the LCT group (Figure 6-4G). Cytosolic lipid droplets have been observed in jejunal enterocytes following lipid absorption in mammals[258]. These lipid droplets play an important role in transient lipid storage and they are closely associated with lipoprotein production. Cytosolic lipid droplets are formed soon after the intestinal enterocytes absorb the lipid digestion products resulting from a typical fatty meal, and part of the absorbed lipids are then exported from the cell by means of chylomicrons [288]. For LCTs, almost all of the FFAs produced by lipid digestion are absorbed by the human body through the chylomicron-lymph pathway, while for MCTs they are primarily transported to the liver without re-esterification via the portal venous system[289]. Hence, it is likely that the highly lipophilic bioactive used in this study (5-DN) was incorporated into the lipid droplets and chylomicrons for the LCT group, and thus avoided being metabolized by the relevant enzymes in the cytoplasm. On the other hand, the 5-DN was more exposed to the metabolic enzymes in the cell when it was co-ingested with MCT nanoemulsions.

The results of this study have important implications for the design of nanoemulsion-based delivery systems for improving the bioavailability of lipophilic bioactives. They show that one must consider the impact of nanoemulsion

composition on the bioaccessibility, absorption, and transformation of any encapsulated bioactive agents.

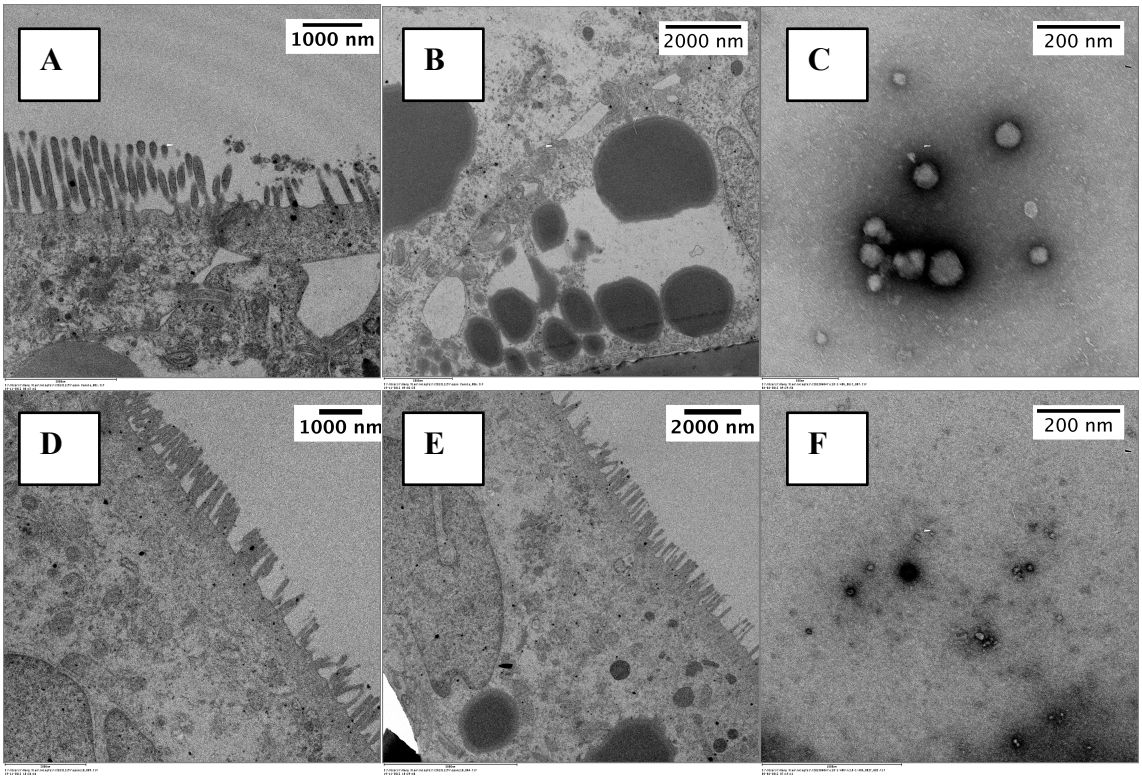

G

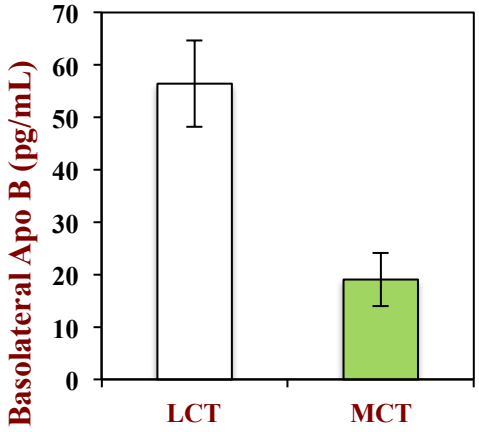

Figure 6-4 Morphologies of Caco-2 cell monolayer incubated with canola based mixed micelle (A&B) and MCT (D&E) based mixed micelle. Secretion and formation of CMs after Caco-2 cell incubated with mixed micelle layer produced by canola oil(C) and MCT (F) emulsion separately for 24h. The secreted Apo B was also determined in (G).

CHAPTER 7

POTENTIAL ADVERSE EFFECTS OF POLYUNSATURATED FATTY ACIDS INFLUENCE OF LIPID OXIDATION ON LYMPHATIC TRANSPORT OF LIPOPHILIC BIOACTIVE COMPONENTS AND CELL MORPHOLOGY

7.1. Introduction

Long chain free fatty acids (FFAs) are one of the major hydrolysis products of ingested dietary lipids (triacylglycerols) in the lumen of the small intestine [290]. After their release, they are incorporated into mixed micelles along with monoacylglycerols, bile salts, phospholipids, cholesterol, and any other lipophilic constituents. The mixed micelle phase typically consists of a compositionally and structurally complex colloidal dispersion consisting of micelles, liposomes, and liquid crystals. FFAs are transported across the mucus layer, and are absorbed by enterocytes where they are re-esterified into triacylglycerols and incorporated into chylomicrons (CMs), which are ultimately transported into the blood circulation via the lymphatic pathway[291]. Polyunsaturated FFAs are important for numerous physiological processes, including stimulation of skin and hair growth, regulation of metabolism, regulation of the immune system, maintenance of bone health, and maintenance of the reproductive system[292-296]. Long chains FFAs also facilitate the absorption of lipophilic vitamins (e.g., A, D, E, and K) and bioactive compounds (e.g. carotenoids and flavonoids) by the lymphatic pathway[297, 298]. In a previous study, we have also shown that long chain FFAs increase the bioavailability of the highly lipophilic polymethoxyflavones (PMFs) found in citrus fruits by promoting

their intestinal lymphatic transport[249], thereby overcoming problems normally associated with their low water solubility[296]. For these reasons, the oral administration of highly lipophilic compounds with dietary fats is considered to be an efficient means of improving their bioavailability[3].

A potential problem associated with utilizing unsaturated lipids to increase the bioavailability of lipophilic bioactives is their high susceptibility to oxidation, which can lead to undesirable off-flavors and to potentially toxic reaction products[299] [300-303]. Some of the undesirable health effects associated with dietary peroxides have been attributed to their incorporation into CMs[304]. Linoleic acid (LA) is an 18-carbon polyunsaturated fatty acid (PUFA) that is commonly found in the human diet, and that is highly susceptible to lipid oxidation when incorporated into foods[305]. The largest source of LA in the human diet is safflower oil (≈78% linoleic acid, C9C12-linoleate)[306]. Other commonly used edible oils, such as soybean and sesame seed oil, also contain relatively high levels of LA. The conjugated form of linoleic acid (CLA) has been reported to reduce the risk of cancer and cardiovascular diseases in humans[299].

The objective of the current study was to evaluate the effect of LA oxidation on the potential biological fate of a model lipophilic bioactive agent: 5-hydroxy-6,7,8,4'tetramethoxylflavone (5-DMT). Consequently, we measured 5-DMT absorption, chylomicron formation, and mucosa layer morphology in the presence of either fresh or oxidized LA using a cell culture model. Caco-2 cells, which are derived from a human colonic adenocarcinoma, form monolayers that have many features similar to those of human enterocyte cells, and are therefore particularly

suitable for studying the absorption and processing of bioactive components in the GIT[10, 164, 166, 228, 307-309]. In particular, this model enables one to study changes in the microvilli and tight junctions of the cell monolayer, as well as monitoring lipoprotein synthesis[303]. The information obtained from this study will facilitate an understanding of how lipid oxidation influences the absorption and processing of lipophilic bioactive agents.

7.2. Materials and methods

7.2.1. Materials

Linoleic acid (LA), taurocholic acid (TC), phosphatungstic acid (PTA), 4% OsO_4, and Optiprep™ density gradient medium were purchased from Sigma Chemicals (St. Louis, MO). All other chemicals and solvents of analytical grade were from Fisher Scientific (Pittsburgh, PA). Apo B human ELISA kit was purchased from Abcam (ab108807).

7.2.2. Cell culture

Caco-2 cells (passage 75 - 85) were cultured in Dulbecco's modified Eagle's medium (DMEM) containing 10% fetal bovine serum (FBS), 1% non-essential amino acid and, 1% penicillin-streptomycin, and incubated at 37°C with 5% CO_2. Cells were sub-cultured when reached 90% confluences. For the evaluation of cytotoxicity and cellular reactive oxygen species (ROS) determination, cells were seeded in 96-well plate (Corning CellBIND Surface, Corning Incorporated, NY, USA) at the concentration around 1.5 x 10^4 cells/well and incubated overnight before use. For

the determination of 5-DMT transport, cells were seeded in transwell plate (Corning Incorporated, NY, USA) and were grown for more than 21 days to obtain a differentiated cell monolayer. Transepithelial electrical resistance (TEER) was measured using the Millicell ERS-2 meter (Millipore Corporation, Bedford, MA, USA).

7.2.3. Promotion and detection the oxidation of LA

A sample of LA was exposed to the air and stored at 55 ºC to promote lipid oxidation at elevated oxygen levels and high temperatures. The change in lipid peroxide value (PV) and 2-thiobarbituric acid reactive substances (TBARS) of the LA sample were measured over time. A rapid, sensitive, iron-based spectrophotometric method was used as described by Shantha and Decker[310], with some modifications. Samples were mixed with 2.8 mL methanol/1-butanol (2:1, v/v), 15 µL of 3.94 M ammonium thiocyanate and 15 µL of ferrous iron solution. After 20 min incubation at room temperature, the absorbance of the solutions was measured at a wavelength of 510 nm using UV-vis spectrophotometer (Genesys 20; Thermo Fisher Scientific Incorporated, MA, USA). TBARS were measured using a method described previously[311] ,with some modifications. The TBARS reagent used consisted of 15% (w/v) trichloroacetic acid, 0.35% (w/v) thiobarbituric acid, 0.25 M hydrochloric acid, and 0.02% (w/v) of butylated hydroxytoluene. Lipid samples were mixed with this reagent and the absorbance of the upper butanol layer was measured at a wavelength of 532 nm using a UV-visible spectrophotometer (Genesys 20; Thermo Fisher Scientific Incorporated, MA, USA).

7.2.4. Measurement of unoxidized lipid fraction

The fraction of the LA that remained in a unoxidized form after subjection of the lipid to air and elevated temperature was measured by gas chromatography (GC). Initially, the lipid sample was esterified using boron trifluoride-methanol. The resulting fatty acid methyl esters (FAMEs) were then analyzed using a gas chromatograph equipped with flame ionization detector (GC-17A; Shimadzu Corporation, Kyoto, Japan) using a DB-23 column (30 m × 0.25 mm; i.d., 0.25 μm, Agilent technologies, J.W. Scientific, Santa Clara, CA, USA). Heptadecanoic acid ($_{C17:0}$) was used as an internal standard.

7.2.5. Determination of cytotoxicity and cellular reactive oxygen species (ROS)

Cytotoxicity of oxidized and unoxidized LA were assessed using the 3-(4, 5-dimethylthiazol-2-yl)-2, 5-diphenyltetrazolium bromide (MTT) assay. Caco-2 cells were seeded in 96-well plates (1.5×10^4 cells/well) and incubated for 24 h. The culture medium was then removed from the cells, a new medium containing the sample was added, and the system was incubated for 24 h. The culture medium was then removed and replaced with 100 μL of 0.5 mg/mL MTT and further incubated for 1 to 2 h according to the level of purple formazan crystal formation. The culture medium was then discarded and the purple formazan crystals were solubilized by addition of DMSO to each well. The absorbance was monitored at 570 nm using a microplate reader (El×800 absorbance microplate reader; BioTek Instruments, Incorporated, VT, USA). The results are expressed as the percentage of viable cells compared to the control (untreated) cells.

The production of cellular ROS was assessed in 96-well plates using a 2', 7'-dichlorodihydrofluorescein (DCFH) assay. The DCFH-DA probe readily diffuses through the cell membrane and is hydrolyzed by intracellular esterase to a non-fluorescent compound (DCFH), which is rapidly oxidized in the presence of ROS to DCF and emits fluorescence. Caco-2 cells were seeded in black-sided clear-bottomed polystyrene 96-well plates and treated the same as described for the MTT assay. Then culture medium was removed and the cells were washed with PBS (pH 7.4). Subsequently, 100 μL of 10 μM DCFH-DA in PBS (pH 7.4) were added and incubated in the dark for 30 min to promote the formation of stable fluorescent compounds. The loading step was terminated and the excess DCFH was removed by washing the cells twice with PBS (pH 7.4) and then adding 100 μL PBS (pH 7.4). Plates were immediately monitored using a fluorescence microplate reader (Synergy 2 multi-mode microplate reader; Bio Tek Instruments, Incorporated, VT, USA) at the excitation wavelength of 485 nm and an emission wavelength of 530 nm. The increase in fluorescence for each treatment was calculated by the relative fluorescence of each treatment compared to control (untreated) cells, normalized by the number of cells as determined by the MTT assay. All treatments were prepared as a FA-BSA complex. Certain amounts of unoxidized or oxidized LA were mixed with bovine serum albumin (BSA) solution dissolved in DMEM.

7.2.6. Determination of 5-DMT transport

Caco-2 cells were seeded in transwell plates (4.5×10^5 cells/well) and cultured for 3 to 4 weeks to be differentiated. Both the apical and basolateral media were replaced with

serum-free complete medium and incubated for 4h before treatment. Cells were then incubated with 2 mL of 5-DMT, 5-DMT+TC, 5-DMT+LA+TC, and 5-DMT+oxidized LA (96 h oxidation)+TC separately. TEER was measured at 1, 2, 4, 8 and 24 h to assess changes in cell monolayer integrity. Periodically, samples of basolateral media (100 μL) were collected and replaced with the same amount of none FBS complete medium. 5-DMT in the collected samples was extracted twice by ethyl acetate with the recovery more than 90%. The 5-DMT concentration was determined as described previously using a HPLC equipped with a multi-channel electrical conductivity detector (Model 6210 CoulArray detector; ESA, Incorporated, MA, USA)[232].

7.2.7 Electron microscopy

Caco-2 cells were grown on transwells for 3 weeks. CMs were collected the same way as we did before[249]. Cells were exposed to different treatments for 24h before fixing and prepared for electron microscopy according to Maurice Leonard et al[255]. Sections were then examined in the transmission electron microscope.

7.2.8. Statistical analysis

All experiments were carried out at least three times using freshly prepared samples and the results are reported as the calculated mean and standard deviation of these measurements. The difference among samples were analyzed by ANOVA with significance level of $p<0.05$.

7.3. Results and discussion

7.3.1. Promotion and detection lipid oxidation

Measurement of the loss of lipid substrate (LA remaining), the formation of primary reaction products (peroxide value), and the formation of secondary reaction products (TBARS) during storage at elevated temperature and oxygen levels clearly indicated that LA oxidation occurred (Figure 7-1). The fraction of LA remaining in the sample decreased appreciably during storage, with less than 40% remaining after 72 days. Initially, the peroxide value increased during storage indicating the formation of primary reaction products, but then it reached a peak around 48 h and decreased due to conversion of primary into secondary reaction products. The TBARs level increased throughout storage indicated that secondary reaction products were rapidly formed. These results indicate that LA samples containing relatively high levels of lipid reaction products could be formed by incubating them at elevated temperatures for prolonged times.

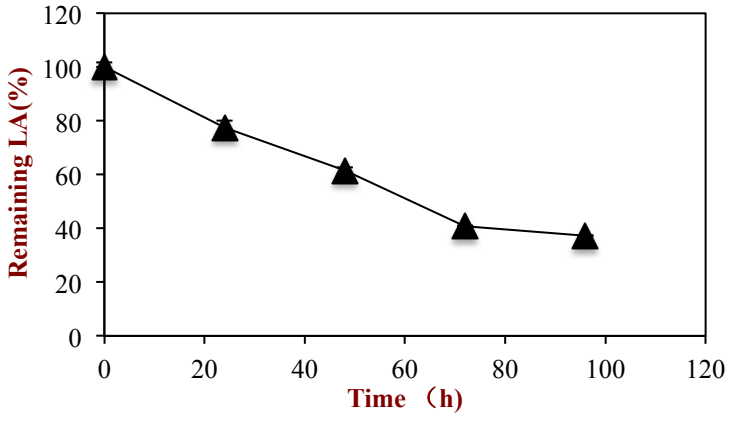

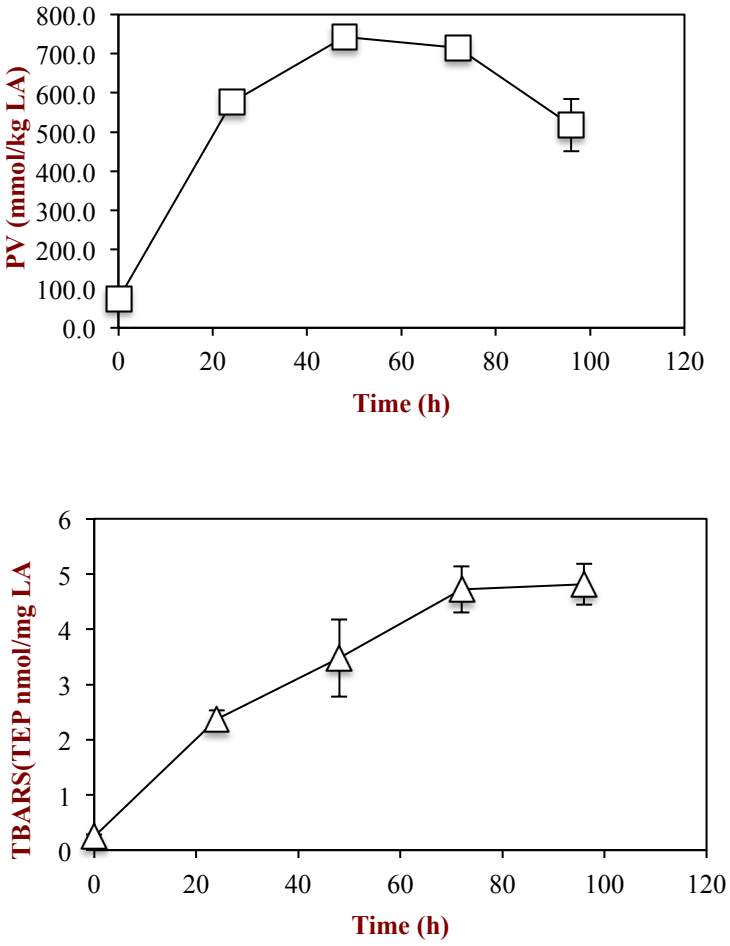

Figure 7-1 PV, TBARS and remaining unoxidized LA were detected every 24h during the stimulated oxidation process. Data represent mean ± SD for n=3 experiments

7.3.2. Cytotoxicity and cellular reactive oxygen species (ROS) determination

Studies have shown that reactive oxygen species (ROS), such as the peroxides formed by LA oxidation, may promote peroxidation of lipids in cell membranes, and may even stimulate programmed cell death[312]. For this reason, we measured the influence of unoxidized and oxidized LA on ROS formation and cytotoxicity of Caco-2 cells after 24 h incubation (Figure 7-2). Oxidized LA was found to increase the

production of ROS in the Caco-2 cells more than unoxidized LA, with higher amounts of ROS being produced for the lipid with the greater extent of oxidation. High concentrations of LA (either unoxidized or oxidized) appeared to exhibit cytotoxicity, as evidenced by the observed decrease in cell viability with increasing LA concentration. In this case, the unoxidized LA appeared to have a bigger impact than the oxidized LA over most of the concentration range studied.

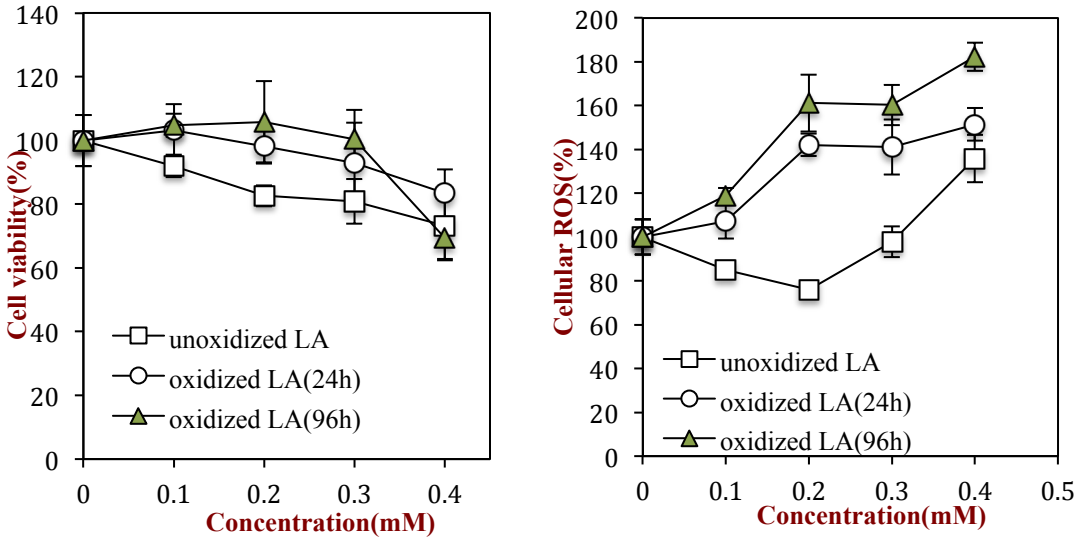

Figure 7-2. MTT assay and ROS assay by Caco-2 cells. Caco-2 cells were incubated by different fatty acids for 24h: unoxidized LA, 24h oxidized LA and 96h oxidized LA. Data represent mean ± SD for n=3 experiments. Different letters indicate statistical difference among the three groups at the given time point ($P<0.05$).

7.3.3. Effect of lipid oxidation on the integrity of Caco-2 monolayer

Changes in the Trans-Epithelial Electric Resistance (TEER) was measured to evaluate the integrity of the Caco-2 monolayer after incubation with the different samples for 24 h. In this series of experiments, the LA samples were compared to a control and a bile salt solution (TC), since high levels of bile salts may impact cell

integrity. The control, TC, and unoxidized LA samples did not decrease the integrity of the cell monolayers, but an appreciable decrease in cell integrity was observed for the oxidized LA (Figure 7-3). Indeed, the TEER value was only 60% of the initial value for the oxidized LA sample after 24 h incubation.

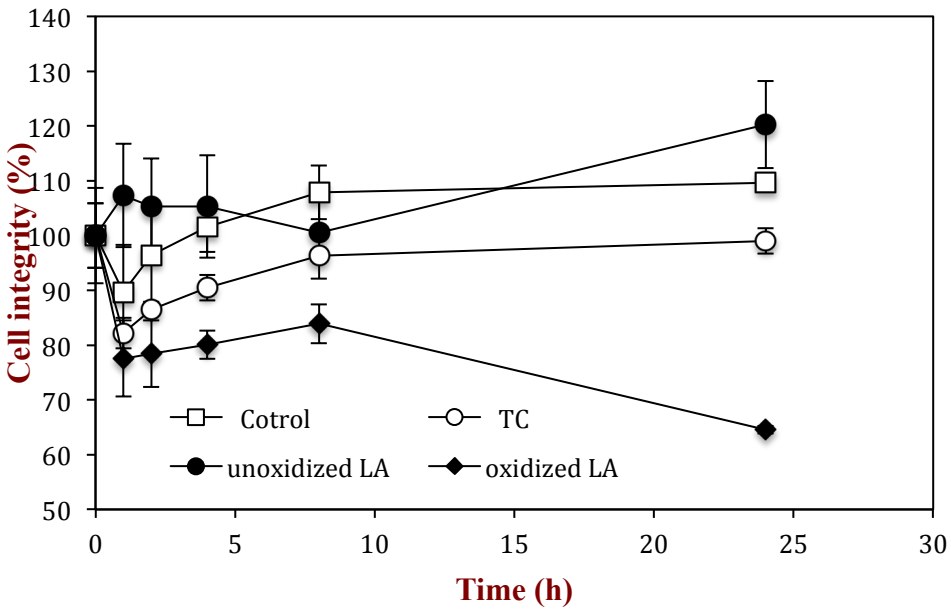

Figure 7-3. TEER of the Caco-2 monolayer. Monolayers were incubated with 0.5 mM TC, 1.6mM unoxidized LA and 1.6mM oxidized LA (96h) were measured at 0,1,2,4,8 and 24h. . Data represent mean ± SD for n=3 experiments.

7.3.4 Lipoproteins formation and structure

In this series of experiments, transmission electron microscopy was used to provide information about the formation and structure of lipoproteins in the Caco-2 cells after incubation with either unoxidized or oxidized LA for 24 h (Figure 7-4). The TEM images clearly show that spherical particles with characteristics indicative

of lipoproteins were formed in both samples containing LA. Previous studies have indicated that relatively large lipoproteins are chylomicrons (CMs), whereas relatively small ones are very low-density lipoproteins (VLDLs)[313]. Our study, indicates that the lipoproteins formed by unoxidized LA were fewer, larger, and more spherically shaped than those formed by oxidized LA (Figure7-4). This result suggests that lipid oxidation may have a pronounced influence on the nature of the lipoproteins formed.

To confirm that the particles observed in the TEM images were lipoproteins, we measured the Apo B content of the various samples[164]. Apo B is synthesized within the enterocytes and then incorporated into the chylomicrons with phospholipids and triglycerides.[7, 9] Consequently, measurement of Apo B levels can be used as a marker to determine whether lipoproteins are present. The size of the lipoproteins formed depends on the amount of lipid added to the triglyceride core, which therefore determines whether a chylomicron or VLDL particle is formed[9]. A significantly higher level of Apo B was observed for oxidized LA than for either the controls or the unoxidized LA (Figure 7-5), which is in agreement with

the larger number of lipoproteins observed in the oxidized LA by TEM (Figure 7- 4).

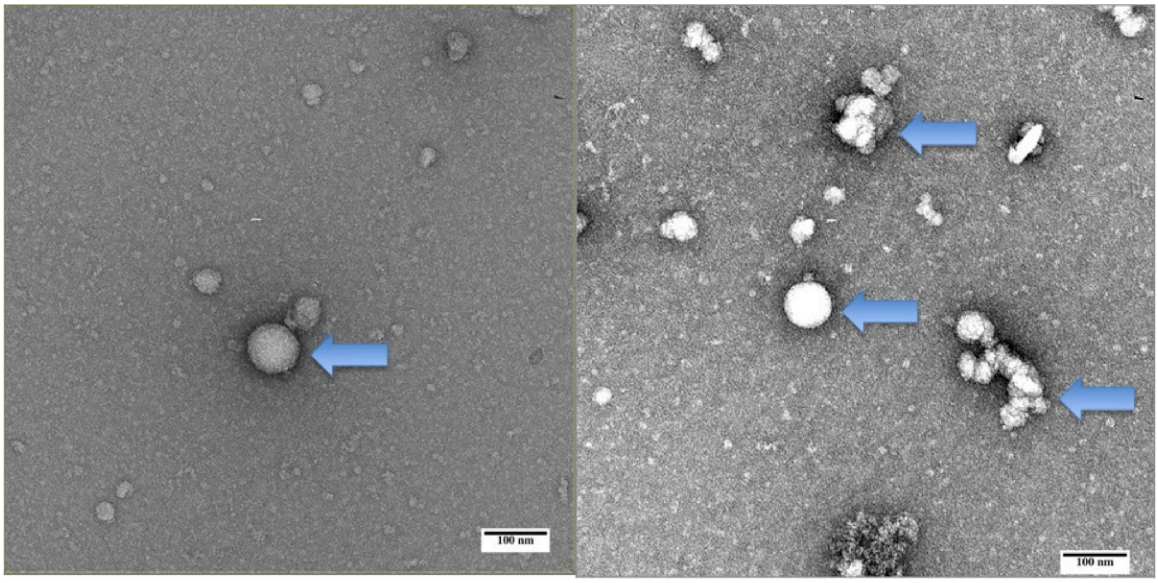

Unoxidized LA Oxidized LA

Figure 7-4 Morphology of lipoproteins secreted by Caco-2 cell monolayer after incubated unoxidized LA-TC(1.6:0.5mM, left) and oxidized LA-TC (96h; 1.6:0.5mM, right) by TEM. Lipoproteins are pointed with arrows.

7.3.5 Effect of lipid oxidation on 5-DMT transport

The transport of 5-DMT by Caco-2 monolayer was also examined. Our previous research already confirmed that oleic acid will facilitate lymphatic transport of 5-hydroxy-6, 7, 8, 3', 4'-pentamethoxylflavone (5-ND) by stimulation and formation of CMs, which is also a high lipophilic nutraceutical derived from citrus fruits[249]. LA has been also demonstrated its potential to assemble into lipoproteins before secretion into the mesenteric lymph[7, 301]. However, the oxidation of LA exhibits no reduced effect on the transport of 5-DMT, the level of 5-DMT in the basolateral side is even higher than that in unoxidized LA after 24h incubation, according to the results of Figure 7- 6. Our hypothesis is that the formation of much more

lipoproteins which were good carriers of 5-DMT, although among them mostly are VLDLs. The other cause is probably because the oxidized LA changed the transport pathway of 5-DMT, since the TEER of monolayer decreased significantly during 24h' incubation (Figure 7-3). As a result, we further studied the morphology of the Caco-2 monolayer by TEM.

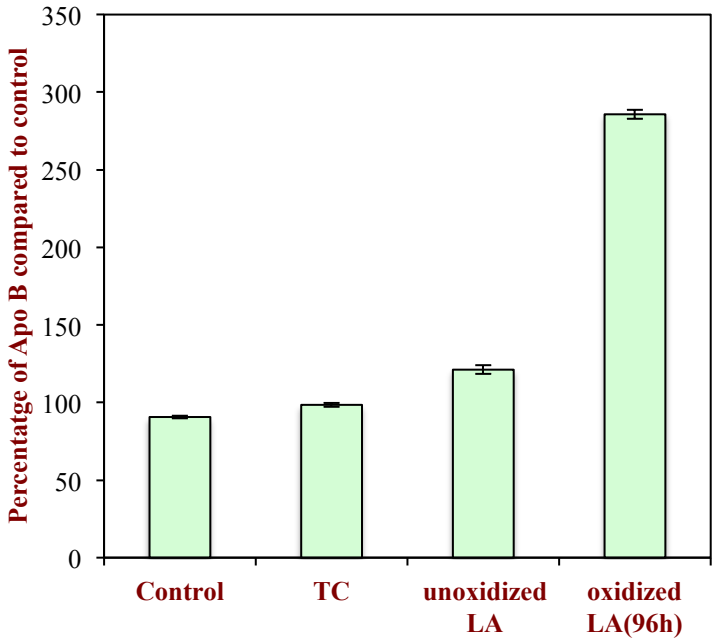

Figure 7-5. Detection of Lipoprotein secretion in the basolateral side of the Caco-2 monolayer after incubation with different treatments for 24h. . Data represent mean ± SD for n=3 experiments.

7.3.6 Change in Caco-2 monolayer morphology

Transmission electron microscopy images revealed that Caco-2 monolayers ncubated with unoxidized LA for 24 h remained in a healthy state: they had numerous thick and uniform microvilli with clearly visible filaments and well-formed tight junctions. Conversely, the images of the monolayers incubated with oxidized LA showed that they were in an unhealthy state: they had few and

irregularly shaped microvilli, loose tight junctions, and damaged membranes[164]. This change in Caco-2 monolayer morphology could result in greater transport of bioactive compounds across the cells, *e.g*., through the tight junctions.

7.4 Discussion

Consumption of PUFAs is considered to be beneficial to human health, and therefore consumers are often encouraged to increase their intake of these "good" lipids [314, 315]. However, PUFAs are highly susceptible to lipid oxidation and so there may be appreciable levels of oxidized FFAs present within products that contain them, such as foods and supplements. Previous studies have shown that oxidized linoleic acid can be taken up by Caco-2 cells and incorporated into lipoproteins[301]. In this study, we have shown that oxidation of an important PUFA (linoleic acid) can affect the lymphatic transport of lipophilic bioactive compounds (5-DMT) and promote adverse changes in cell morphology.

In this study, we produced oxidized LA by heating it in the presence of oxygen for prolonged periods. Auto-oxidation of LA is known to result in the formation of a variety of primary and secondary peroxidation products[316]. In particular, oxidation at elevated temperatures induces radical polymerization reactions that generate dimers, trimers, and larger molecular weight products, as well as scission reactions that generate various smaller molecules [317]. Our lipid oxidation experiments clearly showed that the majority of linoleic acid molecules were converted into primary (peroxides) and secondary (TBARS) reaction products (Figure 7- 1).

The potential cytotoxicity of oxidized lipids has been demonstrated in numerous studies. Lipid peroxides are a major source of dietary oxidants, that have been shown to have mutagenic or carcinogenic potentials[318]. Lipid peroxides have also been shown to be capable of initiating degenerative processes and promoting digestive system disorders[319]. Secondary reaction products formed during lipid oxidation, such as 4-hydroxy-2-nonenal (HNE), 2,4-decadienal (DDE), malondialdehyde (MDA), and crotonaldehyde, have been shown to form exocyclic DNA adducts in human cells and may contribute to cancer development[302, 320, 321]. Oxidized methyl linoleate has been reported to exhibit cytotoxicity in Caco-2 cells, which was attributed to induced apoptotic cell death[322]. Our results indicated that higher levels of ROS were produced in Caco-2 cells after 24 h incubation with highly oxidized LA than with unoxidized LA (Fig. 2). In addition, the integrity of the cell monolayer (TEER) value was reduced in the presence of oxidized LA (Fig. 3), which may have been due to production of ROS or due to changes in cell morphology.

Previous studies have shown that there is not a major difference between the uptake of oxidized and unoxidized fatty acids by Caco-2 cells[148, 301]. Our results confirmed that both unoxidized and oxidized LA could be successfully taken up by enterocytes and packaged into lipoproteins (Figure 7- 4 & 5). However, the number and morphology of the lipoprotein particles formed depended on the oxidation state of the lipid: the lipoproteins formed in the presence of oxidized LA were smaller, more numerous, and more irregularly shaped than those formed in the presence of unoxidized LA. It has been suggested that the size and nature of the lipoproteins

formed within epithelium cells (VLDLs versus CMs) depends on a “core expansion” mechanism involving fusion of “ primordial lipoproteins” with “luminal triglyceride-rich lipid droplets”[9]. This process depends on the type of fatty acids taken up by the epithelium cells. For example, LA has been shown to mainly lead to production of CMs, whereas palmitic acid leads to the production of both VLDLs and CMs[323]. Similarly, it is possible that the unoxidized and oxidized forms of LA had different effects on the “fusion” mechanism mentioned above thereby resulting in different sizes and types of lipoproteins being formed.

The transportation of 5-DMT across the Caco-2 cells was enhanced by incubation with both unoxidized and oxidized LA, when compared to controls containing no fatty acids (Figure 7-6). It is likely that 5-DMT was absorbed by the cells as part of mixed micelles, then packaged into lipoproteins, and then transported through the cells to the basolateral side. These results suggest that oxidized LA would not have a major impact on the bioavailability of co-ingested lipophilic bioactive agents, but that it may alter their subsequent fate in the body (due to the different nature of the lipoproteins formed).

Finally, we examined the influence of the oxidation state of the lipid on the morphology of the Caco-2 cells after a 24 h incubation period (Figure 7-7). Interestingly, the oxidized form of LA appeared to have an adverse impact on the integrity of the cells. In particular, the microvilli and tight junctions of the Caco-2 cells appeared to be damaged after exposure to the oxidized LA. This change in cell morphology may account for the observed decrease in the integrity (TEER) of the Caco-2 monolayer for the oxidized form of LA (Figure 7- 3). It is therefore possible

that some of the bioactive component (5-DMT) was able to travel across the cells via the tight junctions, rather than by being incorporated into lipoproteins, which would affect its subsequent biological fate. Nevertheless, more research is required to establish the relative importance of this mechanism, and its likely consequences on the processing of 5-DMT in the body.

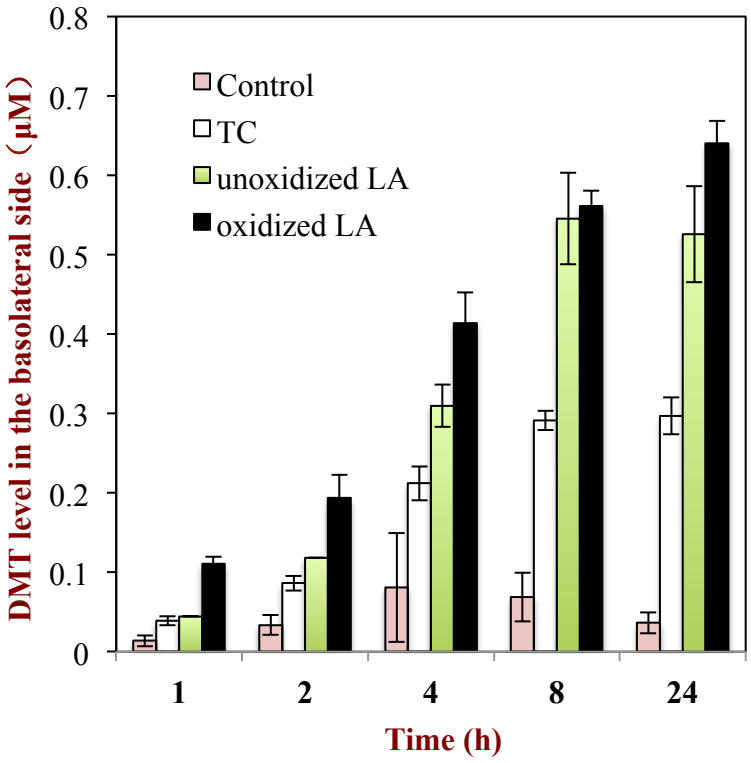

Figure 7-6. Effect of TC (0.5mM), LA (1.6mM), and 96h oxidized LA (96h; 1.6mM) on the transport of (5-DMT) in Caco-2 cell monolayer. Data represent mean ± SD for n=3 experiments.

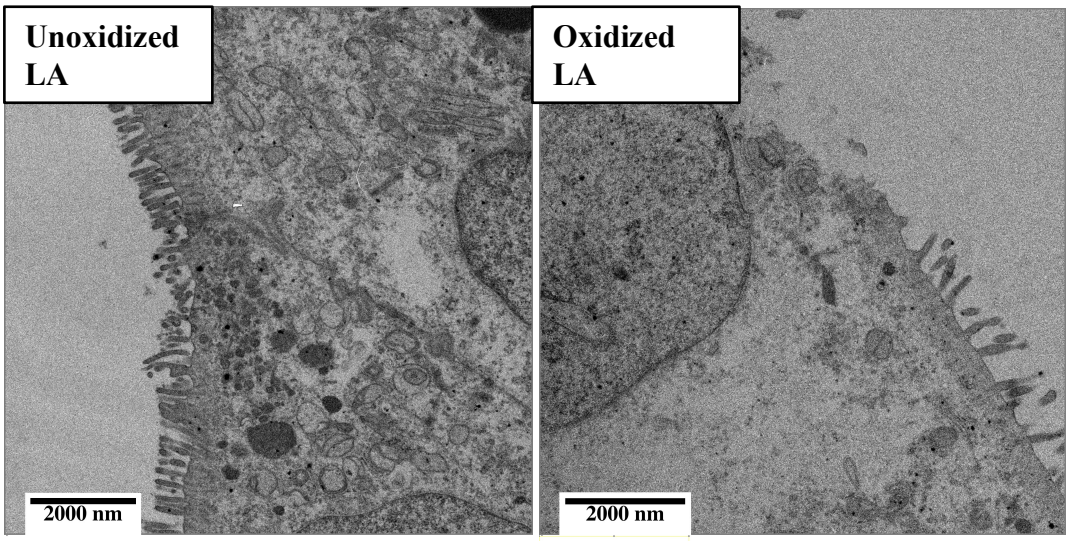

Figure 7-7. Morphology of Caco-2 monolayer after incubation with unoxidized LA and oxidized LA(96h) for 24h

7.5. Conclusion

In summary, ingestion of dietary oxidized lipids will not only cause post health problems, but altered the transport pathway of lipophilic components like PMFs according to our present research, which will definitely change their distribution, metabolism fate in the body.

CHAPTER 8

UPTAKE OF GOLD NANOPARTICLES BY INTESINTAL EPITHELIAL CELLS: IMPACT OF PARTICLE SIZE ON THEIR ABSORPTION, ACCUMULATION, AND TOXICITY

8.1. Introduction

Developments in the nanotechnology field during the past decade or so have led to numerous applications of nanomaterial, such as in computer science, chemistry, cosmetics, agrochemicals, and pharmaceuticals [324, 325]. Nanotechnology has also been utilized within the food industry to improve the microbiological safety, sensory attributes, nutrition value, and shelf life of foods, as well as to develop innovative sensors to monitor food quality and safety [326-328]. Consequently, various types of nanomaterial such as inorganic nanoparticles have been found in a wide range of food products, including the nanoparticles based on silver, titanium dioxide, silica, zinc oxide, etc. [329]. These nanoparticles may be intentionally added to food products as additives because of their specific functional attributes (such as antimicrobial, whitening, or anticaking agents), or they may be unintentionally added to foods (e.g., as a contaminant in an additive that is supposed to contain larger particles). The increasing prevalence of inorganic nanoparticles within food products means that humans come into contact with them more frequently [330]. Hence, it is particularly important to establish whether there are any adverse effects of ingesting inorganic nanoparticles in foods on human health, especially since nanoparticles may have completely different absorption and toxicity patterns in comparison to the larger particles.

A number of studies suggest that ingestion of inorganic nanoparticles may have toxic effects. It has been reported that ingestion of nanomaterials may promote inflammatory bowel disease, DNA fragmentation, liver damage and pregnancy complications, as well as result in abnormal intestinal barrier function and increased intestinal permeability. [331-334]. In particular, prolonged exposure to inorganic nanoparticles may have a detrimental impact on the function of the intestinal membrane [335]. However, detailed information about the gastrointestinal uptake and cytotoxicity of ingested inorganic nanoparticles is currently unavailable, and more studies are needed in this important area.

Gold nanoparticles (AuNPs) have been widely used in the studies of the biological fate and toxicity of inorganic nanoparticles because of their ease of synthesis, high chemical stability, and unique optical properties [336, 337]. Commercially, the main applications of AuNPs are in the medical field, such as for drug delivery and photodynamic therapy. However, AuNPs have also been used in cosmetics, beverages, food packaging materials, and toothpastes, which leads to oral exposure of AuNPs in humans [337-339]. However, a review on the previous studies highlighted the current poor understanding of the gastrointestinal uptake and potential cytotoxicity of AuNPs [340]. Therefore, the objective of this study was to determine the effect of nanoparticle size and concentration on the intestinal absorption and cellular accumulation of AuNPs in the model intestinal epithelial cells, and to assess the potential toxicity caused by the exposure to AuNPs.

Differentiated human intestinal cells (Caco-2 cells) can be grown on a permeable support to form a model intestinal epithelial monolayer. This model

system can be used to carry out systematic studies of the impact of nanoparticle characteristics (such as size, surface chemistry, and concentration) on cellular responses such as absorption and toxicity [259, 335]. Previous studies have shown that different nanoparticles can be absorbed by or transported across this type of epithelial monolayer [338]. In this study, we utilized this model to determine the influence of AuNPs dimensions (15 nm, 50, or 100 nm) on their absorption, accumulation, and toxicity. The results of this study are important for understanding the gastrointestinal fate of inorganic nanoparticles that may be ingested as part of foods.

8.2. Materials and methods

8.2.1 Materials

The following products were purchased from SigmaAldrich Chemicals (St. Louis, MO, USA): 4% osmium tetroxide (OsO_4), phosphatungstic acid (PTA), nitric acid, and hydrochloric acid. AuNPs with different diameters (15, 50, and 100 nm) were purchased from Nanopartz™ (Loveland, CO). A mitochondrial membrane potential probe (JC-1 dye) was purchased from Life Technologies (Thermo Fisher Scientific, Agawam, MA, USA). Hank's balanced salt solution, glutaraldehyde , cacodylate, formvar/carbon Cu grids 200 mesh, epoxy resin were purchased from EM Sciences (Hatfield, PA, USA).

8.2.2. Cell Culture

Caco-2 cells (passage 55~65) were cultured in complete Dulbecco's modified essential medium (DMEM) containing high glucose, 10% fetal bovine serum (FBS), 1% antibiotic, and 1% amino acids as we described previously [221]. Cells were seeded at 3×10^5 cells/mL on transwells (Corning Inc., MA, USA) containing polyester filters (3 μm pore size and 4.7 cm^2 surface area) and grown for 21 days. The transepithelial electrical resistance (TEER) was monitored using a Millicell® ERS-2 epithelial voltammeter (World Precision Instruments, Sarasota, FL). The TEER data is presented as resistance per unit surface area $\Omega\times cm^2$.

8.2.3. Transmission electron microscopy analysis

To visualize the AuNPs, a drop of liquid sample was allowed to air-dry onto a carbon-coated 200 mesh copper grid, and then the sample was stained with 2% PTA. Samples were visualized with a transmission electron microscope (Tecani™ 12 TEM, FEI Company, Hillsboro, OR, USA). To visualize the uptake of AuNPs in intestinal epithelial cells, suspensions of AuNPs (15, 50, or 100 nm) were applied on Caco-2 cell monolayers. After treatment for 0.5 h, 1 h, 2 h, 4 h, 8 h and 24 h, the media in both the apical and basolateral sides were removed and the monolayers were rinsed with Hank's balanced salt solution (HBSS) that had been warmed to 37 ºC. The monolayers were immediately fixed in 2.5% glutaraldehyde and 2% paraformaldehyde (0.1 M sodium cacodylate buffer, pH 7.4) for 2 h at 37 ºC. They were then post-fixed in 1% aqueous osmium tetroxide solution and then embedded in Epoxy resin. Thin sections were obtained using an ultramicrotome with a

diamond knife (DDK, Wilmington, DE). The sections were stained with uranyl acetate followed by lead citrate. The image samples were then viewed with the transmission electron microscope (Tecani™ 12, FEI Company, Hillsboro, OR, USA).

8.2.4. ICP-MS analysis

After treatment with AuNPs, the cell monolayers and medium samples were collected at the specific time period from the apical and basolateral sides of the transwell as described above. A bicinchoninic acid (BCA) kit was used to quantify the protein concentration of the monolayers in each well. Each sample was mixed with 0.5 mL of aqua regia and then the sample was diluted to 10 mL with de-ionized water. A series of standard solutions of Au were prepared under the same conditions. Inductively-coupled plasma (ICP) mass spectrometry (MS) measurements were performed on a mass spectrometer (NexION 300X ICP, PerkinElmer, Cambridge, MA).

8.2.5. Calculation of number of gold nanoparticles

The number of gold nanoparticles in a given sample was calculated from the Au concentration measured by ICP-MS. The number of gold atoms per gold nanoparticle (n) can be estimated from the following expression [341]:

$$n = \frac{D^3}{d^3}$$

Where, D is the diameter of a gold nanoparticle and d is the diameter of a single gold atom, which is approximately 0.28 nm [342]. Hence, the number of AuNPs can be calculated from the measured Au concentration as follows:

$$C_n = \frac{C_m}{N_A \times n}$$

Where C_n = the number of AuNPs per unit volume, C_m = the measured mass of Au per unit volume, and N_A is Avogadro's constant.

8.2.6.Determination of mitochondrial membrane potential

Aqueous suspensions of AuNPs (D = 15, 50, or 100 nm) were applied on to well-differentiated Caco-2 monolayer (TEER > 200 Ω). Four hours after the treatment, the apical and basolateral media were removed and the monolayers were rinsed three times with warmed HBSS. A medium containing 10 μg/mL of JC-1 (mitochondrial membrane potential probe) in warmed DMEM solution was added to the Caco-2 cell monolayers. After the incubation for 15 minutes (37 ºC, 5% carbon dioxide, and 100% humidity), the monolayers were washed twice with HBSS, placed onto a microscope slide. After adding a fluorescent dye (DAPI) to the samples, the slides were rapidly sealed and stored overnight at 4 ºC. The microstructure of the samples was observed using a confocal fluorescent microscope (Olympus FV-1000, Waltham, MA). The JC-1 treated coverslips were excited at 488 nm, and the emission was recorded simultaneously at 527 and 590 nm by independent detectors [343]. Two-photon excitation of JC-1 labeled Caco-2 cell monolayers allowed for the real-time

analysis of mitochondria membrane potential. The data were analyzed using the following expression as described previously [344]:

$$\text{Ratio} = 5 \times I_{red}/I_{green}$$

Here I_{red} and I_{green} are the intensities of the signals in the red and green regions of the spectra. The factor "5" is used to transform the ratiometric results into an 8-bit scale of 256 levels.

8.2.7. Statistical Analysis

All values are expressed as means ± standard deviations (SD) unless stated otherwise. The difference among samples were analyzed by ANOVA with significance level of $p < 0.05$.

8.3. Results and discussion

8.3.1. Properties of gold nanoparticles

The AuNPs used in this study have been reported to be monodispersed spheres in an aqueous sodium citrate buffer that acted as a stabilizer to prevent particle aggregation [345]. The manufacturer reported that the droplet diameters of the three AuNPs samples used were 15, 50, and 100 nm, respectively, and that all of the particles had a negative charge (around -40 mV). The initial gold concentration was given as 50 ppm for all the AuNPs suspensions when they were adjusted to an optical density of 1 cm^{-1}. The morphology of the AuNPs was confirmed using transmission electron microscopy (Figure 8.1). All of the samples contained fairly

uniform spheres with dimensions that conformed to those stated by the manufacturer. Nevertheless, the TEM images suggested that some of the particles clustered together and formed aggregates. These aggregates may have been present within the initial samples, or they may have been introduced as a result of the method used to prepare the samples for TEM analysis. Previous studies have shown that inorganic nanoparticles (1 to 100 nm) might affect normal cellular functions, including inducing cell death, in a manner that depended on their particle size [346, 347]. We therefore hypothesized that the initial size of the AuNPs used in this study can influence their absorption, accumulation and cytotoxicity in the intestinal epithelial cells.

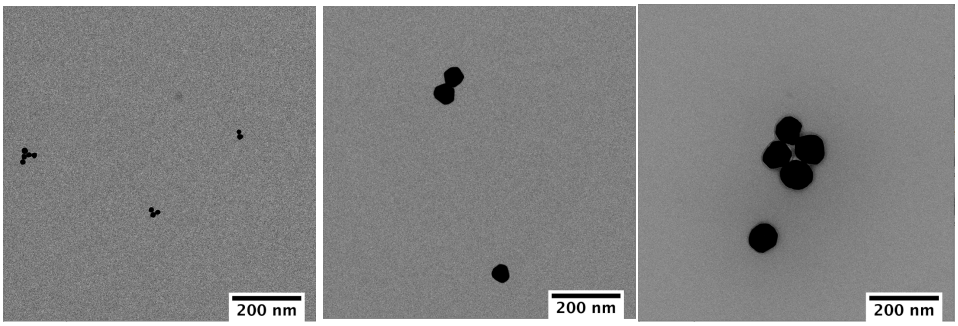

Figure 8-1 Morphology of the initial gold nanoparticle suspensions (nominal diameters of 15, 50 and 100 nm) used in this study. All images were taken under transmission electron microscopy as described in the Method.

8.3.2. Migration of gold nanoparticles within intestinal epithelium

It is well known that particle characteristics (such as size, shape, and surface chemistry) play an important role in determining the interactions of inorganic nanoparticles with biological membranes [348]. In this study we focused on the role

of particle size on cellular uptake by using AuNPs with the same shape (spherical) and surface chemistry (bare gold), but different diameters (15, 50, and 100 nm).

Caco-2 cells were cultured in the transwells to form well-differentiated and polarized monolayers. The monolayers were used to mimic absorptive functions of intestinal epithelium. Aqueous suspensions of AuNPs (15, 50, or 100 nm) were then placed on the apical side of the polarized monolayers for different incubation periods. The migration of AuNPs across the model intestinal cells was visualized by transmission electron microscope. The results were shown in Figure 3 (the most apparent AuNPs were highlighted by circles, and arrows indicate the direction from apical to basolateral side across microvilli). It is clear that the migration of AuNPs across the intestinal epithelial cells showed a distinct size-dependent pattern: the smaller the particle size, the faster the migration (Figure 8.2.). At 0.5 hour, 15 nm AuNPs have already been observed within the microvilli (Figure 8.2A), whereas no 50 or 100 nm AuNPs were found anywhere in the cells (Fig.8. 2E and 2I). After 1 hour of incubation, an appreciable number of 15 and 50 nm AuNPs could be observed in the cytoplasm (Fig.ure 8.2B and 2F). In contrast, only a few 100 nm AuNPs had entered the microvilli after 2 hours of incubation (Figure 8.2J). At 1-2 hour, the 15 and 50 nm AuNPs have migrated into various cellular organelles, such as the mitochondria and lysosome (Figure 8. 2B, 2C and 2G). In contrast， not until 4h's incubation, 100 nm AuNPs were found in the mitochondria and lysosome (Figure 8.2K). Some of AuNPs appeared as aggregates in lysosomes (Figure 8. 2G and 2K), After 24 hour of incubation, all AuNPs (15, 50, and 100 nm) were found

throughout the entire cell monolayer (Figure 8. 2D, 2H, and 2L). It is noteworthy that some of the nanoparticles were observed in the cell nuclei (Figure 8.2 H and 2L), which suggested that AuNPs may have the potential to induce genotoxicity. In general, the smallest gold nanoparticles (15 nm) were internalized at a faster rate than the large ones (50 or 100 nm).

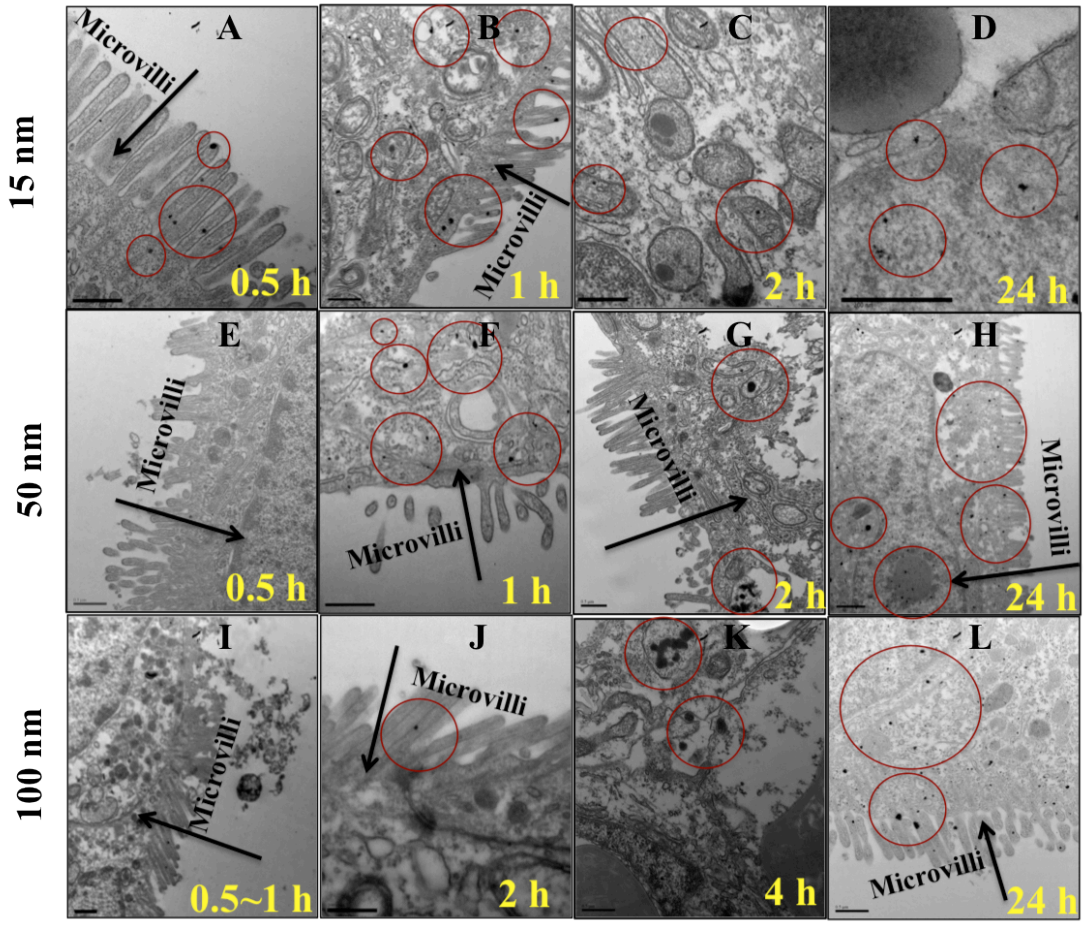

Figure 8-2 The absorption of AuNPs by intestinal epithelial cells. Caco-2 cell monolayers were incubated with AuNPs (15 nm, 50 nm, or 100 nm) for various time periods (up to 24 hour). After thorough wash, Caco-2 cell monolayers were processed for TEM (transmission electron microscope) analysis to visualize AuNPs absorbed by the cells. AuNPs are highlighted by the circles. Arrows indicate the direction from apical to basolateral side across microvilli. Different magnifications were used in different images. Scale bar represent 500 nm. Representative images were selected from replicates of at least 3.

8.3.3. Transport of gold nanoparticles across the intestinal epithelium

Microscopic analysis is useful for obtaining direct visualization of the migration and location of AuNPs in epithelial cells, but it is less useful for providing quantitative information about the amount of AuNPs that has been transported across the intestinal epithelial monolayer and that has been accumulated in side of the epithelial cells For this reason, quantitative analysis of the gold concentration was carried out using a highly sensitive ICP-MS method [336]. This method utilized acid digestion to dissolve the gold nanoparticles, and then the gold concentration is determined by mass spectrometry.

We established the influence of initial particle size of AuNPs on the transport of the AuNPs across the epithelial monolayers into the basolateral compartment of the transwells. After incubating the Caco-2 monolayers with AuNPs in the apical compartment of the transwells, a fixed volume of medium was collected from the basolateral compartment of the transwells at different times and then the amount of gold was quantified by ICP-MS (Figure 8. 3). The concentrations of gold in the basolateral compartment increased with increasing incubation time for all three types of AuNPs studied. For 15 and 50 nm nanoparticles (Figure 8. 3A and 3B), the higher the initial level of AuNPs in the apical compartment, the higher the basolateral concentration of gold that was detected at the same time point, particularly at 8 and 24 hour of incubation. This effect can be attributed to the fact that there were more gold nanoparticles per unit surface area in contact with the apical cell membrane (microvilli) at the higher concentration of AuNPs, and so

endocytosis occurred more frequently. Interestingly, a much higher concentration of intermediate sized nanoparticles (50 nm) were transported across the epithelial cell monolayer into the basolateral compartment than small (15 nm) or large (100 nm) ones (Figure 8.3B). A possible explanation of this phenomenon is the size-dependent nature of the receptor-mediated endocytosis [349, 350]. The endocytosis of nanoparticles depends on two competitive processes that require two different energies: (i) the binding energy between ligands and receptors; and (ii) the free energy for particle envelopment. When nanoparticles have diameters below about 40 nm, they do not produce a sufficiently large free energy change to become completely enveloped by the surface of the membrane. Conversely, when the nanoparticles have diameters greater than about 80 nm, the lack of free receptors limits the ligand-receptor binding energy. This much higher transport rate of 50 nm AuNPs across the intestinal epithelium may lead to higher levels of AuNPs in the systemic circulation, which may have a profound impact on the tissue/organ distribution and potential toxicity of these AuNPs in human body.

In contrast to 15 and 50 nm AuNPs, the transport of 100 nm AuNPs across the epithelial monolayer into the basolateral compartment of the transwells was found to be concentration independent (Figure 8.3C). At 2.5 and 5 μg/mL, the basolateral concentration of AuNPs remained relatively low after 24 hours of incubation, but at 10 μg/mL there was a steep increase (Figure 3C). Correspondingly, the TEER of the monolayers decreased drastically to values below 100 $\Omega.cm^2$, which suggests the monolayers had become leaky, hence the drastically increase in transport of AuNPs

across the epithelium. Standard TEER values of healthy cells are around 260 ± 65 Ω.cm^2 [259]. The 10 µg/mL of AuNPs suspension caused the same problem after 24 hours of incubation (Figure 8. 3B). These results suggested that AuNPs (50 and 100 nm) at the concentration of 10 µg/mL damaged the integrity of the epithelial monolayers.

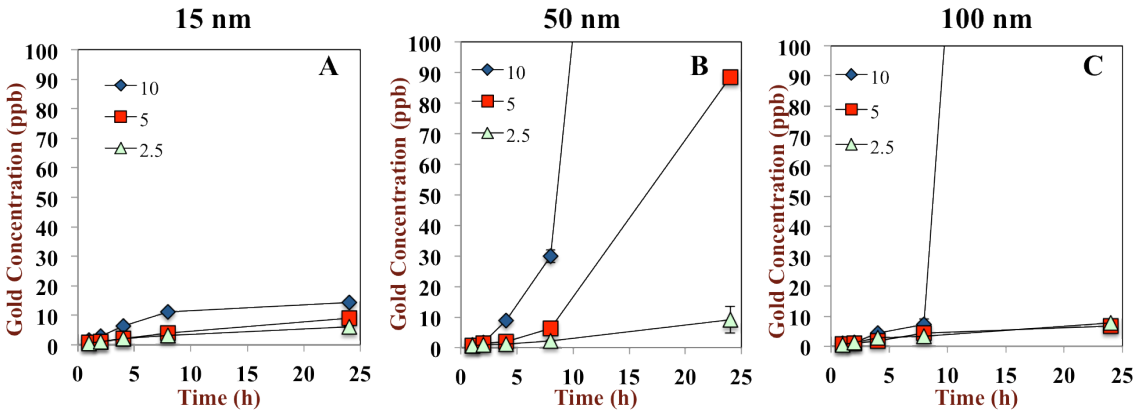

Figure 8-3 Transport of AuNPs across intestinal epithelium. Change in the concentration of gold measured in the basolateral compartment after incubating Caco-2 cell monolayers with AuNPs in the apical compartment of the transwells. Suspensions containing different concentrations of gold nanoparticles were used (shown in figure): 2.5, 5 and 10 µg/mL in the apical medium.

8.3.4. Accumulation of gold nanoparticles within the intestinal epithelium

Based on the above results, we used the nanoparticle suspensions with intermediate gold concentration (5 µg/mL that is not detrimental to the integrity of the epithelial monolayer) to further quantify the cellular accumulation of AuNPs within the Caco-2 cell monolayers. The data on the gold concentration were analyzed in two different but complementary ways (Figure 8.4). First, the mass of gold was normalized by the amount of cellular protein in each sample, so the results are presented as mass of gold per unit mass of protein (Figure 8. 4A). Since the

diameter of the AuNPs was known, it was also possible to calculate the number of nanoparticles per unit mass of protein (Figure 8. 4B). The incubation of Caco-2 monolayers with AuNPs was stopped after different incubation times and the amount of gold that had accumulated in the monolayer was quantified by ICP-MS as described in the Methods. The cellular accumulation of AuNPs clearly showed a size-dependent pattern, which depend on the way that the particle concentration was represented. In terms of total particle mass, the smaller the particle size, the lower the total amount of gold accumulated in the epithelial cells: 15 nm < 50 nm < 100 nm. Conversely, in terms of total particle number, the smaller the particle size, the greater the total accumulation of gold within the epithelial cells: 100 nm < 50 nm < 15 nm. This latter trend is similar to that reported previously for *in vivo* permeation of AuNPs through rat intestine [351].

The results suggest that smaller gold nanoparticles can more easily penetrate into cells, which leads to a greater number of small particles inside the cells. However, the total mass of gold that accumulates in the cells is greater for the larger AuNPs (even though they penetrate into the cells more slowly) because the number of gold atoms per particle is proportional to the cube of the particle size. These results also indicated that larger AuNPs had a slower excretion rate from inside of epithelial cells to the basolateral compartment. This highly size-dependent pattern of cellular accumulation of AuNPs may have a profound impact on the potential

toxicity of these AuNPs in the epithelial cells.

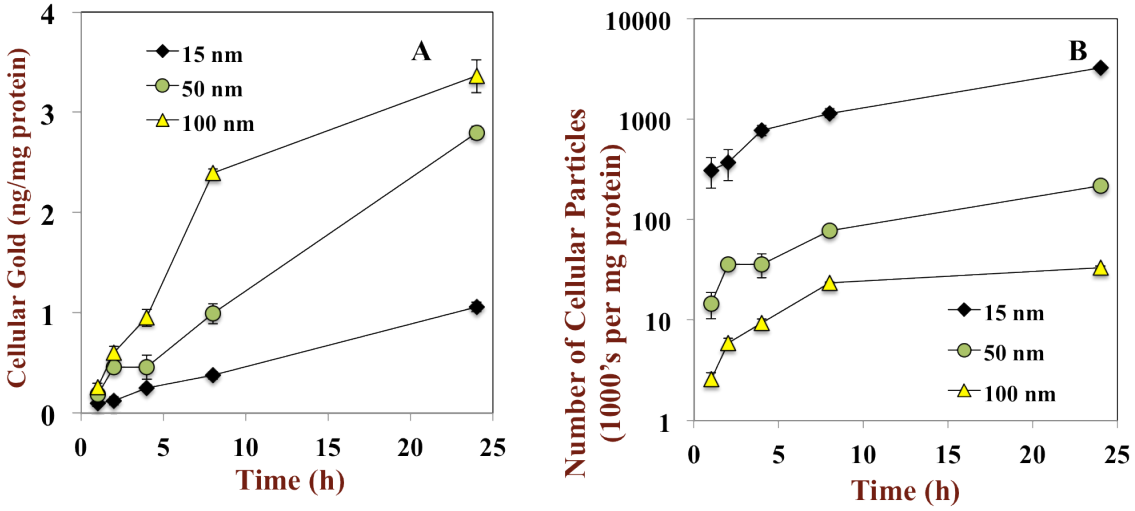

Figure 8-4 Accumulation of AuNPs within the intestinal epithelium. Change in the amount of gold measured in the Caco-2 monolayers after incubating Caco-2 cell monolayers with 5 µg/mL of AuNPs in the apical compartment of the transwells. Amount of gold was expressed as either particle mass (A) or particle number (B) in the Caco-2 cell monolayer.

8.3.5. Effect of gold nanoparticles on mitochondria potential

The ICP-MS results provided valuable quantitative information about endocytosis, accumulation, and excretion of the AuNPs by the Caco-2 intestinal epithelial cell monolayers. The TEM images indicated that the gold nanoparticles progressively spread throughout the model epithelium cells after absorption, and were eventually accumulated within different cellular organelles such as endosomes, lysosomes, Golgi apparatus, mitochondria, and nucleus (Figure 8.2.). The accumulation of AuNPs within these cellular substructures may promote cytotoxicity, since previous studies have shown that AuNPs can depolarize the membranes of the mitochondria in mammalian cells [340]. A decrease in mitochondrial membrane potential is an early indicator of cell death [335]. In

addition, impaired mitochondrial function has been shown to result in elevated levels of DNA damages [352]. Hence, we determined the mitochondria potential using a mitochondrion-specific dye (JC-1) after the Caco-2 cell monolayers had been incubated with AuNPs (5 μg/mL in apical medium) for 4 h. At this incubation time, the TEM images showed that the nanoparticles had accumulated within the mitochondria (Figure 2). Cells with high mitochondria membrane potential (healthy) promote the formation of dye aggregates that fluoresce red, whereas cells with low mitochondria membrane potential (damaged) remain monomeric JC-1 that fluoresce green [353]. As a result, the decrease of the red/green intensity ratio provides an indication of the damage of the mitochondria membrane function.

Our results showed a distinct size-dependent trend in the mitochondria toxicity caused by the gold nanoparticles: the larger the nanoparticles, the higher the toxicity, as evidenced by a decrease in the intensity of red florescence when the particle diameter increased (Figure 8.5A). Quantification of the ratio of red/green florescence further confirmed that the larger the AuNPs the lower the relative red florescence (Figure 8.5B) This finding is consistent with our results by ICP-MS that showed the cellular accumulation of total mass of gold follows the trend 100 nm > 50 nm > 15 nm (Figure 8.4A).

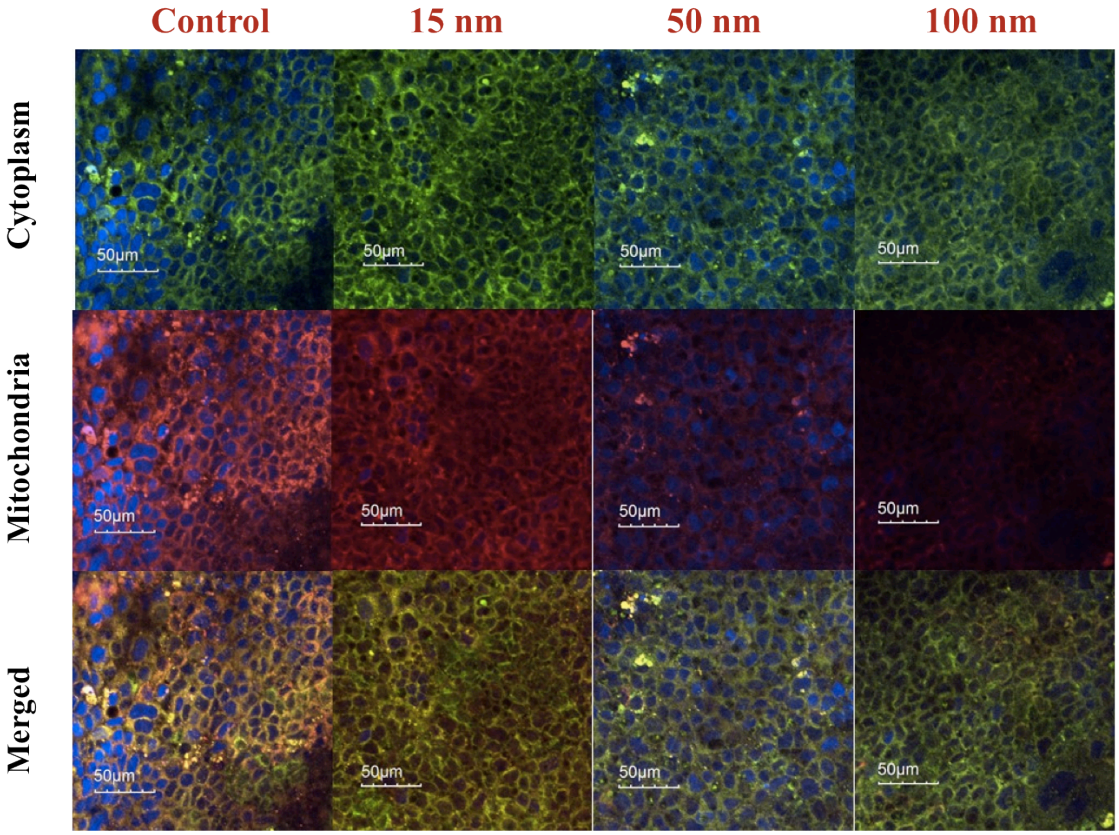
Control
15 nm
50 nm
100 nm
Cytoplasm
Mitochondria
Merged
50μm

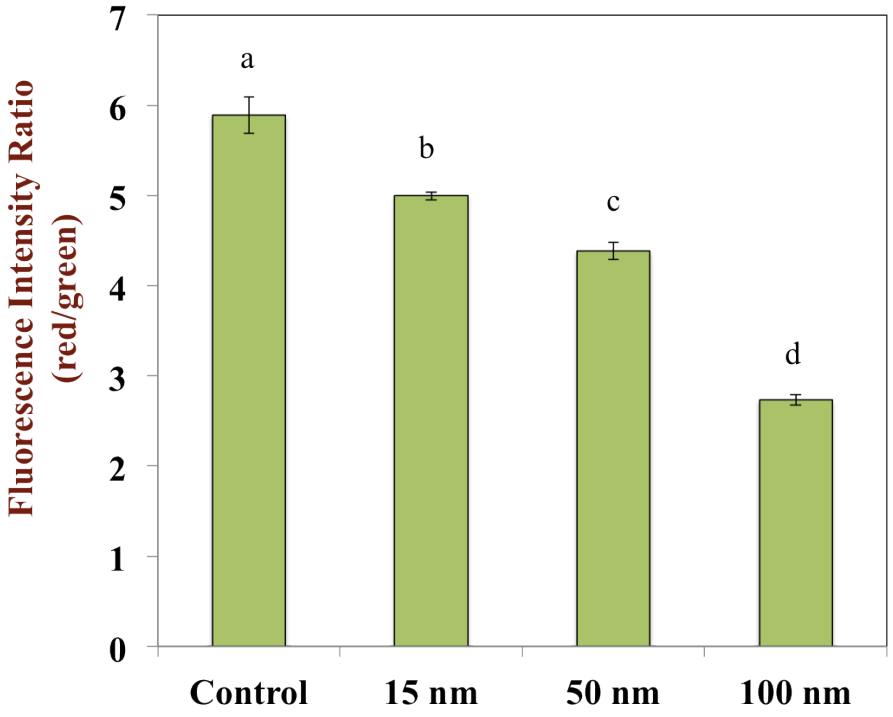
Fluorescence Intensity Ratio (red/green)
7
6
5
4
3
2
1
0
a
b
c
d
Control
15 nm
50 nm
100 nm

Figure 8-5 The effects of AuNPs on the mitochondrial membrane potentials of intestinal epithelial cells. Caco-2 cell monolayers were incubated with AuNPs (15 nm, 50 nm or 100 nm) for 4h separately. Mitochondria toxicity of AuNPs was visualized by confocal microscope using a red fluorescent dye JC-1 (A). Cells with high mitochondria membrane potential (healthy) promote the formation of dye aggregates that fluoresce red, whereas cells with low mitochondria membrane potential (damaged) remain monomeric JC-1 that fluoresce green. The red/green ratio was quantified using image J (B). Representative images were selected from replicates of 3. Different letters indicate statistical difference among the three groups at the given time point ($P<0.05$).

8.4. Conclusion

In summary, the absorption, accumulation, and transfer of AuNPs in the intestinal epithelial cells were highly dependent on their particle diameter (15, 50 or 100 nm). AuNPs with intermediate sizes (50 nm) were the most efficiently transported across the intestinal epithelium: uptaken from the apical side and excreted into the basolateral side. The smaller AuNPs (15 nm) were more rapidly absorbed by the intestinal epithelial cells and more quickly spread throughout the interior of the cells. Conversely, the larger AuNPs (100 nm) tended to accumulate within the intestinal epithelial cells since their rate of excretion into the basolateral side was slow. The increasing accumulation of the total mass of gold caused by AuNPs resulted in increasing mitochondria toxicity to the intestinal epithelial cells. Overall, this study provided detailed information on the impact of particle size on the absorption, accumulation and cytotoxicity of AuNPs in the intestinal epithelium.

CHAPTER 9

ADDITIONAL INFORMATION: IMPACT OF MIXED MICELLE ON THE FTE OF GOLD NANOPARTICLES IN THE INTESTINAL EPITHELIUM

9.1 Transport of gold nanoparticles across the intestinal epithelium

In this study, we determined the effect of mixed micelles (oleic acid-taurocholate) on the transport of gold nanoparticles (AuNPs) across the intestinal epithelium. Caco-2 cell monolayer was used as the intestinal epithelium model. AuNPs sized 15 nm, 50 nm and 100 nm (final concentration 2.5 ppm) were added on the Caco-2 cell monolayer model with or without mixed micelle in them. The final concentration of mixed micelles is constant (1.6: 0.5 mM) which is sufficient to produce abundant lipid droplets and chylomicrons as indicated in our previous research[4]. We first detected the amount of AuNPs changing in the basolateral side. Basolateral samples were collected at 4 h, 8 h and 24 h separately.

Significant difference was found when mixed micelle was incubated together with AuNPs: the amount of AuNPs dramatically increased after 24 h's incubation compared to the control group, especially AuNPs sized 50 nm and 100 nm, the total transported particles is tripled (mass/number)(Figure 9. 1). Hence, mixed micelles could improve the transport of AuNPs across the intestinal epithelium and AuNPs with larger size seems more efficient. We have the assumption that the improvement of the transport is related with the intestinal lipid absorption. The chylomicron-lymphatic pathway may interfere the fate of AuNPs through intestinal epithelium.

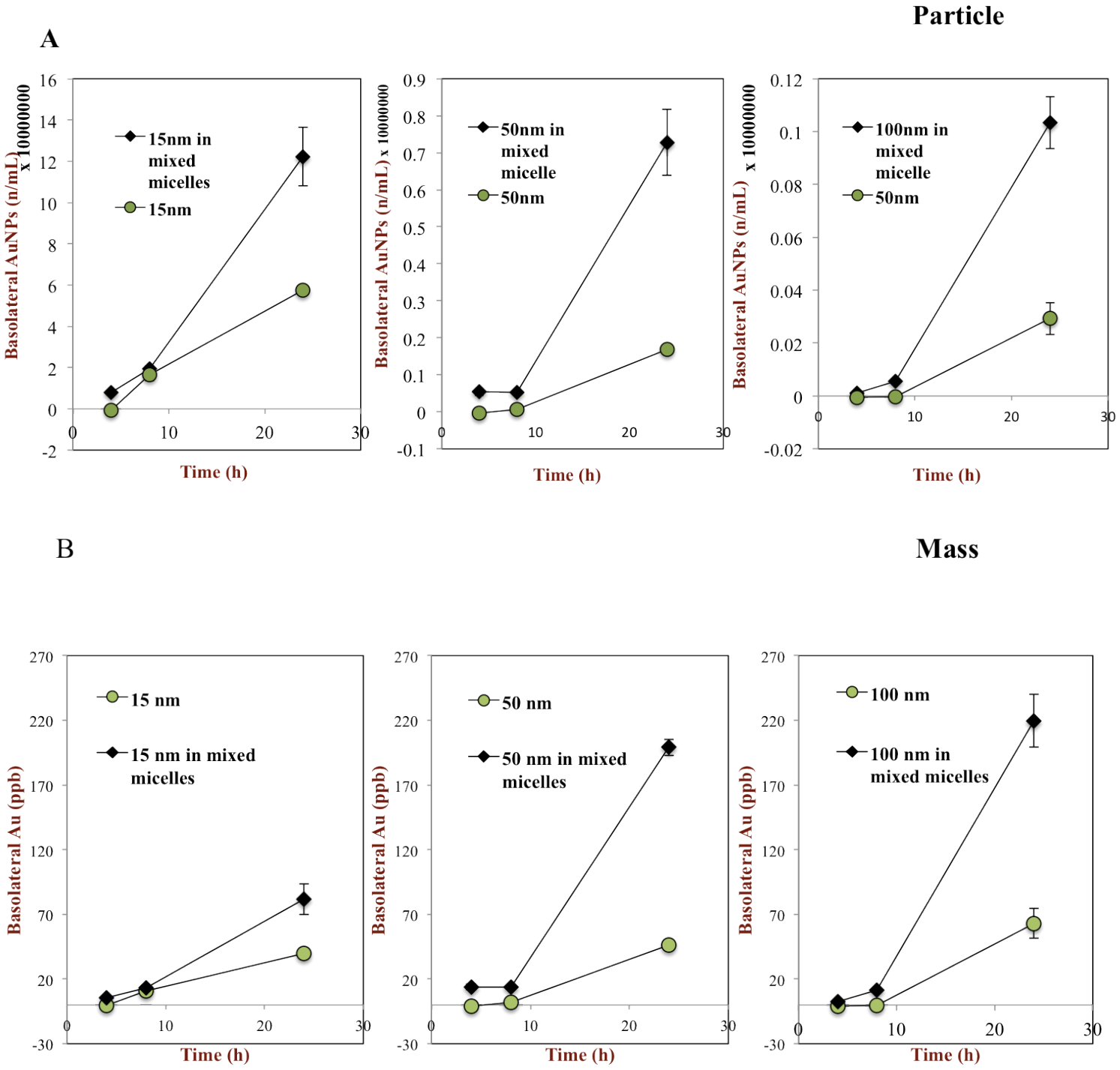

Figure 9-1 Transport of AuNPs sized 15 nm, 50 nm and 50 with or without mixed micelles (oleic acid- taurocholate) across Caco-2 cell monolayer. The amount of AuNPs was detected by ICP-MS. Results was shown both particle (A) and mass version (B).

9.2 Accumulation of gold nanoparticles in the intestinal epithelium

Cellular accumulation of AuNPs was also monitored. Interestingly, the amount of AuNPs retention in the monolayer was remarkably lower compared to the control group after 24 h incubation, especially for the AuNPs sized 100 nm, which was regarded as the most difficult to be expelled once taken into the cells according to our previous research（Figure 9.2）. Less AuNPs were found trapped in the monolayer compared to the control group, but the difference was not as significant as 15 nm and 100 nm particles. Mixed micelles were also shown to slightly affect the absorption of AuNPs at the first 4 h except the AuNPs sized 50 nm. Although the excretion rate of AuNPs greatly improved by the mixed micelles, the accumulation of AuNPs didn't decrease because AuNPs sized around 50 nm was confirmed to be the most efficient for uptake into mammal cells, according to the mechanism of size-dependent nature of the receptor-mediated endocytosis[340, 349, 350].

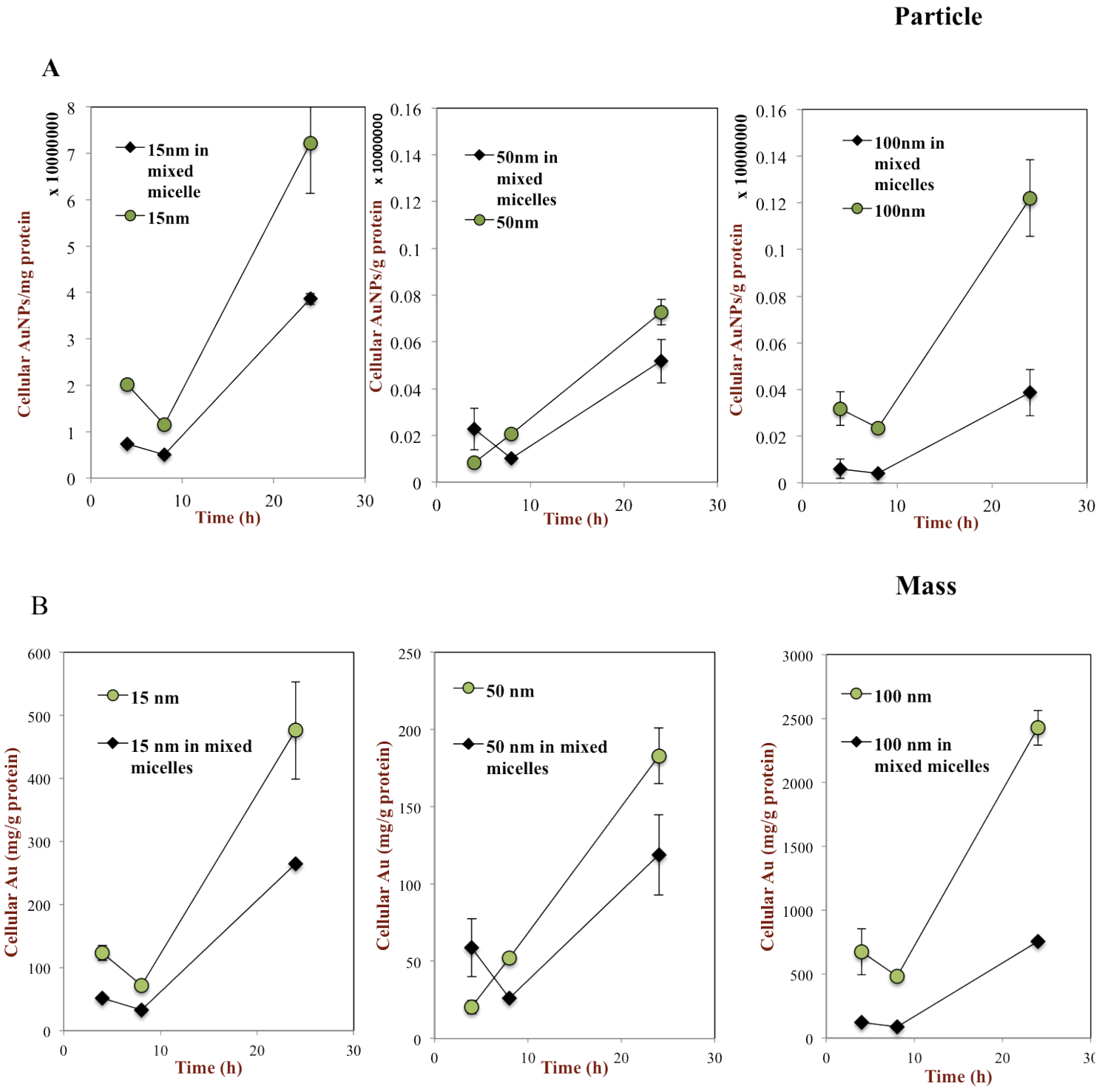

Figure 9-2 Effect of mixed micelles on cellular accumulation of gold nanoparticles with different size (15 nm, 50 nm and 100 nm) in Caco-2 cell monolayer.

CHAPTER 10

CONCLUSIONS

The overall goal of this work is to determine the role of lipid-based systems in the biological fate of lipophilic nutraceuticals and inorganic nanoparticles in the gastrointestinal tract. Two *in vitro* models were applied in this research, an in vitro digestion model and a Caco-2 cell monolayer model.

Our study based on the Caco-2 cell model showed that the transport of the highly lipophilic component 5-DN significantly enhanced in the present of mixed micelles ($C_{18:1}$-TC). The present of mixed micelles improved the solubilization 5-DN. Besides, they also stimulated the formation and secretion of chylomicrons. We assumed that chylomicrons might incorporate the lipophilic 5-DN molecules and protect them from metabolism by the enzymes in the cells. Thus the oral bioavailability of 5-DN increased. We further compared three different long chain fatty acid based mixed micelles ($C_{18:1}$-TC, $C_{18:2}$-TC and $C_{18:3}$-TC). Among them, oleic acid was found to be the most effective at improving the bioavailability of 5-DN. The efficiency of transport across the Caco-2 cell monolayer decreased in the following order: $C_{18:1} > C_{18:3} > C_{18:3}$. Same trend was found in the amount and size of the formed lipid droplets and chylomicrons. Hence, the bioavailability of 5-DN can be controlled through regulating the type of the ingested lipids.

It is also interesting to investigate the effect of lipid phase properties (MCT versus LCT) on digestion, bioaccessibility, and absorption of 5-DN using an in vitro digestion model combined with a Caco-2 cell monolayer model. Higher

bioaccessibility of 5-DN was found in MCT nanoemulsion than canola nanoemulsion, 13% vs.7% respectively. However, only 30% 5-DN crossed Caco-2 monolayer while half of them were metabolized for MCT nanoemulsion, up to 60% 5-DN and only 10% were metabolized in canola nanoemulsion. Results also demonstrated more lipid droplets and CMs were formed by LCT, which were responsible for transportation of 5-DN to the lymph. LCT-based emulsion was more potent in enhancing the bioavailability through increased lymphatic transport.

Ingestion of oxidized lipids was confirmed to affect the chylomicron-based lymphatic transport in this study. We compared the effect of oxidized and unoxidized linoleic acid (LA) on the transport of a highly lipophilic bioactive compound (5-DMT) using Caco-2 cell model. Our results suggest that oxidized LA affected the morphology of the Caco-2 monolayer, and especially the tight junctions, which may influence their subsequent distribution and metabolism in the human body.

Inorganic nanomaterials have been increasingly utilized in many consumer products, which has led to concerns about their potential toxicity. In this study, we determined the influence of particle size and concentration of gold nanoparticles (AuNPs) on their absorption, accumulation and cytotoxicity in model intestinal epithelial cells. As the mean particle diameter of the AuNPs decreased (from 100 to 50 to 15 nm) their rate of absorption by the intestinal epithelium cells increased, but their cellular accumulation in the epithelial cells decreased. Moreover, accumulation of AuNPs caused cytotoxicity in the intestinal epithelial cells, which was evidenced by depolarization of mitochondria membranes.

The impact of mixed micelles on the absorption and accumulation of inorganic nanoparticles in the gastrointestinal tract were also evaluated. Mixed micelles ($C_{18:1}$-TC) significantly improve the transport of AuNPs across the Cao-2 cell monolayer and meanwhile decreased the accumulation of AuNPs in the monolayer.

In summary, this study provides important information for the creation of lipid-based delivery systems designed to increase the oral bioavailability of lipophilic compounds in foods and drugs. Meanwhile, we also noticed that lipid based delivery system might also affect the fate of nanoparticle based food additive in the GI tract.

BIBLIOGRAPHY

1. McClements, D.J., *Emulsion Design to Improve the Delivery of Functional Lipophilic Components*, Annual Review of Food Science and Technology, Vol 1, 2010, 1: p. 241-269.

2. Somashekar, D., et al., *Effect of culture conditions on lipid and gamma-linolenic acid production by mucoraceous fungi*, Process Biochemistry, 2003, 38 (12): p. 1719-1724.

3. Porter, C.J., N.L. Trevaskis, W.N. Charman, *Lipids and lipid-based formulations: optimizing the oral delivery of lipophilic drugs*, Nat Rev Drug Discov, 2007, 6 (3): p. 231-248.

4. Yao, M.F., et al., *Controlling the gastrointestinal fate of nutraceutical-enriched lipid nanoparticles: From mixed micelles to chylomicrons* submitted, 2014: p.

5. Yao, M.F., H. Xiao, D.J. McClements, *Delivery of Lipophilic Bioactives: Assembly, Disassembly, and Reassembly of Lipid Nanoparticles*, Annual Review of Food Science and Technology, Vol 5, 2014, 5: p. 53-81.

6. Porter, C.J.H., et al., *Enhancing intestinal drug solubilisation using lipid-based delivery systems*, Advanced Drug Delivery Reviews, 2008, 60 (6): p. 673-691.

7. Trevaskis, N.L., W.N. Charman, C.J. Porter, *Lipid-based delivery systems and intestinal lymphatic drug transport: a mechanistic update*, Adv Drug Deliv Rev, 2008, 60 (6): p. 702-716.

8. During, A., et al., *Carotenoid uptake and secretion by CaCo-2 cells: beta-carotene isomer selectivity and carotenoid interactions*, J Lipid Res, 2002, 43 (7): p. 1086-1095.

9. Hussain, M.M., *A proposed model for the assembly of chylomicrons*, Atherosclerosis, 2000, 148 (1): p. 1-15.

10. Luchoomun, J., M.M. Hussain, *Assembly and secretion of chylomicrons by differentiated Caco-2 cells. Nascent triglycerides and preformed phospholipids are preferentially used for lipoprotein assembly*, J Biol Chem, 1999, 274 (28): p. 19565-19572.

11. Gonnet, M., L. Lethuaut, F. Boury, *New trends in encapsulation of liposoluble vitamins*, J Control Release, 2010, 146 (3): p. 276-290.

12. Weiss, J., et al., *Solid lipid nanoparticles as delivery systems for bioactive food components*, Food Biophysics, 2008, 3 (2): p. 146-154.

13. Jingling Tang, J.S., *Self-Emulsifying Drug Delivery Systems: Strategy for Improving Oral De- livery of Poorly Soluble Drugs*, Current Drug Therapy,, 2007, 2 (1): p. 85-93.

14. McClements, D.J., et al., *Structural design principles for delivery of bioactive components in nutraceuticals and functional foods*, Crit Rev Food Sci Nutr, 2009, 49 (6): p. 577-606.

15. During, A., et al., *Carotenoid uptake and secretion by CaCo-2 cells: beta-carotene isomer selectivity and carotenoid interactions*, J Lipid Res, 2002, 43 (7): p. 1086-1095.

16. Humberstone, A.J., W.N. Charman, *Lipid-based vehicles for the oral delivery of poorly water soluble drugs*, Advanced Drug Delivery Reviews, 1997, 25 (1): p. 103-128.

17. Kuentz, M., *Lipid-based formulations for oral delivery of lipophilic drugs*, Drug Discovery Today: Technologies, 2012, 9 (2): p. 97-104.

18. Porter, C.J., W.N. Charman, *Lipid-based formulations for oral administration: opportunities for bioavailability enhancement and lipoprotein targeting of lipophilic drugs*, J Recept Signal Transduct Res, 2001, 21 (2-3): p. 215-257.

19. Pouton, C.W., *Lipid formulations for oral administration of drugs: non-emulsifying, self-emulsifying and 'self-microemulsifying' drug delivery systems*, Eur J Pharm Sci, 2000, 11 Suppl 2: p. S93-98.

20. Pouton, C.W., C.J. Porter, *Formulation of lipid-based delivery systems for oral administration: materials, methods and strategies*, Adv Drug Deliv Rev, 2008, 60 (6): p. 625-637.

21. Vors, C., et al., *Modulating absorption and postprandial handling of dietary fatty acids by structuring fat in the meal: a randomized crossover clinical trial*, American Journal of Clinical Nutrition, 2013, 97 (1): p. 23-36.

22. Patel, A.R., K.P. Velikov, *Colloidal delivery systems in foods: A general comparison with oral drug delivery*, Lwt-Food Science and Technology, 2011, 44 (9): p. 1958-1964.

23. McClements, D.J., Y. Li, *Structured emulsion-based delivery systems: Controlling the digestion and release of lipophilic food components*, Advances in Colloid and Interface Science, 2010, 159 (2): p. 213-228.

24. McClements, D.J., E.A. Decker, Y. Park, *Controlling lipid bioavailability through physicochemical and structural approaches*, Crit Rev Food Sci Nutr, 2009, 49 (1): p. 48-67.

25. Wilde, P.J., B.S. Chu, *Interfacial & colloidal aspects of lipid digestion*, Adv Colloid Interface Sci, 2011, 165 (1): p. 14-22.

26. Chakraborty, S., et al., *Lipid--an emerging platform for oral delivery of drugs with poor bioavailability*, Eur J Pharm Biopharm, 2009, 73 (1): p. 1-15.

27. Kohli, K., et al., *Self-emulsifying drug delivery systems: an approach to enhance oral bioavailability*, Drug Discov Today, 2010, 15 (21-22): p. 958-965.

28. Acosta, E., *Bioavailability of nanoparticles in nutrient and nutraceutical delivery*, Current Opinion in Colloid & Interface Science, 2009, 14 (1): p. 3-15.

29. McClements, D.J., *Emulsion Design to Improve the Delivery of Functional Lipophilic Components*, in: Annual Review of Food Science and Technology, Vol 1, 2010, p. 241-269.

30. Sagalowicz, L., M.E. Leser, *Delivery systems for liquid food products*, Current Opinion in Colloid & Interface Science, 2010, 15 (1-2): p. 61-72.

31. Velikov, K.P., E. Pelan, *Colloidal delivery systems for micronutrients and nutraceuticals*, Soft Matter, 2008, 4 (10): p. 1964-1980.

32. Versantvoort, C.H.M., E. Van de Kamp, C.J.M. Rompelberg, *Development and applicability of an in vitro digestion model in assessing the bioaccessibility of contaminants from food*, in, Inspectorate of Health Inspection, Bilthoven, 2004, p. 1-87.

33. Fernandez-Garcia, E., et al., *Carotenoids bioavailability from foods: From plant pigments to efficient biological activities*, Food Research International, 2012, 46 (2): p. 438-450.

34. Bauer, E., S. Jakob, R. Mosenthin, *Principles of physiology of lipid digestion*, Asian-Australasian Journal of Animal Sciences, 2005, 18 (2): p. 282-295.

35. Fave, G., T.C. Coste, M. Armand, *Physicochemical properties of lipids: New strategies to manage fatty acid bioavailability*, Cellular and Molecular Biology, 2004, 50 (7): p. 815-831.

36. Bermudez, B., et al., *Digestion and absorption of olive oil*, Grasas Y Aceites, 2004, 55 (1): p. 1-10.

37. Mohanty, C., M. Das, S.K. Sahoo, *Emerging role of nanocarriers to increase the solubility and bioavailability of curcumin*, Expert Opinion on Drug Delivery, 2012, 9 (11): p. 1347-1364.

38. Cone, R.A., *Barrier properties of mucus*, Advanced Drug Delivery Reviews, 2009, 61 (2): p. 75-85.

39. Ensign, L.M., R. Cone, J. Hanes, *Oral drug delivery with polymeric nanoparticles: The gastrointestinal mucus barriers*, Advanced Drug Delivery Reviews, 2012, 64 (6): p. 557-570.

40. Singh, H., A. Ye, D. Horne, *Structuring food emulsions in the gastrointestinal tract to modify lipid digestion*, Progress in Lipid Research, 2008: p.

41. McClements, D.J., E.A. Decker, J. Weiss, *Emulsion-based delivery systems for lipophilioc bioactive components*, Journal of Food Science, 2007, 72 (8): p. R109-R124.

42. Brodskaya, E.N., *Computer simulations of micellar systems*, Colloid Journal, 2012, 74 (2): p. 154-171.

43. Torchilin, V.P., *Micellar nanocarriers: Pharmaceutical perspectives*, Pharmaceutical Research, 2007, 24 (1): p. 1-16.

44. Leser, M.E., et al., *Self-assembly of polar food lipids*, Advances in Colloid and Interface Science, 2006, 123: p. 125-136.

45. Israelachvili, J., *Intermolecular and Surface Forces, Third Edition*, Third Edition ed., Academic Press, London, UK, 2011.

46. Huang, Q.R., H.L. Yu, Q.M. Ru, *Bioavailability and Delivery of Nutraceuticals Using Nanotechnology*, Journal of Food Science, 2010, 75 (1): p. R50-R57.

47. Marze, S., *Bioaccessibility of Nutrients and Micronutrients from Dispersed Food Systems: Impact of the Multiscale Bulk and Interfacial Structures*, Critical Reviews in Food Science and Nutrition, 2013, 53 (1): p. 76-108.

48. Flanagan, J., H. Singh, *Microemulsions: A potential delivery system for bioactives in food*, Critical Reviews in Food Science and Nutrition, 2006, 46 (3): p. 221-237.

49. Spernath, A., A. Aserin, *Microemulsions as carriers for drugs and nutraceuticals*, Adv Colloid Interface Sci, 2006, 128: p. 47-64.

50. Spernath, A., et al., *Food-grade microemulsions based on nonionic emulsifiers: Media to enhance lycopene solubilization*, Journal of Agricultural and Food Chemistry, 2002, 50 (23): p. 6917-6922.

51. Garti, N., et al., *Nano-sized self-assemblies of nonionic surfactants as solubilization reservoirs and microreactors for food systems*, Soft Matter, 2005, 1 (3): p. 206-218.

52. Yaghmur, A., A. Aserin, N. Garti, *Phase behavior of microemulsions based on food-grade nonionic surfactants: effect of polyols and short-chairs alcohols*, Colloids and Surfaces a-Physicochemical and Engineering Aspects, 2002, 209 (1): p. 71-81.

53. Rao, J.J., D.J. McClements, *Formation of Flavor Oil Microemulsions, Nanoemulsions and Emulsions: Influence of Composition and Preparation Method*, Journal of Agricultural and Food Chemistry, 2011, 59 (9): p. 5026-5035.

54. Sharma, A., U.S. Sharma, *Liposomes in drug delivery: progress and limitations*, International Journal of Pharmaceutics, 1997, 154 (2): p. 123-140.

55. Maherani, B., et al., *Liposomes: A Review of Manufacturing Techniques and Targeting Strategies*, Current Nanoscience, 2011, 7 (3): p. 436-452.

56. Reineccius, G.A., *Liposomes for controlled-release in the food-industry*, in: Risch, S.J., G.A. Reineccius (Eds.) Encapsulation and Controlled Release of Food Ingredients, 1995, p. 113-131.

57. Taylor, T.M., et al., *Liposomal nanocapsules in food science and agriculture*, Critical Reviews in Food Science and Nutrition, 2005, 45 (7-8): p. 587-605.

58. McClements, D.J., *Edible nanoemulsions: fabrication, properties, and functional performance*, Soft Matter, 2011, 7 (6): p. 2297-2316.

59. McClements, D.J., J. Rao, *Food-Grade Nanoemulsions: Formulation, Fabrication, Properties, Performance, Biological Fate, and Potential Toxicity*, Critical Reviews in Food Science and Nutrition, 2011, 51 (4): p. 285-330.

60. McClements, D.J., *Nanoemulsions versus microemulsions: terminology, differences, and similarities*, Soft Matter, 2012, 8 (6): p. 1719-1729.

61. Koroleva, M.Y., E.V. Yurtov, *Nanoemulsions: the properties, methods of preparation and promising applications*, Russian Chemical Reviews, 2012, 81 (1): p. 21-43.

62. Silva, H.D., M.A. Cerqueira, A.A. Vicente, *Nanoemulsions for Food Applications: Development and Characterization*, Food and Bioprocess Technology, 2012, 5 (3): p. 854-867.

63. Solans, C., I. Sole, *Nano-emulsions: Formation by low-energy methods*, Current Opinion in Colloid & Interface Science, 2012, 17 (5): p. 246-254.

64. McClements, D.J., *Food Emulsions: Principles, Practice, and Techniques*, 2nd ed., CRC Press, Boca Raton, 2005.

65. Jores, K., et al., *Investigations on the structure of solid lipid nanoparticles (SLN) and oil-loaded solid lipid nanoparticles by photon correlation spectroscopy, field-flow fractionation and transmission electron microscopy*, Journal of Controlled Release, 2004, 95 (2): p. 217-227.

66. Muller, R.H., K. Mader, S. Gohla, *Solid lipid nanoparticles (SLN) for controlled drug delivery - a review of the state of the art*, European Journal of Pharmaceutics and Biopharmaceutics, 2000, 50 (1): p. 161-177.

67. Bunjes, H., *Structural properties of solid lipid based colloidal drug delivery systems*, Current Opinion in Colloid & Interface Science, 2011, 16 (5): p. 405-411.

68. Lesmes, U., D.J. McClements, *Structure-function relationships to guide rational design and fabrication of particulate food delivery systems*, Trends in Food Science & Technology, 2009, 20 (10): p. 448-457.

69. Fathi, M., M.R. Mozafari, M. Mohebbi, *Nanoencapsulation of food ingredients using lipid based delivery systems*, Trends in Food Science & Technology, 2012, 23 (1): p. 13-27.

70. Muller, R.H., M. Radtke, S.A. Wissing, *Solid lipid nanoparticles (SLN) and nanostructured lipid carriers (NLC) in cosmetic and dermatological preparations*, Adv Drug Deliv Rev, 2002, 54 Suppl 1: p. S131-155.

71. Mcclements, D.J., E.A. Decker, Y. Park, *Controlling Lipid Bioavailability through Physicochemical and Structural Approaches*, Crit Rev Food Sci Nutr, 2009, 49 (1): p. 48-67.

72. Matalanis, A., O.G. Jones, D.J. McClements, *Structured biopolymer-based delivery systems for encapsulation, protection, and release of lipophilic compounds*, Food Hydrocolloids, 2011, 25 (8): p. 1865-1880.

73. Singh, H., A. Ye, D. Horne, *Structuring food emulsions in the gastrointestinal tract to modify lipid digestion*, Prog Lipid Res, 2009, 48 (2): p. 92-100.

74. van Aken, G.A., *Relating Food Emulsion Structure and Composition to the Way It Is Processed in the Gastrointestinal Tract and Physiological Responses: What Are the Opportunities?*, Food Biophysics, 2010, 5 (4): p. 258-283.

75. Barrett, K.E., *Gastrointestinal Physiology*, McGraw-Hill, New York, NY, 2006.

76. Basit, A.W., *Advances in colonic drug delivery*, Drugs, 2005, 65 (14): p. 1991-2007.

77. McClements, D.J., E.A. Decker, Y. Park, *Physicochemical and structural aspects of lipid digestion*, in: McClements, D.J. (Ed.) Understanding and Controlling the Microstructure of Complex Foods, CRC Press, Boca Raton, FL, 2007, p. 483-503.

78. Johnson, L.R., *Gastrointestinal Physiology, 6th Edition*, Mosby, St. Louis, MI, 2001.

79. Singh, H., A.Q. Ye, D. Horne, *Structuring food emulsions in the gastrointestinal tract to modify lipid digestion*, Progress in Lipid Research, 2009, 48 (2): p. 92-100.

80. Golding, M., et al., *Impact of gastric structuring on the lipolysis of emulsified lipids*, Soft Matter, 2011, 7 (7): p. 3513-3523.

81. McClements, D.J., H. Xiao, *Potential biological fate of ingested nanoemulsions: influence of particle characteristics*, Food & Function, 2012, 3 (3): p. 202-220.

82. Hu, S.W., et al., *Integrity and stability of oral liposomes containing bile salts studied in simulated and ex vivo gastrointestinal media*, International Journal of Pharmaceutics, 2013, 441 (1-2): p. 693-700.

83. Li, Y., et al., *Modulation of lipid digestibility using structured emulsion-based delivery systems: Comparison of in vivo and in vitro measurements*, Food & Function, 2012, 3 (5): p. 528-536.

84. Augustin, M.A., et al., *Intestinal passage of microencapsulated fish oil in rats following oral administration*, Food & Function, 2011, 2 (11): p. 684-696.

85. Liu, Y.W., et al., *Investigation into the bioaccessibility and microstructure changes of beta-carotene emulsions during in vitro digestion*, Innovative Food Science & Emerging Technologies, 2012, 15: p. 86-95.

86. Tokle, T., et al., *Impact of dietary fiber coatings on behavior of protein-stabilized lipid droplets under simulated gastrointestinal conditions*, Food & Function, 2012, 3 (1): p. 58-66.

87. Singh, H., A. Sarkar, *Behaviour of protein-stabilised emulsions under various physiological conditions*, Advances in Colloid and Interface Science, 2011, 165 (1): p. 47-57.

88. Mackie, A., A. Macierzanka, *Colloidal aspects of protein digestion*, Current Opinion in Colloid & Interface Science, 2010, 15 (1-2): p. 102-108.

89. Mun, S., E.A. Decker, D.J. McClements, *Influence of emulsifier type on in vitro digestibility of lipid droplets by pancreatic lipase*, Food Research International, 2007, 40 (6): p. 770-781.

90. Nik, A.M., S. Langmaid, A.J. Wright, *Digestibility and beta-carotene release from lipid nanodispersions depend on dispersed phase crystallinity and interfacial properties*, Food & Function, 2012, 3 (3): p. 234-245.

91. Gallier, S., A. Ye, H. Singh, *Structural changes of bovine milk fat globules during in vitro digestion*, Journal of Dairy Science, 2012, 95 (7): p. 3579-3592.

92. Troncoso, E., J.M. Aguilera, D.J. McClements, *Fabrication, characterization and lipase digestibility of food-grade nanoemulsions*, Food Hydrocolloids, 2012, 27 (2): p. 355-363.

93. Wilde, P.J., B.S. Chu, *Interfacial & colloidal aspects of lipid digestion*, Advances in Colloid and Interface Science, 2011, 165 (1): p. 14-22.

94. Ye, A., J. Cui, H. Singh, *Proteolysis of milk fat globule membrane proteins during in vitro gastric digestion of milk*, Journal of Dairy Science, 2011, 94 (6): p. 2762-2770.

95. McClements, D.J., *Crystals and crystallization in oil-in-water emulsions: Implications for emulsion-based delivery systems*, Advances in Colloid and Interface Science, 2012, 174 (0): p. 1-30.

96. Li, Y., et al., *Nanoemulsion-based delivery systems for poorly water-soluble bioactive compounds: Influence of formulation parameters on polymethoxyflavone crystallization*, Food Hydrocolloids, 2012, 27 (2): p. 517-528.

97. Bonnaire, L., et al., *Influence of lipid physical state on the in vitro digestibility of emulsified lipids*, Journal of Agricultural and Food Chemistry, 2008, 56 (10): p. 3791-3797.

98. Madenci, D., S.U. Egelhaaf, *Self-assembly in aqueous bile salt solutions*, Current Opinion in Colloid & Interface Science, 2010, 15 (1-2): p. 109-115.

99. Porter, C.J., W.N. Charman, *Transport and absorption of drugs via the lymphatic system*, Adv Drug Deliv Rev, 2001, 50 (1-2): p. 1-2.

100. Di Maio, S., R.L. Carrier, *Gastrointestinal contents in fasted state and post-lipid ingestion: In vivo measurements and in vitro models for studying oral drug delivery*, Journal of Controlled Release, 2011, 151 (2): p. 110-122.

101. Shen, H., P. Howles, P. Tso, *From interaction of lipidic vehicles with intestinal epithelial cell membranes to the formation and secretion of chylomicrons*, Adv Drug Deliv Rev, 2001, 50 Suppl 1: p. S103-125.

102. Porter, C.J., W.N. Charman, *In vitro assessment of oral lipid based formulations*, Adv Drug Deliv Rev, 2001, 50 Suppl 1: p. S127-147.

103. Mullertz, A., et al., *Insights into Intermediate Phases of Human Intestinal Fluids Visualized by Atomic Force Microscopy and Cryo-Transmission Electron Microscopy ex Vivo*, Molecular Pharmaceutics, 2012, 9 (2): p. 237-247.

104. Darwich, A.S., et al., *Interplay of Metabolism and Transport in Determining Oral Drug Absorption and Gut Wall Metabolism: A Simulation Assessment Using the "Advanced Dissolution, Absorption, Metabolism (ADAM)" Model*, Current Drug Metabolism, 2010, 11 (9): p. 716-729.

105. Mazer, N.A., G.B. Benedek, M.C. Carey, *Quasi-elastic light-scattering-studies of aqueous biliary lipid systems - mixed micelle formation in bile-salt lecithin solutions*, Biochemistry, 1980, 19 (4): p. 601-615.

106. Schwebel, H.J., et al., *The apparent solubilizing capacity of simulated intestinal fluids for poorly water-soluble drugs*, Pharmaceutical Development and Technology, 2011, 16 (3): p. 278-286.

107. Charman, W.N., et al., *Physicochemical and physiological mechanisms for the effects of food on drug absorption: The role of lipids and pH*, J Pharm Sci, 1997, 86 (3): p. 269-282.

108. Porter, C.J.H., N.L. Trevaskis, W.N. Charman, *Lipids and lipid-based formulations: optimizing the oral delivery of lipophilic drugs*, Nature Reviews Drug Discovery, 2007, 6 (3): p. 231-248.

109. Xiao, C., G.F. Lewis, *Regulation of chylomicron production in humans*, Biochimica Et Biophysica Acta-Molecular and Cell Biology of Lipids, 2012, 1821 (5): p. 736-746.

110. Ahmed, K., et al., *Nanoemulsion- and emulsion-based delivery systems for curcumin: Encapsulation and release properties*, Food Chem, 2012, 132 (2): p. 799-807.

111. Wang, P., et al., *Preliminary study into the factors modulating beta-carotene micelle formation in dispersions using an in vitro digestion model*, Food Hydrocolloids, 2012, 26 (2): p. 427-433.

112. Li, Y., M. Hu, D.J. McClements, *Factors affecting lipase digestibility of emulsified lipids using an in vitro digestion model: Proposal for a standardised pH-stat method*, Food Chemistry, 2011, 126 (2): p. 498-505.

113. Li, Y., D.J. McClements, *New Mathematical Model for Interpreting pH-Stat Digestion Profiles: Impact of Lipid Droplet Characteristics on in Vitro Digestibility*, Journal of Agricultural and Food Chemistry, 2010, 58 (13): p. 8085-8092.

114. Reis, P., et al., *Lipases at interfaces: A review*, Advances in Colloid and Interface Science, 2009, 147-48: p. 237-250.

115. Li, Y., D.J. McClements, *Inhibition of lipase-catalyzed hydrolysis of emulsified triglyceride oils by low-molecular weight surfactants under simulated gastrointestinal conditions*, European Journal of Pharmaceutics and Biopharmaceutics, 2011, 79 (2): p. 423-431.

116. Troncoso, E., J.M. Aguilera, D.J. McClements, *Influence of particle size on the in vitro digestibility of protein-coated lipid nanoparticles*, Journal of Colloid and Interface Science, 2012, 382: p. 110-116.

117. Nik, A.M., M. Corredig, A.J. Wright, *Release of lipophilic molecules during in vitro digestion of soy protein-stabilized emulsions*, Molecular Nutrition & Food Research, 2011, 55: p. S278-S289.

118. Sy, C., et al., *Effects of physicochemical properties of carotenoids on their bioaccessibility, intestinal cell uptake, and blood and tissue concentrations*, Molecular Nutrition & Food Research, 2012, 56 (9): p. 1385-1397.

119. Hussain, N., V. Jaitley, A.T. Florence, *Recent advances in the understanding of uptake of microparticulates across the gastrointestinal lymphatics*, Advanced Drug Delivery Reviews, 2001, 50 (1-2): p. 107-142.

120. Iqbal, J., M.M. Hussain, *Intestinal lipid absorption*, American Journal of Physiology-Endocrinology and Metabolism, 2009, 296 (6): p. E1183-E1194.

121. Porter, C.J.H., W.N. Charman, *Uptake of drugs into the intestinal lymphatics after oral administration*, Advanced Drug Delivery Reviews, 1997, 25 (1): p. 71-89.

122. Kindel, T., D.M. Lee, P. Tso, *The mechanism of the formation and secretion of chylomicrons*, Atherosclerosis Supplements, 2010, 11 (1): p. 11-16.

123. Li, Y., et al., *Controlling lipid nanoemulsion digestion using nanolaminated biopolymer coatings*, Journal of Microencapsulation, 2011, 28 (3): p. 166-175.

124. Abumrad, N.A., N.O. Davidson, *Role of the gut in lipid homeostasis*, Physiological Reviews, 2012, 92 (3): p. 1061-1085.

125. Powell, J.J., et al., *Origin and fate of dietary nanoparticles and microparticles in the gastrointestinal tract*, Journal of Autoimmunity, 2010, 34 (3): p. J226-J233.

126. Sugano, K., *Estimation of effective intestinal membrane permeability considering bile micelle solubilisation*, International Journal of Pharmaceutics, 2009, 368 (1-2): p. 116-122.

127. Usami, M., et al., *Effect of gamma-linolenic acid or docosahexaenoic acid on tight junction permeability in intestinal monolayer cells and their mechanism by protein kinase C activation and/or eicosanoid formation*, Nutrition, 2003, 19 (2): p. 150-156.

128. Duraisamy, Y., et al., *Differential incorporation of docosahexaenoic acid into distinct cholesterol-rich membrane raft domains*, Biochem Biophys Res Commun, 2007, 360 (4): p. 885-890.

129. Jewell, C., K.D. Cashman, *The effect of conjugated linoleic acid and medium-chain fatty acids on transepithelial calcium transport in human intestinal-like Caco-2 cells*, Br J Nutr, 2003, 89 (5): p. 639-647.

130. Shima, M., et al., *Effects of medium-chain fatty acids and their acylglycerols on the transport of penicillin V across Caco-2 cell monolayers*, Biosci Biotechnol Biochem, 1997, 61 (7): p. 1150-1155.

131. Kotake-Nara, E., A. Nagao, *Effects of Mixed Micellar Lipids on Carotenoid Uptake by Human Intestinal Caco-2 Cells*, Bioscience Biotechnology and Biochemistry, 2012, 76 (5): p. 875-882.

132. Rozner, S., et al., *Do food microemulsions and dietary mixed micelles interact?*, Colloids and Surfaces B-Biointerfaces, 2010, 77 (1): p. 22-30.

133. Delorme, V., et al., *Effects of Surfactants on Lipase Structure, Activity, and Inhibition*, Pharmaceutical Research, 2011, 28 (8): p. 1831-1842.

134. Thongngam, M., D.J. McClements, *Isothermal titration calorimetry study of the interactions between chitosan and a bile salt (sodium taurocholate)*, Food Hydrocolloids, 2005, 19 (5): p. 813-819.

135. Helgason, T., et al., *Examination of the interaction of chitosan and oil-in-water emulsions under conditions simulating the digestive system using confocal microscopy*, Journal of Aquatic Food Product Technology, 2008, 17 (3): p. 216-233.

136. Tsujita, T., et al., *Antiobesity action of epsilon-polylysine, a potent inhibitor of pancreatic lipase*, Journal of Lipid Research, 2006, 47 (8): p. 1852-1858.

137. Sarkar, A., D.S. Horne, H. Singh, *Interactions of milk protein-stabilized oil-in-water emulsions with bile salts in a simulated upper intestinal model*, Food Hydrocolloids, 2010, 24 (2-3): p. 142-151.

138. Devraj, R., et al., *In vitro digestion testing of lipid-based delivery systems: Calcium ions combine with fatty acids liberated from triglyceride rich lipid solutions to form soaps and reduce the solubilization capacity of colloidal digestion products*, International Journal of Pharmaceutics, 2013, 441 (1-2): p. 323-333.

139. Hu, M., et al., *Role of calcium and calcium-binding agents on the lipase digestibility of emulsified lipids using an in vitro digestion model*, Food Hydrocolloids, 2010, 24 (8): p. 719-725.

140. Bendsen, N.T., et al., *Effect of dairy calcium on fecal fat excretion: a randomized crossover trial*, International Journal of Obesity, 2008, 32 (12): p. 1816-1824.

141. Yanez, J.A., et al., *Intestinal lymphatic transport for drug delivery*, Adv Drug Deliv Rev, 2011, 63 (10-11): p. 923-942.

142. Porter, C.J., S.A. Charman, W.N. Charman, *Lymphatic transport of halofantrine in the triple-cannulated anesthetized rat model: effect of lipid vehicle dispersion*, J Pharm Sci, 1996, 85 (4): p. 351-356.

143. Sun, M., et al., *Intestinal absorption and intestinal lymphatic transport of sirolimus from self-microemulsifying drug delivery systems assessed using the single-pass intestinal perfusion (SPIP) technique and a chylomicron flow blocking approach: linear correlation with oral bioavailabilities in rats*, Eur J Pharm Sci, 2011, 43 (3): p. 132-140.

144. Lehner, R., J.H. Lian, A.D. Quiroga, *Lumenal Lipid Metabolism Implications for Lipoprotein Assembly*, Arteriosclerosis Thrombosis and Vascular Biology, 2012, 32 (5): p. 1087-1093.

145. Pan, X.Y., M.M. Hussain, *Gut triglyceride production*, Biochimica Et Biophysica Acta-Molecular and Cell Biology of Lipids, 2012, 1821 (5): p. 727-735.

146. Lairon, D., *Macronutrient intake and modulation on chylomicron production and clearance*, Atherosclerosis Supplements, 2008, 9 (2): p. 45-48.

147. Hamidi, M., M. Foroozesh, A. Zarrin, *Lipoproteins: From physiological roles to drug delivery potentials*, Critical Reviews in Therapeutic Drug Carrier Systems, 2006, 23 (6): p. 497-523.

148. O'Driscoll, C.M., *Lipid-based formulations for intestinal lymphatic delivery*, Eur J Pharm Sci, 2002, 15 (5): p. 405-415.

149. Tso, P., W.J. Simmonds, *The absorption of lipid and lipoprotein synthesis*, Lab Res Methods Biol Med, 1984, 10: p. 191-216.

150. Lu, Y., S. Kim, K. Park, *In vitro-in vivo correlation: Perspectives on model development*, International Journal of Pharmaceutics, 2011, 418 (1): p. 142-148.

151. Lipinski, C.A., et al., *Experimental and computational approaches to estimate solubility and permeability in drug discovery and development settings*, Adv Drug Deliv Rev, 2001, 46 (1-3): p. 3-26.

152. Lipinski, C.A., et al., *Experimental and computational approaches to estimate solubility and permeability in drug discovery and development settings*, Advanced Drug Delivery Reviews, 2012, 64: p. 4-17.

153. Martel, S., et al., *Large, chemically diverse dataset of logP measurements for benchmarking studies*, Eur J Pharm Sci, 2012, 48 (1-2): p. 21-29.

154. Kendrick, J.S., L. Chan, J.A. Higgins, *Superior role of apolipoprotein B48 over apolipoprotein B100 in chylomicron assembly and fat absorption: an investigation of apobec-1 knock-out and wild-type mice*, Biochem J, 2001, 356 (Pt 3): p. 821-827.

155. Rifai, N., J.R. Merrill, R.G. Holly, *Postprandial effect of a high fat meal on plasma lipid, lipoprotein cholesterol and apolipoprotein measurements*, Ann Clin Biochem, 1990, 27 (Pt 5): p. 489-493.

156. Tso, P., M.B. Lindstrom, B. Borgstrom, *Factors regulating the formation of chylomicrons and very-low-density lipoproteins by the rat small intestine*, Biochim Biophys Acta, 1987, 922 (3): p. 304-313.

157. Tso, P., et al., *Evidence for separate pathways of chylomicron and very low-density lipoprotein assembly and transport by rat small intestine*, Am J Physiol, 1984, 247 (6 Pt 1): p. G599-610.

158. Ringman, J.M., et al., *A potential role of the curry spice curcumin in Alzheimer's disease*, Curr Alzheimer Res, 2005, 2 (2): p. 131-136.

159. Fraser, R., W.J. Cliff, F.C. Courtice, *The effect of dietary fat load on the size and composition of chylomicrons in thoracic duct lymph*, Q J Exp Physiol Cogn Med Sci, 1968, 53 (4): p. 390-398.

160. Hayashi, H., et al., *Fat feeding increases size, but not number, of chylomicrons produced by small intestine*, Am J Physiol, 1990, 259 (5 Pt 1): p. G709-719.

161. Glickman, R.M., K. Kirsch, *Lymph chylomicron formation during the inhibition of protein synthesis. Studies of chylomicron apoproteins*, J Clin Invest, 1973, 52 (11): p. 2910-2920.

162. Sheehe, D.M., J.B. Green, M.H. Green, *Influence of dietary fat saturation on lipid absorption in the rat*, Atherosclerosis, 1980, 37 (2): p. 301-310.

163. Holm, R., et al., *Comparison of total oral bioavailability and the lymphatic transport of halofantrine from three different unsaturated triglycerides in lymph-cannulated conscious rats*, Eur J Pharm Sci, 2001, 14 (4): p. 331-337.

164. Bateman, P.A., et al., *Differences in cell morphology, lipid and apo B secretory capacity in caco-2 cells following long term treatment with saturated and monounsaturated fatty acids*, Biochim Biophys Acta, 2007, 1771 (4): p. 475-485.

165. Jackson, K.G., et al., *Olive oil increases the number of triacylglycerol-rich chylomicron particles compared with other oils: an effect retained when a second standard meal is fed*, Am J Clin Nutr, 2002, 76 (5): p. 942-949.

166. van Greevenbroek, M.M., et al., *Effects of saturated, mono-, and polyunsaturated fatty acids on the secretion of apo B containing lipoproteins by Caco-2 cells*, Atherosclerosis, 1996, 121 (1): p. 139-150.

167. Schurgers, L.J., et al., *Novel effects of diets enriched with corn oil or with an olive oil/sunflower oil mixture on vitamin K metabolism and vitamin K-dependent proteins in young men*, J Lipid Res, 2002, 43 (6): p. 878-884.

168. Jackson, K.G., et al., *Acute effects of meal fatty acids on postprandial NEFA, glucose and apo E response: implications for insulin sensitivity and lipoprotein regulation?*, Br J Nutr, 2005, 93 (5): p. 693-700.

169. van Greevenbroek, M.M., et al., *Palmitic acid and linoleic acid metabolism in Caco-2 cells: different triglyceride synthesis and lipoprotein secretion*, J Lipid Res, 1995, 36 (1): p. 13-24.

170. Ranheim, T., et al., *Effect of chronic incubation of CaCo-2 cells with eicosapentaenoic acid (20:5, n-3) and oleic acid (18:1, n-9) on triacylglycerol production*, Biochem J, 1994, 303 (Pt 1): p. 155-161.

171. Field, F.J., E. Albright, S.N. Mathur, *Regulation of triglyceride-rich lipoprotein secretion by fatty acids in CaCo-2 cells*, J Lipid Res, 1988, 29 (11): p. 1427-1437.

172. Holm, R., et al., *Comparison of the lymphatic transport of halofantrine administered in disperse systems containing three different unsaturated fatty acids*, Pharm Res, 2001, 18 (9): p. 1299-1304.

173. Porsgaard, T., et al., *Size and number of lymph particles measured by a particle sizer during absorption of structured oils in rats*, Lipids, 2005, 40 (3): p. 273-279.

174. Caliph, S.M., W.N. Charman, C.J. Porter, *Effect of short-, medium-, and long-chain fatty acid-based vehicles on the absolute oral bioavailability and intestinal lymphatic transport of halofantrine and assessment of mass balance in lymph-cannulated and non-cannulated rats*, J Pharm Sci, 2000, 89 (8): p. 1073-1084.

175. Wermuth, C.G., *The practice of medicinal chemistry*, 2008.

176. Chitchumroonchokchai, C., S.J. Schwartz, M.L. Failla, *Assessment of lutein bioavailability from meals and a supplement using simulated digestion and Caco-2 human intestinal cells*, Journal of Nutrition, 2004, 134 (9): p. 2280-2286.

177. Levy, E., et al., *Metabolic fate of chylomicrons obtained from rats maintained on diets varying in fatty acid composition*, J Am Coll Nutr, 1991, 10 (1): p. 69-78.

178. Kinoshita, M., et al., *Determination of apolipoprotein B-48 in serum by a sandwich ELISA*, Clin Chim Acta, 2005, 351 (1-2): p. 115-120.

179. Blanchette-Mackie, E.J., R.O. Scow, *Sites of lipoprotein lipase activity in adipose tissue perfused with chylomicrons. Electron microscope cytochemical study*, J Cell Biol, 1971, 51 (1): p. 1-25.

180. Lusis, A.J., P. Pajukanta, *A treasure trove for lipoprotein biology*, Nat Genet, 2008, 40 (2): p. 129-130.

181. Cooper, A.D., *Hepatic uptake of chylomicron remnants*, J Lipid Res, 1997, 38 (11): p. 2173-2192.

182. Kei, A.A., et al., *A review of the role of apolipoprotein C-II in lipoprotein metabolism and cardiovascular disease*, Metabolism-Clinical and Experimental, 2012, 61 (7): p. 906-921.

183. Vine, D.F., D.R. Glimm, S.D. Proctor, *Intestinal lipid transport and chylomicron production: Possible links to exacerbated atherogenesis in a rodent model of the metabolic syndrome*, Atherosclerosis Supplements, 2008, 9 (2): p. 69-76.

184. Jackson, K.G., S.D. Poppitt, A.M. Minihane, *Postprandial lipemia and cardiovascular disease risk: Interrelationships between dietary, physiological and genetic determinants*, Atherosclerosis, 2012, 220 (1): p. 22-33.

185. Jagla, A., J. Schrezenmeir, *Postprandial triglycerides and endothelial function*, Experimental and Clinical Endocrinology & Diabetes, 2001, 109 (4): p. S533-S547.

186. Napolitano, M., et al., *The fatty acid composition of chylomicron remnants influences their propensity to oxidate*, Nutr Metab Cardiovasc Dis, 2004, 14 (5): p. 241-247.

187. McClements, D.J., *Utilizing food effects to overcome challenges in delivery of lipophilic bioactives: structural design of medical and functional foods*, Expert Opin Drug Deliv, 2013, 10 (12): p. 1621-1632.

188. McClements, D.J., H. Xiao, *Excipient foods: designing food matrices that improve the oral bioavailability of pharmaceuticals and nutraceuticals*, Food & Function, 2014, 5 (7): p. 1320-1333.

189. McClements, D.J., *Emulsion design to improve the delivery of functional lipophilic components*, Annu Rev Food Sci Technol, 2010, 1: p. 241-269.

190. Xu, J., et al., *Improved stability and controlled release of omega 3/omega 6 polyunsaturated fatty acids by spring dextrin encapsulation*, Carbohydrate Polymers, 2013, 92 (2): p. 1633-1640.

191. Paramera, E.I., S.J. Konteles, V.T. Karathanos, *Stability and release properties of curcumin encapsulated in Saccharomyces cerevisiae, beta-cyclodextrin and modified starch*, Food Chem, 2011, 125 (3): p. 913-922.

192. Yu, H.L., Q.R. Huang, *Improving the Oral Bioavailability of Curcumin Using Novel Organogel-Based Nanoemulsions*, J Agric Food Chem, 2012, 60 (21): p. 5373-5379.

193. Zimet, P., Y.D. Livney, *Beta-lactoglobulin and its nanocomplexes with pectin as vehicles for omega-3 polyunsaturated fatty acids*, Food Hydrocolloids, 2009, 23 (4): p. 1120-1126.

194. Haham, M., et al., *Stability and bioavailability of vitamin D nanoencapsulated in casein micelles*, Food & Function, 2012, 3 (7): p. 737-744.

195. Schiborr, C., et al., *The oral bioavailability of curcumin from micronized powder and liquid micelles is significantly increased in healthy humans and differs between sexes*, Molecular Nutrition & Food Research, 2014, 58 (3): p. 516-527.

196. Zhou, H.F., et al., *Novel Lipid-Free Nanoformulation for Improving Oral Bioavailability of Coenzyme Q10*, Biomed Research International, 2014: p.

197. Herrera, E., C. Barbas, *Vitamin E: action, metabolism and perspectives*, J Physiol Biochem, 2001, 57 (2): p. 43-56.

198. Qian, C., et al., *Nanoemulsion delivery systems: influence of carrier oil on beta-carotene bioaccessibility*, Food Chem, 2012, 135 (3): p. 1440-1447.

199. Borel, P., et al., *Chylomicron beta-carotene and retinyl palmitate responses are dramatically diminished when men ingest beta-carotene with medium-chain rather than long-chain triglycerides*, Journal of Nutrition, 1998, 128 (8): p. 1361-1367.

200. Yang, Y., D.J. McClements, *Vitamin E bioaccessibility: influence of carrier oil type on digestion and release of emulsified alpha-tocopherol acetate*, Food Chem, 2013, 141 (1): p. 473-481.

201. Gong, Y.H., et al., *An Excellent Delivery System for Improving the Oral Bioavailability of Natural Vitamin E in Rats*, Aaps Pharmscitech, 2012, 13 (3): p. 961-966.

202. Cho, H.T., et al., *Droplet size and composition of nutraceutical nanoemulsions influences bioavailability of long chain fatty acids and Coenzyme Q10*, Food Chem, 2014, 156: p. 117-122.

203. Thanatuksorn, P., et al., *Improvement of the oral bioavailability of coenzyme Q(10) by emulsification with fats and emulsifiers used in the food industry*, Lwt-Food Science and Technology, 2009, 42 (1): p. 385-390.

204. Mignet, N., J. Seguin, G.G. Chabot, *Bioavailability of polyphenol liposomes: a challenge ahead*, Pharmaceutics, 2013, 5 (3): p. 457-471.

205. Zou, L.P., S.; Liu, W.; Gan, L.; Liu, W.; Liang,R.; Liu, C.; Niu, J.; Cao, Y.; Liu, Z.; Chen,X., *Improved in vitro digestion stability of (−)-epigallocatechin gallate through nanoliposome encapsulation*, Food Research International, 2014, 64: p. 492-499.

206. Yao, M., H. Xiao, D.J. McClements, *Delivery of lipophilic bioactives: assembly, disassembly, and reassembly of lipid nanoparticles*, Annu Rev Food Sci Technol, 2014, 5: p. 53-81.

207. Xiao, Y., et al., *Preparation and oral bioavailability study of curcuminoid-loaded microemulsion*, J Agric Food Chem, 2013, 61 (15): p. 3654-3660.

208. Chen, Y.J., et al., *Development of lycopene micelle and lycopene chylomicron and a comparison of bioavailability*, Nanotechnology, 2014, 25 (15): p.

209. Sanguansri, P., M.A. Augustin, *Nanoscale materials development - a food industry perspective*, Trends in Food Science & Technology, 2006, 17 (10): p. 547-556.

210. Ezhilarasi, P.N., et al., *Nanoencapsulation Techniques for Food Bioactive Components: A Review*, Food and Bioprocess Technology, 2013, 6 (3): p. 628-647.

211. Gutierrez, F.J., et al., *Methods for the nanoencapsulation of beta-carotene in the food sector*, Trends in Food Science & Technology, 2013, 32 (2): p. 73-83.

212. Joyea, I.J., G. Davidov-Pardoa, D.J. McClements, *Nanotechnology for increased micronutrient bioavailability*, Trends in Food Science & Technology, 2014: p.

213. Parada, J., J.M. Aguilera, *Food microstructure affects the bioavailability of several nutrients*, Journal of Food Science, 2007, 72 (2): p. R21-R32.

214. Harde, H., M. Das, S. Jain, *Solid lipid nanoparticles: an oral bioavailability enhancer vehicle*, Expert Opin Drug Deliv, 2011, 8 (11): p. 1407-1424.

215. Salvia-Trujillo, L., et al., *Modulating beta-carotene bioaccessibility by controlling oil composition and concentration in edible nanoemulsions*, Food Chem, 2013, 139 (1-4): p. 878-884.

216. Sun, Y., et al., *Nanoemulsion-based delivery systems for nutraceuticals: Influence of carrier oil type on bioavailability of pterostilbene*, Submitted, 2014: p.

217. Salvia-Trujillo, L., et al., *Influence of particle size on lipid digestion and beta-carotene bioaccessibility in emulsions and nanoemulsions*, Food Chem, 2013, 141 (2): p. 1472-1480.

218. Speranza, A., et al., *Influence of emulsifier structure on lipid bioaccessibility in oil-water nanoemulsions*, J Agric Food Chem, 2013, 61 (26): p. 6505-6515.

219. Oehlke, K., et al., *Potential bioavailability enhancement of bioactive compounds using food-grade engineered nanomaterials: a review of the existing evidence*, Food & Function, 2014, 5 (7): p. 1341-1359.

220. Grolier, P., S. Agoudavi, V. Azaisbraesco, *Comparative Bioavailability of Diet-Based, Oil-Based and Emulsion-Based Preparations of Vitamin-a and Beta-Carotene in Rat*, Nutrition Research, 1995, 15 (10): p. 1507-1516.

221. Yao, M.F., et al., *Enhanced lymphatic transport of bioactive lipids: cell culture study of polymethoxyflavone incorporation into chylomicrons*, Food & Function, 2013, 4 (11): p. 1662-1667.

222. Kondoh, M., A. Takahashi, K. Yagi, *Spiral progression in the development of absorption enhancers based on the biology of tight junctions*, Advanced Drug Delivery Reviews, 2012, 64 (6): p. 515-522.

223. Hu, B., et al., *Optimization of fabrication parameters to produce chitosan-tripolyphosphate nanoparticles for delivery of tea catechins*, J Agric Food Chem, 2008, 56 (16): p. 7451-7458.

224. Kenny, O., *Effects of Ingredient Incorporation into Sausage Meat on the Micellarisation and uptake of a-tocopherol by Caco-2 Human Intestinal Cell*, Food Sci Tech Int, 2008, 14 (1): p. 79-86.

225. Hofmann, A.F., B. Borgstrom, *Physico-chemical state of lipids in intestinal content during their digestion and absorption*, Fed Proc, 1962, 21: p. 43-50.

226. Trevaskis, N.L., W.N. Charman, C.J. Porter, *Targeted drug delivery to lymphocytes: a route to site-specific immunomodulation?*, Mol Pharm, 2010, 7 (6): p. 2297-2309.

227. Beyrich, T., A. Mehr, *[The problem of plastic containers for liquid drug preparations. 17. Photometric determination of oxygen permeability with indigo carmine]*, Pharmazie, 1975, 30 (11): p. 715-717.

228. Levy, E., et al., *Caco-2 cells and human fetal colon: a comparative analysis of their lipid transport*, Biochim Biophys Acta, 1999, 1439 (3): p. 353-362.

229. Levy, E., M. Mehran, E. Seidman, *Caco-2 Cells as a Model for Intestinal Lipoprotein Synthesis and Secretion*, Faseb Journal, 1995, 9 (8): p. 626-635.

230. Xiao, H., et al., *Monodemethylated polymethoxyflavones from sweet orange (Citrus sinensis) peel inhibit growth of human lung cancer cells by apoptosis*, Mol Nutr Food Res, 2009, 53 (3): p. 398-406.

231. Qiu, P., et al., *Inhibitory effects of 5-hydroxy polymethoxyflavones on colon cancer cells*, Mol Nutr Food Res, 2010, 54 Suppl 2: p. S244-252.

232. Dong, P., et al., *Simultaneous determination of four 5-hydroxy polymethoxyflavones by reversed-phase high performance liquid chromatography with electrochemical detection*, J Chromatogr A, 2010, 1217 (5): p. 642-647.

233. Anderson, L.J., J.K. Boyles, M.M. Hussain, *A rapid method for staining large chylomicrons*, J Lipid Res, 1989, 30 (11): p. 1819-1824.

234. Levin, M.S., et al., *Trafficking of Exogenous Fatty-Acids within Caco-2 Cells*, J Lipid Res, 1992, 33 (1): p. 9-19.

235. Murota, K., J. Storch, *Uptake of micellar long-chain fatty acid and sn-2-monoacylglycerol into human intestinal Caco-2 cells exhibits characteristics of protein-mediated transport*, J Nutr, 2005, 135 (7): p. 1626-1630.

236. Raimondi, F., et al., *Bile acids modulate tight junction structure and barrier function of Caco-2 monolayers via EGFR activation*, Am J Physiol Gastrointest Liver Physiol, 2008, 294 (4): p. G906-913.

237. David L. Nelson, M.M.C., *Lehninger principles of biochemistry*, W.H.Freeman and Company, 41 Madsion Avenue, New York, NY 10010, 2005.

238. Aspenstrom-Fagerlund, B., et al., *Oleic acid and docosahexaenoic acid cause an increase in the paracellular absorption of hydrophilic compounds in an experimental model of human absorptive enterocytes*, Toxicology, 2007, 237 (1-3): p. 12-23.

239. Zheng, J., et al., *Identification of novel bioactive metabolites of 5-demethylnobiletin in mice*, Mol Nutr Food Res, 2013: p.

240. Caliph, S.M., W.N. Charman, C.J.H. Porter, *Effect of short-, medium-, and long-chain fatty acid-based vehicles on the absolute oral bioavailability and intestinal lymphatic transport of halofantrine and assessment of mass balance in lymph-cannulated and non-cannulated rats*, Journal of Pharmaceutical Sciences, 2000, 89 (8): p. 1073-1084.

241. Attili-Qadri, S., et al., *Oral delivery system prolongs blood circulation of docetaxel nanocapsules via lymphatic absorption*, Proc Natl Acad Sci U S A, 2013, 110 (43): p. 17498-17503.

242. Szebeni, J., et al., *Prevention of infusion reactions to PEGylated liposomal doxorubicin via tachyphylaxis induction by placebo vesicles: a porcine model*, J Control Release, 2012, 160 (2): p. 382-387.

243. Ng, K.K., J.F. Lovell, G. Zheng, *Lipoprotein-inspired nanoparticles for cancer theranostics*, Acc Chem Res, 2011, 44 (10): p. 1105-1113.

244. Yeap, Y.Y., et al., *Intestinal Bile Secretion Promotes Drug Absorption from Lipid Colloidal Phases via Induction of Supersaturation*, Molecular Pharmaceutics, 2013, 10 (5): p. 1874-1889.

245. Williams, H.D., et al., *Strategies to address low drug solubility in discovery and development*, Pharmacol Rev, 2013, 65 (1): p. 315-499.

246. Hofmann, A.F., B. Borgstroem, *The Intraluminal Phase of Fat Digestion in Man: The Lipid Content of the Micellar and Oil Phases of Intestinal Content Obtained during Fat Digestion and Absorption*, J Clin Invest, 1964, 43: p. 247-257.

247. Shiau, Y.F., *Mechanisms of intestinal fat absorption*, Am J Physiol, 1981, 240 (1): p. G1-9.

248. van Greevenbroek, M.M., T.W. de Bruin, *Chylomicron synthesis by intestinal cells in vitro and in vivo*, Atherosclerosis, 1998, 141 Suppl 1: p. S9-16.

249. Mingfei Yao, J.C., Jinkai Zheng, Mingyue Song, D. J. McClements and Hang Xiao, *Enhanced lymphatic transport of bioactive lipids: Cell culture study of polymethoxyflavone incorporation into chylomicrons*, Food&Function, 2013: p.

250. Nelson, R., *Oleic acid suppresses overexpression of ERBB2 oncogene*, Lancet Oncol, 2005, 6 (2): p. 69.

251. Mozaffarian, D., J.H. Wu, *Omega-3 fatty acids and cardiovascular disease: effects on risk factors, molecular pathways, and clinical events*, J Am Coll Cardiol, 2011, 58 (20): p. 2047-2067.

252. Abeywardena, M.Y., R.J. Head, *Longchain n-3 polyunsaturated fatty acids and blood vessel function*, Cardiovasc Res, 2001, 52 (3): p. 361-371.

253. Djousse, L., et al., *Dietary linolenic acid is inversely associated with calcified atherosclerotic plaque in the coronary arteries - The national heart, lung, and blood institute family heart study*, Circulation, 2005, 111 (22): p. 2921-2926.

254. Wijendran, V., K.C. Hayes, *Dietary n-6 and n-3 fatty acid balance and cardiovascular health*, Annual Review of Nutrition, 2004, 24: p. 597-615.

255. Leonard, M., et al., *Evaluation of the Caco-2 monolayer as a model epithelium for iontophoretic transport*, Pharmaceutical Research, 2000, 17 (10): p. 1181-1188.

256. Mullertz, A., et al., *Insights into intermediate phases of human intestinal fluids visualized by atomic force microscopy and cryo-transmission electron microscopy ex vivo*, Mol Pharm, 2012, 9 (2): p. 237-247.

257. Almgren, M., *Mixed micelles and other structures in the solubilization of bilayer lipid membranes by surfactants*, Biochim Biophys Acta, 2000, 1508 (1-2): p. 146-163.

258. Demignot, S., F. Beilstein, E. Morel, *Triglyceride-rich lipoproteins and cytosolic lipid droplets in enterocytes: key players in intestinal physiology and metabolic disorders*, Biochimie, 2014, 96: p. 48-55.

259. Hubatsch, I., E.G.E. Ragnarsson, P. Artursson, *Determination of drug permeability and prediction of drug absorption in Caco-2 monolayers*, Nature Protocols, 2007, 2 (9): p. 2111-2119.

260. Usami, M., et al., *Effect of eicosapentaenoic acid (EPA) on tight junction permeability in intestinal monolayer cells*, Clin Nutr, 2001, 20 (4): p. 351-359.

261. Olofsson, S.O., et al., *Lipid droplets as dynamic organelles connecting storage and efflux of lipids*, Biochim Biophys Acta, 2009, 1791 (6): p. 448-458.

262. Schmitz, G., V.F. R, *Lipid droplets as dynamic organelles of fat deposition and release*, Biochim Biophys Acta, 2009, 1791 (6): p. 397-398.

263. Luchoomun, J., M.M. Hussain, *Assembly and secretion of chylomicrons by differentiated Caco-2 cells - Nascent triglycerides and preformed phospholipids are preferentially used for lipoprotein assembly*, Journal of Biological Chemistry, 1999, 274 (28): p. 19565-19572.

264. Harris, W.S., et al., *N-3 fatty acids and chylomicron metabolism in the rat*, J Lipid Res, 1997, 38 (3): p. 503-515.

265. Van Veld, P.A., et al., *Dietary fat inhibits the intestinal metabolism of the carcinogen benzo[a]pyrene in fish*, J Lipid Res, 1987, 28 (7): p. 810-817.

266. Kobayashi, H., R. Watanabe, P.L. Choyke, *Improving conventional enhanced permeability and retention (EPR) effects; what is the appropriate target?*, Theranostics, 2013, 4 (1): p. 81-89.

267. Qian, C., et al., *Nanoemulsion delivery systems: Influence of carrier oil on beta-carotene bioaccessibility*, Food Chem, 2012, 135 (3): p. 1440-1447.

268. Martinez, M., et al., *Applying the Biopharmaceutics Classification System to veterinary pharmaceutical products Part I: Biopharmaceutics and formulation considerations*, Adv Drug Deliv Rev, 2002, 54 (6): p. 805-824.

269. McClements, D.J., *Design of Nano-Laminated Coatings to Control Bioavailability of Lipophilic Food Components*, Journal of Food Science, 2010, 75 (1): p. R30-R42.

270. Ting, Y.W., et al., *Common delivery systems for enhancing in vivo bioavailability and biological efficacy of nutraceuticals*, Journal of Functional Foods, 2014, 7: p. 112-128.

271. Cho, H.T., et al., *Droplet size and composition of nutraceutical nanoemulsions influences bioavailability of long chain fatty acids and Coenzyme Q10*, Food Chem, 2014, 156: p. 117-122.

272. Li, J., et al., *Influence of gastric digestive reaction on subsequent in vitro intestinal digestion of sodium caseinate-stabilized emulsions*, Food Funct, 2012, 3 (3): p. 320-326.

273. Leonard, M., et al., *Evaluation of the Caco-2 monolayer as a model epithelium for iontophoretic transport*, Pharm Res, 2000, 17 (10): p. 1181-1188.

274. Yao, M., et al., *Enhanced lymphatic transport of bioactive lipids: cell culture study of polymethoxyflavone incorporation into chylomicrons*, Food Funct, 2013, 4 (11): p. 1662-1667.

275. Brown, M.J., et al., *Carotenoid bioavailability is higher from salads ingested with full-fat than with fat-reduced salad dressings as measured with electrochemical detection*, American Journal of Clinical Nutrition, 2004, 80 (2): p. 396-403.

276. Yang, Y., D.J. McClements, *Vitamin E bioaccessibility: Influence of carrier oil type on digestion and release of emulsified alpha-tocopherol acetate*, Food Chem, 2013, 141 (1): p. 473-481.

277. Rudkowska, I., et al., *Phytosterols mixed with medium-chain triglycerides and high-oleic canola oil decrease plasma lipids in overweight men*, Metabolism, 2006, 55 (3): p. 391-395.

278. Yu, H.L., Q.R. Huang, *Investigation of the cytotoxicity of food-grade nanoemulsions in Caco-2 cell monolayers and HepG2 cells*, Food Chem, 2013, 141 (1): p. 29-33.

279. Lo, Y.L., C.Y. Hsu, J.D. Huang, *Comparison of effects of surfactants with other MDR reversing agents on intracellular uptake of epirubicin in Caco-2 cell line*, Anticancer Research, 1998, 18 (4C): p. 3005-3009.

280. Liu, Y., et al., *Effects of milk proteins on release properties and particle morphology of beta-carotene emulsions during in vitro digestion*, Food Funct, 2014, 5 (11): p. 2940-2947.

281. Ritzoulis, C., et al., *Interactions between pig gastric mucin and sodium caseinate in solutions and in emulsions*, Food Hydrocolloids, 2012, 29 (2): p. 382-388.

282. Sek, L., et al., *Evaluation of the in-vitro digestion profiles of long and medium chain glycerides and the phase behaviour of their lipolytic products*, Journal of Pharmacy and Pharmacology, 2002, 54 (1): p. 29-41.

283. Matthies, A., et al., *Daidzein and Genistein Are Converted to Equol and 5-Hydroxy-Equol by Human Intestinal Slackia isoflavoniconvertens in Gnotobiotic Rats*, Journal of Nutrition, 2012, 142 (1): p. 40-46.

284. Zheng, J.K., et al., *Identification of novel bioactive metabolites of 5-demethylnobiletin in mice*, Molecular Nutrition & Food Research, 2013, 57 (11): p. 1999-2007.

285. Swift, L.L., et al., *Medium-Chain Fatty-Acids - Evidence for Incorporation into Chylomicron Triglycerides in Humans*, American Journal of Clinical Nutrition, 1990, 52 (5): p. 834-836.

286. Bouchoux, J., et al., *The proteome of cytosolic lipid droplets isolated from differentiated Caco-2/TC7 enterocytes reveals cell-specific characteristics*, Biology of the Cell, 2011, 103 (11): p. 499-517.

287. Galluser, M., et al., *Comparison of different lipid substrates on intestinal adaptation in the rat*, Gut, 1993, 34 (8): p. 1069-1074.

288. Walther, T.C., R.V. Farese, Jr., *Lipid droplets and cellular lipid metabolism*, Annu Rev Biochem, 2012, 81: p. 687-714.

289. Bach, A.C., V.K. Babayan, *Medium-Chain Triglycerides - an Update*, American Journal of Clinical Nutrition, 1982, 36 (5): p. 950-962.

290. Trotter, P.J., J. Storch, *Fatty acid uptake and metabolism in a human intestinal cell line (Caco-2): comparison of apical and basolateral incubation*, J Lipid Res, 1991, 32 (2): p. 293-304.

291. Wang, T.Y., et al., *New insights into the molecular mechanism of intestinal fatty acid absorption*, Eur J Clin Invest, 2013, 43 (11): p. 1203-1223.

292. von Schacky, C., *The role of omega-3 fatty acids in cardiovascular disease*, Curr Atheroscler Rep, 2003, 5 (2): p. 139-145.

293. Trushina, E.N., O.K. Mustafina, M.N. Volgarev, *[The mechanism of action of polyunsaturated fatty acids on the immune system]*, Vopr Pitan, 2003, 72 (3): p. 35-40.

294. Innis, S.M., *Perinatal biochemistry and physiology of long-chain polyunsaturated fatty acids*, J Pediatr, 2003, 143 (4 Suppl): p. S1-8.

295. do Nascimento, C.M., L.M. Oyama, *Long-chain polyunsaturated fatty acids essential for brain growth and development*, Nutrition, 2003, 19 (1): p. 66.

296. Gil, A., M. Ramirez, M. Gil, *Role of long-chain polyunsaturated fatty acids in infant nutrition*, Eur J Clin Nutr, 2003, 57 Suppl 1: p. S31-34.

297. Martin, M.M.a.K.R., *Inestinal absorption of fat-soluble vitamins*, in: Charles M. Mansbach II , P.T., Arnis Kuksis (Ed.) Intestinal Lipid Metabolism, Kluwer Academic/plenum Publishers, New York 2000, p. 367-378.

298. Zolfaghari, R., A.C. Ross, *Recent advances in molecular cloning of fatty acid desaturase genes and the regulation of their expression by dietary vitamin A and retinoic acid*, Prostaglandins Leukot Essent Fatty Acids, 2003, 68 (2): p. 171-179.

299. Kaleem, A., et al., *Effect of chemical form, heating, and oxidation products of linoleic acid on rumen bacterial population and activities of biohydrogenating enzymes*, J Dairy Sci, 2013, 96 (11): p. 7167-7180.

300. Santoro, N., et al., *Oxidized fatty acids: A potential pathogenic link between fatty liver and type 2 diabetes in obese adolescents?*, Antioxid Redox Signal, 2014, 20 (2): p. 383-389.

301. Penumetcha, M., N. Khan, S. Parthasarathy, *Dietary oxidized fatty acids: an atherogenic risk?*, J Lipid Res, 2000, 41 (9): p. 1473-1480.

302. Esterbauer, H., *Cytotoxicity and genotoxicity of lipid-oxidation products*, Am J Clin Nutr, 1993, 57 (5 Suppl): p. 779S-785S; discussion 785S-786S.

303. Maestre, R., et al., *Alterations in the intestinal assimilation of oxidized PUFAs are ameliorated by a polyphenol-rich grape seed extract in an in vitro model and Caco-2 cells*, J Nutr, 2013, 143 (3): p. 295-301.

304. Staprans, I., et al., *Effect of dietary lipid peroxides on metabolism of serum chylomicrons in rats*, Am J Physiol, 1993, 264 (3 Pt 1): p. G561-568.

305. Rong, R., et al., *Dietary oxidized fatty acids may enhance intestinal apolipoprotein A-I production*, J Lipid Res, 2002, 43 (4): p. 557-564.

306. Norris, L.E., et al., *Comparison of dietary conjugated linoleic acid with safflower oil on body composition in obese postmenopausal women with type 2 diabetes mellitus*, Am J Clin Nutr, 2009, 90 (3): p. 468-476.

307. van Greevenbroek, M.M., D.W. Erkelens, T.W. de Bruin, *Caco-2 cells secrete two independent classes of lipoproteins with distinct density: effect of the ratio of unsaturated to saturated fatty acid*, Atherosclerosis, 2000, 149 (1): p. 25-31.

308. Yvonne O'Callaghan* , N.O.B., *Bioaccessibility, cellular uptake and transepithelial transport of a-tocopherol and retinol from a range of supplemented foodstuffs assessed using the caco-2 cell model*, International Journal of Food Science &Technology, 2010, 45: p. 1436-1442.

309. Anwar, K., H.J. Kayden, M.M. Hussain, *Transport of vitamin E by differentiated Caco-2 cells*, J Lipid Res, 2006, 47 (6): p. 1261-1273.

310. Shantha, N.C., E.A. Decker, *Rapid, Sensitive, Iron-Based Spectrophotometric Methods for Determination of Peroxide Values of Food Lipids*, Journal of Aoac International, 1994, 77 (2): p. 421-424.

311. Mcdonald, R.E., H.O. Hultin, *Some Characteristics of the Enzymatic Lipid-Peroxidation System in the Microsomal Fraction of Flounder Skeletal-Muscle*, Journal of Food Science, 1987, 52 (1): p. 15-&.

312. Jambunathan, N., *Determination and detection of reactive oxygen species (ROS), lipid peroxidation, and electrolyte leakage in plants*, Methods Mol Biol, 2010, 639: p. 292-298.

313. Lopez-Soldado, I., M. Avella, K.M. Botham, *Comparison of the effects of dietary saturated, mono-unsaturated and polyunsaturated fatty acids on very-low-density lipoprotein secretion when delivered to hepatocytes in chylomicron remnant-like particles*, Biochem Soc Trans, 2007, 35 (Pt 3): p. 440-441.

314. Thiebaut, A.C., et al., *Dietary intakes of omega-6 and omega-3 polyunsaturated fatty acids and the risk of breast cancer*, Int J Cancer, 2009, 124 (4): p. 924-931.

315. Sioen, I.A., et al., *Dietary intakes and food sources of fatty acids for Belgian women, focused on n-6 and n-3 polyunsaturated fatty acids*, Lipids, 2006, 41 (5): p. 415-422.

316. Frankel, E.N., *Lipid oxidation, second edition(Oily Press Lipid Library Series)*, 2005.

317. Kubow, S., *Routes of formation and toxic consequences of lipid oxidation products in foods*, Free Radic Biol Med, 1992, 12 (1): p. 63-81.

318. Ames, B.N., *Dietary carcinogens and anti-carcinogens*, J Toxicol Clin Toxicol, 1984, 22 (3): p. 291-301.

319. Parks, D.A., G.B. Bulkley, D.N. Granger, *Role of oxygen-derived free radicals in digestive tract diseases*, Surgery, 1983, 94 (3): p. 415-422.

320. Medeiros, M.H., *Exocyclic DNA adducts as biomarkers of lipid oxidation and predictors of disease. Challenges in developing sensitive and specific methods for clinical studies*, Chem Res Toxicol, 2009, 22 (3): p. 419-425.

321. Reddy, B.S., C. Burill, J. Rigotty, *Effect of diets high in omega-3 and omega-6 fatty acids on initiation and postinitiation stages of colon carcinogenesis*, Cancer Res, 1991, 51 (2): p. 487-491.

322. Alghazeer, R., H. Gao, N.K. Howell, *Cytotoxicity of oxidised lipids in cultured colonal human intestinal cancer cells (caco-2 cells)*, Toxicol Lett, 2008, 180 (3): p. 202-211.

323. Ockner, R.K., F.B. Hughes, K.J. Isselbacher, *Very low density lipoproteins in intestinal lymph: role in triglyceride and cholesterol transport during fat absorption*, J Clin Invest, 1969, 48 (12): p. 2367-2373.

324. Yun, Y., Y.W. Cho, K. Park, *Nanoparticles for oral delivery: Targeted nanoparticles with peptidic ligands for oral protein delivery*, Adv Drug Deliv Rev, 2013, 65 (6): p. 822-832.

325. Fisichella, M., et al., *Intestinal toxicity evaluation of TiO2 degraded surface-treated nanoparticles: a combined physico-chemical and toxicogenomics approach in caco-2 cells*, Particle and Fibre Toxicology, 2012, 9: p.

326. Chaudhry, Q., et al., *Applications and implications of nanotechnologies for the food sector*, Food Additives and Contaminants Part a-Chemistry Analysis Control Exposure & Risk Assessment, 2008, 25 (3): p. 241-258.

327. Duncan, T.V., *Applications of nanotechnology in food packaging and food safety: Barrier materials, antimicrobials and sensors*, Journal of Colloid and Interface Science, 2011, 363 (1): p. 1-24.

328. Weiss, J., D.J. McClements, P. Takhistov, *Functional materials in food nanotechnology*, Food Australia, 2007, 59 (6): p. 274-275.

329. Wang, H.F., et al., *Progress in the characterization and safety evaluation of engineered inorganic nanomaterials in food*, Nanomedicine, 2013, 8 (12): p. 2007-2025.

330. Abbott, L.C., A.D. Maynard, *Exposure Assessment Approaches for Engineered Nanomaterials*, Risk Analysis, 2010, 30 (11): p. 1634-1644.

331. Weber, C.R., et al., *Claudin-1 and claudin-2 expression is elevated in inflammatory bowel disease and may contribute to early neoplastic transformation*, Laboratory Investigation, 2008, 88 (10): p. 1110-1120.

332. Yamashita, K., et al., *Silica and titanium dioxide nanoparticles cause pregnancy complications in mice*, Nature Nanotechnology, 2011, 6 (5): p. 321-328.

333. Lagopati, N., et al., *Effect of nanostructured TiO(2) crystal phase on photoinduced apoptosis of breast cancer epithelial cells*, Int J Nanomedicine, 2014, 9: p. 3219-3230.

334. Wang, J., et al., *Acute toxicity and biodistribution of different sized titanium dioxide particles in mice after oral administration*, Toxicol Lett, 2007, 168 (2): p. 176-185.

335. Thubagere, A., B.M. Reinhard, *Nanoparticle-Induced Apoptosis Propagates through Hydrogen-Peroxide-Mediated Bystander Killing: Insights from a Human Intestinal Epithelium In Vitro Model*, Acs Nano, 2010, 4 (7): p. 3611-3622.

336. Liang, M., et al., *Cellular Uptake of Densely Packed Polymer Coatings on Gold Nanoparticles*, Acs Nano, 2010, 4 (1): p. 403-413.

337. Ghosh, P., et al., *Gold nanoparticles in delivery applications*, Adv Drug Deliv Rev, 2008, 60 (11): p. 1307-1315.

338. Frohlich, E., E. Roblegg, *Models for oral uptake of nanoparticles in consumer products*, Toxicology, 2012, 291 (1-3): p. 10-17.

339. El-Sayed, I.H., X. Huang, M.A. El-Sayed, *Surface plasmon resonance scattering and absorption of anti-EGFR antibody conjugated gold nanoparticles in cancer diagnostics: applications in oral cancer*, Nano Lett, 2005, 5 (5): p. 829-834.

340. Dykman, L.A., N.G. Khlebtsov, *Uptake of Engineered Gold Nanoparticles into Mammalian Cells*, Chemical Reviews, 2014, 114 (2): p. 1258-1288.

341. Gu, Y.J., et al., *Nuclear penetration of surface functionalized gold nanoparticles*, Toxicology and Applied Pharmacology, 2009, 237 (2): p. 196-204.

342. Coulter, J.A., et al., *Cell type-dependent uptake, localization, and cytotoxicity of 1.9 nm gold nanoparticles*, International Journal of Nanomedicine, 2012, 7: p. 2673-2685.

343. Wadia, J.S., et al., *Mitochondrial membrane potential and nuclear changes in apoptosis caused by serum and nerve growth factor withdrawal: Time course and modification by (-)-deprenyl*, Journal of Neuroscience, 1998, 18 (3): p. 932-947.

344. Keil, V.C., et al., *Ratiometric high-resolution imaging of JC-1 fluorescence reveals the subcellular heterogeneity of astrocytic mitochondria*, Pflugers Archiv-European Journal of Physiology, 2011, 462 (5): p. 693-708.

345. Polte, J., et al., *Mechanism of gold nanoparticle formation in the classical citrate synthesis method derived from coupled in situ XANES and SAXS evaluation*, J Am Chem Soc, 2010, 132 (4): p. 1296-1301.

346. Datta, S.R., A. Brunet, M.E. Greenberg, *Cellular survival: a play in three Akts*, Genes Dev, 1999, 13 (22): p. 2905-2927.

347. Jiang, W., et al., *Nanoparticle-mediated cellular response is size-dependent*, Nature Nanotechnology, 2008, 3 (3): p. 145-150.

348. Nel, A.E., et al., *Understanding biophysicochemical interactions at the nano-bio interface*, Nature Materials, 2009, 8 (7): p. 543-557.

349. Yang, P.H., et al., *Transferrin-mediated gold nanoparticle cellular uptake*, Bioconjugate Chemistry, 2005, 16 (3): p. 494-496.

350. Wang, S.H., et al., *Size-dependent endocytosis of gold nanoparticles studied by three-dimensional mapping of plasmonic scattering images*, J Nanobiotechnology, 2010, 8: p. 33.

351. Sonavane, G., et al., *In vitro permeation of gold nanoparticles through rat skin and rat intestine: Effect of particle size*, Colloids and Surfaces B-Biointerfaces, 2008, 65 (1): p. 1-10.

352. Taggart, L.E., et al., *The role of mitochondrial function in gold nanoparticle mediated radiosensitisation*, Cancer Nanotechnol, 2014, 5 (1): p. 5.

353. Wang, L.M., et al., *Selective Targeting of Gold Nanorods at the Mitochondria of Cancer Cells: Implications for Cancer Therapy*, Nano Lett, 2011, 11 (2): p. 772-780.